R-921/1-ARPA
November 1971

Soviet Chemical Laser Research

Yuri Ksander

A Report prepared for

ADVANCED RESEARCH PROJECTS AGENCY

Rand
SANTA MONICA, CA. 90406

This research is supported by the Advanced Research Projects Agency under Contract No. DAHC15 67 C 0141. Views or conclusions contained in this study should not be interpreted as representing the official opinion or policy of Rand or of ARPA.

DOCUMENT CONTROL DATA

1. ORIGINATING ACTIVITY	2a. REPORT SECURITY CLASSIFICATION
The Rand Corporation	UNCLASSIFIED
	2b. GROUP ----

3. REPORT TITLE

SOVIET CHEMICAL LASER RESEARCH

4. AUTHOR(S) (Last name, first name, initial)

Ksander, Yuri

5. REPORT DATE	6a. TOTAL NO. OF PAGES	6b. NO. OF REFS.
November 1971	173	---

7. CONTRACT OR GRANT NO.	8. ORIGINATOR'S REPORT NO.
DAHC15 67 C 0141	R-921/1-ARPA

9a. AVAILABILITY/LIMITATION NOTICES	9b. SPONSORING AGENCY
DDC-A	Advanced Research Projects Agency

10. ABSTRACT

Reviews recent Soviet open literature on chemical lasers, published mainly in January-October 1971. Two research teams have been added to the five discussed in R-921: a second Lebedev Institute group, nominally under Prokhorov, and Letokhov's group at the Institute of Spectroscopy. A lack of papers from Khokhlov's Moscow State University group suggests that they may be doing classified work. For specialists familiar with U.S. chemical laser research, this report describes Soviet work on (1) kinetics of chemical reactions, (2) photodissociation lasers, (3) photorecombination lasers, (4) beam pumped lasers, and (5) controlled chemical reactions. The principal laser researchers continue to ignore the practical problems of optics and of beam propagation in the atmosphere, while the many studies of atmospheric propagation nowhere mention chemical lasers. Although steady progress is evident, work remains heavily theoretical, with no evidence of the keenly competitive pace found in the U.S.

11. KEY WORDS

Chemistry
Lasers
USSR--Science
Bibliography

ARPA ORDER NO.: 189-1

R-921/1-ARPA
November 1971

Soviet Chemical Laser Research

Yuri Ksander

A Report prepared for

ADVANCED RESEARCH PROJECTS AGENCY

Rand
SANTA MONICA, CA. 90406

Bibliographies of Selected Rand Publications

Rand maintains a number of special subject bibliographies containing abstracts of Rand publications in fields of wide current interest. The following bibliographies are available upon request:

Aerodynamics • Arms Control • Civil Defense
Communication Satellites • Communication Systems
Communist China • Computer Simulation • Computing Technology
Decisionmaking • Game Theory • Maintenance
Middle East • Policy Sciences • Program Budgeting
SIMSCRIPT and Its Applications • Southeast Asia
Space Technology and Planning • Statistics • Systems Analysis
USSR/East Europe • Weapon Systems Acquisition
Weather Forecasting and Control

To obtain copies of these bibliographies, and to receive information on how to obtain copies of individual publications, write to: Communications Department, Rand, 1700 Main Street, Santa Monica, California 90406.

Published by The Rand Corporation

PREFACE

This report has been prepared in the course of a continuing Rand study of Soviet high-power lasers sponsored by the Advanced Research Projects Agency. It is the second in the series, outlining Soviet work on chemical lasers as reflected in the open-source literature and covering -- with some exceptions -- the period from January through October 1971. The first report [1] reviewed the Soviet work published during the 1963-1970 period. In addition to this, an edited translation of a review article by Basov et al. [2] containing a list of known chemical lasers, as of August 1, 1970, was prepared within the scope of this study.

The present report begins with a brief summary of the highlights of the current Soviet chemical laser research. A list of facilities which support the work in this area, featuring the group leaders, is given. An assessment is made of certain factors which appear to affect the present Soviet programs.

The main body of the report consists of five sections, each section discussing the theoretical and/or experimental data on a specific aspect of chemical lasers such as vibrational kinetics, reaction rate control, etc. These sections were written for chemical laser specialists with a high degree of familiarity with the counterpart work in the United States; references to U.S. work are made only in those instances where they help to elucidate the Soviet work or where they serve as a point of reference.

The report concludes with a list of major Soviet publications with their abbreviations. An author index follows the complete list of references.

SUMMARY

At year end, 1971, the Soviet chemical laser literature continues to hold to an upward course compared with the 1969-1970 period. The basic structure of institutional effort in this area remains virtually unchanged since the publication of the first report in this series [1]. The original five research groups increased to seven. The additional groups are Prokhorov's at the Lebedev Institute, in which N. V. Karlov is the *de facto* leader, and Letokhov's at the newly formed Institute of Spectroscopy of which Letokhov is vice-director. The group leaders, their affiliations, and the number of contributing authors at each Institute ( )[≠] are as follows:

1. N. G. Basov
2. A. M. Prokhorov

} Lebedev Institute (43);

3. V. L. Tal'roze, Chemical Physics Institute, AN SSSR (25);
4. G. G. Dolgov-Savel'yev, Institute of Nuclear Physics, Siberian Branch AN SSSR (7);
5. S. I. Pekar, Institute of Semiconductors, AN UkrSSR (2);
6. R. V. Khokhlov, Moscow State University (16); and,
7. V. S. Letokhov, Institute of Spectroscopy, AN SSSR (2).

In terms of the publishing activity in chemical lasers, the keenest pace exists among researchers from the Lebedev Institute, historically the prime center of all laser studies in the USSR. The Lebedev Institute researchers are credited with ~50% of all the Soviet articles in this report. Highly conspicuous is the near total absence of papers from Khokhlov's group during 1971. It is conceivable that scientists in this group are currently addressing themselves to those problems in which the information is being withheld from the open-source literature.

[≠] It should be emphasized that these numbers are based only on the published literature (1963-1971) and not on a direct knowledge of Soviet research itself. Consequently, the reported degree of activity can be credible only to the extent to which the frequency and relative importance of publications in chemical lasers can be considered to reflect the actual situation.

The Soviet researchers continue to dwell heavily on the studies of reaction kinetics. In fact, these studies which are mostly theoretical constitute the bulk of their overall program and are consciously undertaken in an effort to optimize the existing chemical lasers and/or to design new ones. Particularly noteworthy among these are Tal'roze's rate measurements of the HF-producing reaction and his studies of vibrational energy transfer in HF(DF) + CO_2 mixtures.

Interest in the transfer chemical lasers is certainly gaining momentum in the USSR. Among the recent significant advances in this area is the development by Basov of their first purely chemical cw DF + CO_2 laser.[≠] This device -- which is largely patterned after Cool's -- was operated by the mixing of DF and CO_2 in a subsonic longitudinal flow and produced a steady maximum power output of ~2w. There are indications that Basov is interested in scaling of the chemical lasers to higher power outputs. This implies that transverse flow devices in the 1 kw range with subsonic or supersonic mixing may well be under development at the Lebedev Institute.

Dolgov-Savel'yev's experiments with the second-harmonic initiation of HF mixtures is highly significant as it appears to open up new possibilities for studying chemical reactions occurring during very short times (10^{-7} sec and less). In particular, it is hoped that using such short pumping pulses will help solve the question concerning the role of chain branching in the production of population inversion. So far, the only argument for branching appears to hinge on the weak dependence of power on the pump intensity.

Nearly all of the Soviet work on the reaction rate control merits a mention. Particularly useful are the Gordeyets studies on the nonresonant vibrational energy transfer which also indicate attainment of rapid dissociation rates under non-equilibrium conditions by way of

---

[≠]According to Chester, "true chemical laser" is a better term than "pure chemical laser" since "true" provides for lasers with sparkplug ignition which "pure" excludes (Laser Focus, November 1971, p. 26).

manipulating the gas temperature and the vibrational energy content. In the same area, Letokhov's and Karlov's experiments with the two-step photodissociation of HCl and CF_3I (proposed) molecules should be heavily underscored. Equally significant are the independent experiments of Basov and Karlov on the effect of 10.6μ CO_2 laser radiation on a number of gaseous systems such as BCl_3 - CO_2, N_2F_4 - NO, N_2F_4 - NO - N_2, N_2F_4 - NO - CF_4, SF_6 - NO, SiH_4 - BCl_3, SiH_4 - SF_6, etc. These experiments confirm the possibility of controllable chemical reactions.

Research in the electron-beam-pumping of molecular mixtures as a means of uniform volumetric initiation of gases is rapidly gaining momentum in the Soviet Union. The most recent advances in this area are due to Basov, who claims to have obtained 200j/liter energy densities from 1.2-Mev electron-beam-pumped CO_2 kept at 16--20 atm pressure, with an overall efficiency of 20% at 10.6μ. Similar experiments with high-pressure xenon resulted in ~50% efficiency at 1672Å. Beam-pumped liquid He and Ne are being considered at the Lebedev Institute as potential vacuum uv laser candidates at wavelengths down to 600Å.

Pekar's work on the photorecombination laser is continuing steadily and concerns in the most part the kinetics of addition and substitution reactions. In Pekar's laboratory, Kochelap is advocating the use of thermal methods for increasing the concentration of active molecules necessary to achieve a chemical reaction. Kochelap and Pekar have proposed a simple quasi-thermodynamic method of calculating laser gain and for establishing the population inversion criteria.

Soviet researchers are steadily pursuing photodissociation laser studies. A Q-switched CF_3I photodissociation laser was used by Andreyeva for studying the reaction kinetics of atomic iodine. A repetitively pulsed IBr, capable of delivering 1 kw (peak) 5-μsec pulses at 6--7 pps, was developed by Dudkin.

Topics in two areas which heavily involve the chemical laser -- optics and beam propagation in the atmosphere -- are not discussed in this report. Scarcity of materials in one area and overabundance and occasional irrelevance in the other, are responsible for the intentional omission of these from the present report. In the case of optics, only a few significant studies concerned with mirrors, windows, and mode control were retrieved, indicating a disappointing low-profile research throughout the community working in support of the chemical laser programs.

In the second case -- beam propagation in the atmosphere -- a large number of materials was retrieved, the majority dating back to the mid-'60s. A close examination of these revealed that atmospheric studies -- heavily dominated by highly formal theoretical analyses -- are concentrated in at least six major institutions:

1. Institute of Physics of the Atmosphere, AN SSSR (V. I. Tatarskiy);
2. Institute of Physics, AN BSSR (A. P. Ivanov);
3. Siberian Scientific-Research Physico-Technological Institute at Tomsk University (V. Ye. Zuyev);
4. Lebedev Institute of Physics, AN SSSR (F. V. Bunkin);
5. State Geophysical Observatory; and,
6. Central Aerological Observatory.

Works by principal chemical laser researchers (Tal'roze, Orayevskiy, et al.) continue to show a flagrant disregard for a substantive treatment of the propagation problems. Conversely, chemical lasers as such are nowhere mentioned directly in the Soviet literature dealing with beam propagation in the atmosphere. The experimental field and chamber work appears to be handled with mostly sub-micron lasers, although theoretical models postulate non-chemical lasers in the range from 1 to 10 microns and up.

Evidently, some groups -- notably Basov's, Prokhorov's, and Tal'roze's -- are showing dramatic gains by Soviet standards. Others appear to be standing still. A close-up look at what is happening in specific groups pinpoints a rather spotty pattern of approach to the overall chemical laser problem. Yet, despite the fact that the results achieved in the last ten months (January through October) were a little less than sparkling, they generally give evidence of a steady progress with a prospect for sharper focusing on truly important problems in the near-term future.

The general impression gained from perusing the Soviet chemical laser literature is that U.S. and Soviet interests coincide at very many points, clash at few. Their people appear to be highly talented, albeit lack confidence and/or funding to press on and innovate. Frequently, their research appears to be heavily bogged down in theoretical analyses, while their eyes are turned to the West, eagerly awaiting experimental developments.

This prevailing Soviet attitude is a trap that stands in the way of real breakthroughs in chemical lasers, and a lack there of a keenly competitive pace -- such as the one in the United States -- can well be regarded as one reason for the technological gap in chemical lasers. In order to stimulate advancement -- without undue strain -- and to broaden their goals while responding to a rising demand for chemical laser devices, the Soviets will have to revise their programs and proceed with renewed strength and philosophy.

Above all, the traditional Soviet reticence to fully discuss results and their inter- and intramural xenophobia would have to go before real progress can be made and the technological gap narrowed or closed. As things stand at the present time, the diffusion of information within the Soviet scientific community is hampered by inordinate -- and occasionally deliberate -- publication delays and costs. Ironically, Soviet researchers seem to be able to obtain Western literature more readily than their own. This is possible through an efficient distribution network of translations of foreign journals. Problems in the laser research created by poor communication channels are further

complicated by highly dominant leadership of the system by Basov, whose motives for the advancement of a specific laser field are not always altruistic nor, for that matter, fully understood.

CONTENTS

CONTENTS (cont.)

FIGURES

FIGURES (cont.)

FIGURES (cont.)

FIGURES (cont.)

TABLES

I. KINETICS OF CHEMICAL REACTIONS

A. DIRECT ENERGY TRANSFER

1. HF/DF Laser

When he first looked at the HF spectra, Basov reported that laser emission from HF originates from very high (6th and lower) vibrational levels [1]. The greatest number of transitions was claimed to be occurring between the 2 → 1 and 5 → 4 bands. The failure to observe HF 1 → 0 transitions was partly blamed by Basov on deexcitation by means of the nonresonant v-v energy transfer process.

In an unpublished article [3], Basov reiterates in more detail his findings on HF spectra and he supplements these findings with some additional data concerning HF mixtures as well as more recent experiences with DF molecules.

The HF/DF experiments were performed using Gross' setup (J. Chem. Phys., 48, 3821, 1968) and the reaction was initiated by 0.25-j 1-μsec electric pulses with the repetition rate of 1 pulse per 10 sec. The flow rate was 300 mtorr.ℓ.sec^{-1}. The resonator consisted of a 3-m radius mirror and a plane Au-coated mirror, spaced 120 cm apart. The laser power was extracted through a d = 0.5 mm hole in the plane mirror. The 2.6 --5.1 μ emission was detected with Au-doped Ge photoresistors operating at 77°K. The spectra were obtained with a LiF prism monochromator.

The more recent results show that the emission spectra of excited HF molecules include the P-branch transitions of the 1-0 and 6-5 bands and the DF spectra exhibit transitions in the 1-0 and 9-8 bands. These are shown in Fig. 1.

The pulse duration for the HF and DF molecules ranges from 2 to 35 μsec and from 2 to 45 μsec, respectively. The authors regard the presence of $P_{1-0}(9)$ HF transition -- occurring with a rather high 18 μsec delay -- significant and they speculate that this transition is excited by the $P_{2-1}(8)$ laser transition. The analysis of the energy distribution shows that the emission energy maximum in each vibrational band occurs at close values of J, viz., P(6)-P(8) for HF

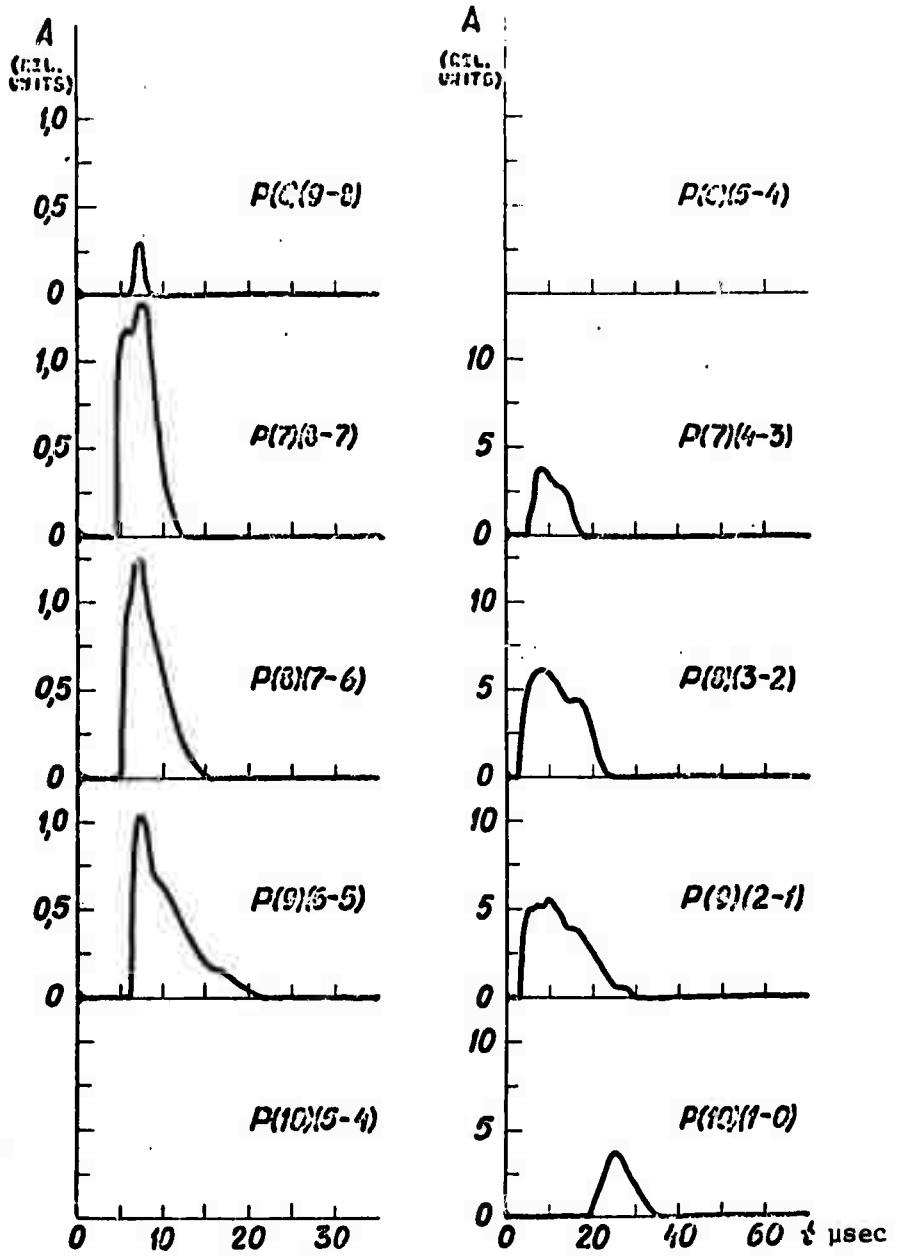

Fig. 1

Stimulated emission pulses on different transitions of (a) HF and (b) DF molecules excited in the process of $H_2(D_2) + F_2 \rightarrow HF(DF)$ reaction.

and P(7) for DF. The authors explain this effect in terms of a fast thermalization of the rotational levels of HF/DF molecules.

The relative distribution of the vibrational HF/DF is shown in Fig. 2.

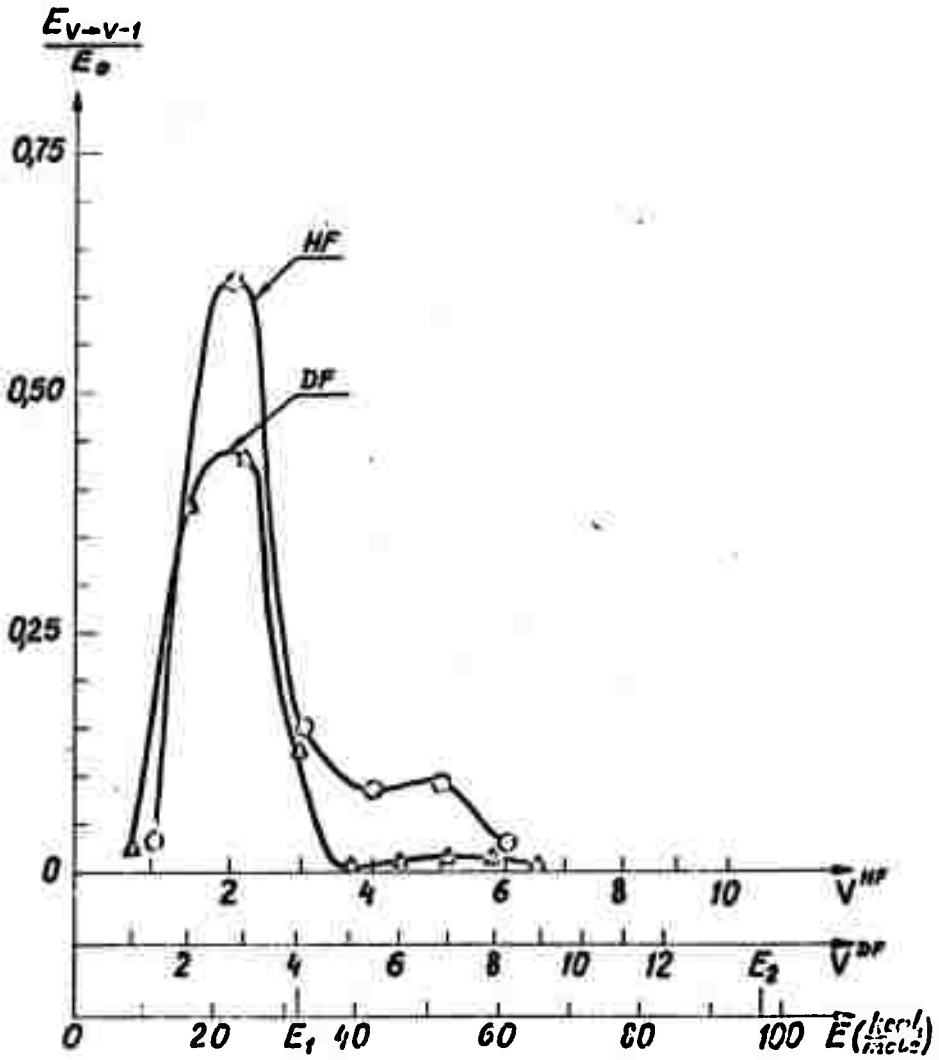

Fig. 2

Relative distribution of different bands of HF and DF molecules.

The curves are normalized, and the lower abscissa indicates energy in kcal/mole, where E_1 and E_2 (32 and 97 kcal/mole, respectively) are the maximum values of energy released in the respective $F + H_2$ and $H + F_2$ reactions. Energy values in the upper vibrational levels are denoted by the two other scales. The two-maximum structure of the curves clearly reflects the complex mechanism of the chemical reaction in which the population inversion is produced by two reactions with different exothermicities.

The most recent advancement in the laboratory of Dolgov-Savel'yev is the use of the second harmonic of the ruby laser to produce photolysis of $H_2 + F_2$ mixture [4]. This is an important development as the use of short laser pulses on the order of 10^{-8} sec opens up new possibilities of studying rapid chemical reactions occurring during times of 10^{-7} sec and less. This technique was used to analyze the initial stage of the laser pulse which is dominated by the reaction $F + H_2 \rightarrow HF(v=2) + H$.

Two sets of experiments were performed: experiments in which the reaction was initiated by flash photolysis using IFP-20000 flash lamps and by the second harmonic of a Q-switched ruby laser.

a. Photolytic Excitation

The experimental setup used in this experiment was similar to the one described in [1]. The duration of the pumping pulse was somewhat shorter (3 μsec at halfwidth). The spectral resolution was done by means of IKM-1 monochromator with a 200 lines/mm diffraction grating. The spectral width of the slit was 2 cm^{-1}. The radiation detector was a GeAu crystal at a liquid nitrogen temperature. The total pressure of the $H_2 + F_2$ mixture was 24 torr.

Figure 3 shows the pumping pulse and the spectrally unresolved laser pulse. In Fig. 4b and 4c, the typical emission oscillograms of individual transitions are shown: Table 1 shows the frequencies of the observed v-r transitions.

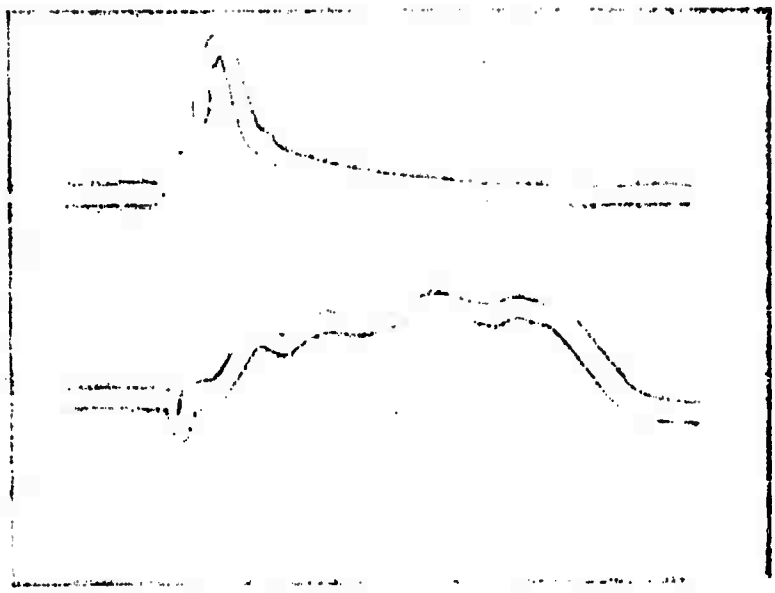

Fig. 3

Pumping (above) and laser (below) pulses. Total scan time 60 μsec.

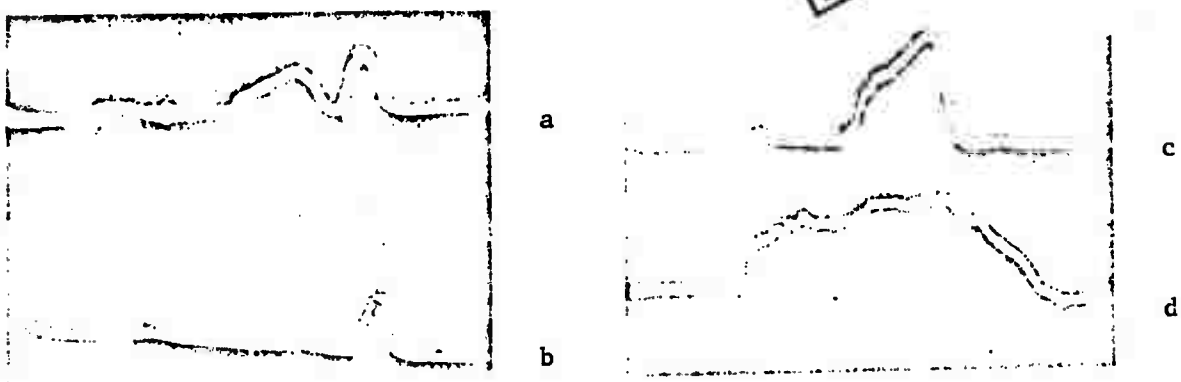

Fig. 4

Oscillograms of individual v-r transitions ($\tau_{pump} \approx 8$ μsec): a -- unresolved transitions $P_{3-2}(8)$ and $P_{2-1}(11)$; b -- $P_{2-1}(11)$; c -- $P_{3-2}(8)$; d -- total laser pulse. Total scan time 60 μsec.

Table 1

Experimental and calculated frequencies of v-r transitions

Transition	ν_{exp}, cm^{-1}	ν_{cal} cm^{-1}	Transition	ν_{exp}, cm^{-1}	ν_{cal} cm^{-1}
P_{2-1} (3)	3667	3666,39	P_{3-2} (5)	3416	3417,98
P_{2-1} (4)	3623	3622.61	P_{3-2} (6)	3375	3373,33
P_{2-1} (5)	3578	3577.53	P_{3-2} (7)	3327	3327.50
P_{2-1} (6)	3532	3531.21	P_{3-2} (8)	3281	3280,57
P_{2-1} (7)	3482	3483,09	P_{3-2} (9)	—	3232.57
P_{2-1} (8)	3435	3435.03	P_{3-2} (10)	—	3183,57
P_{2-1} (9)	3386	3385.29	P_{3-2} (11)	—	3133.62
P_{2-1} (10)	3335	3334.53	P_{3-2} (12)	3081	3082,77
P_{2-1} (11)	3283	3282.79	P_{4-3} (7)	3175	3175.22
P_{2-1} (12)	3231	3230,13	P_{4-3} (8)	3130	3129,94
P_{2-1} (13)	3177	3175.61	P_{5-4} (2)	3229	3227,63

Figure 5 shows the temporal variation of intensities of the tabulated transitions averaged over several oscillograms. A simple comparison of the oscillograms shows that the entire period of oscillation may be divided into three stages. The first stage, lasting 6 μsec, exhibits a rapid growth of laser pulse and a relatively rapid -- nearly exponential -- decrease in the intensity of individual transitions (shown as I in Fig. 5). The duration of an individual transition is 3-4 μsec. This period is associated with the initial excitation of reaction, as a result of which a large number of free fluorine atoms is formed which react with the hydrogen molecules, thus producing excited HF molecules. Subsequently, after the initiation, the system enters the second stage (II in Fig. 5), during which the reaction $H + F_2 \rightarrow HF^* + F$ begins to "work" (transitions $v(3 \rightarrow 2)$, $v(4 \rightarrow 3)$ and others begin to appear). The duration of individual transitions increases up to 20 μsec. During this time (6 -- 30 μsec from the onset of laser action), a large number of cascade transitions such as $P_{4-3}(7) \rightarrow P_{3-2}(8)$ is observed. The temperature of the mixture slowly increases during this stage. The third stage (III in Fig. 5) is characterized by a sharp rise in the rotational temperature. The duration of transition decreases to 5 μsec and the laser action is disrupted.

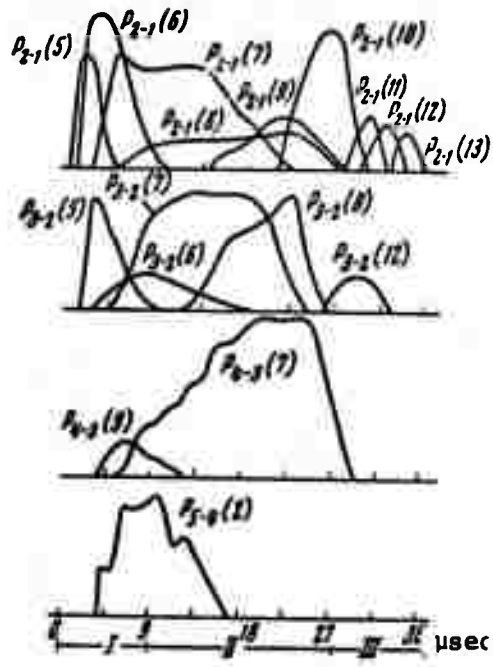

Fig. 5

Spectral resolution of laser pulse ($\tau_{pump} \approx 8\mu sec$)

b. Second Harmonic Excitation

The experiment with an HF mixture initiated by 25 nanosec pulses were carried out on a setup shown in Fig. 6. The pumping was due to the second harmonic of the ruby laser which operated in two regimes: (1) free running, with 10j and 250 μsec pulses, and (2) Q-switched 1j, and 25 nanosec pulses. The second harmonic was produced by KDP crystal and the use of f = 100 cm optics resulted in a 10% energy conversion of the ruby laser radiation. The fundamental frequency was isolated by a 5 mm thick UFS-6 filter and the second harmonic was coupled to the mixture by an aperture in one of the mirrors. The cell consisted of a copper tube 2 cm bore and 100 cm long with CaF_2 Brewster flats. The cell and the gas feeder tubes were cooled by liquid nitrogen vapor down to 100-150°K. The temperature control was by means of a copper-constantan thermocouple. At these temperatures, the mixture could be introduced without detonation at pressures up to 100 torr, and it did not contain undesirable fluorides. The input (λ = 3470Å) and output (λ = 3μ) energies

were measured by IEK-1 calorimeter. The spectral composition of the laser beam was measured by IKM-1 monochromator and a GeAu crystal at the liquid nitrogen temperature.

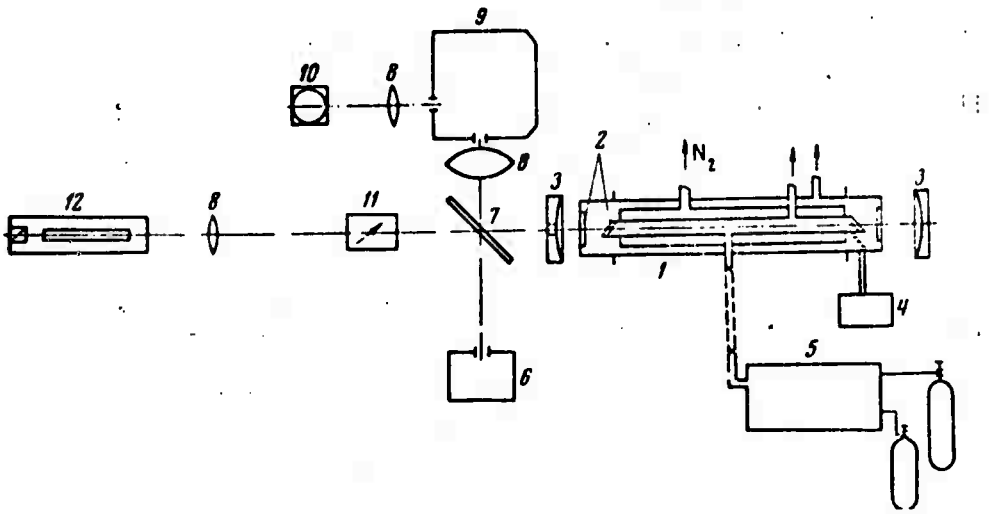

Fig. 6

Experimental ruby-laser setup: 1 -- liquid nitrogen cooled cell; 2 -- CaF_2 windows; 3 -- mirrors; 4 -- thermocouple; 5 -- gas supply system; 6 -- IEK-1 calorimeter; 7 -- plane-parallel plate; 8 -- optics; 9 -- IKM-1 monochromator; 10 -- GeAu detector; 11 -- KDP crystal; 12 -- ruby laser.

Normally, in the case of photolytically- and discharge-initiated reactions in a gas mixture, the measurement of the quantum yield encounters a number of difficulties associated with the measurement of the absorbed energy. In Dolgov-Savel'yev's experiment with the second harmonic ruby laser, the quantum yield appears to have been measured accurately. Experiments were carried out for the total mixture pressure of 40 torr ($P_{H_2} = P_{F_2}$) at T = 100°K. The coefficient of absorption of fluorine at λ = 3470Å was $1.31 \times 10^{-4} cm^{-1}/torr$. The energy absorbed in the mixture was W_{ab} = 0.005 j and the laser energy was W_l = 0.1j. Thus, the ratio $W_l/W_{ab} = 20$, and the laser quantum yield was $W_l\lambda_l/W_{ab}\lambda_{ab} = 108$.

It should be pointed out that the quantum yield determined in this manner depends on the conditions of the experiment and characterizes "chemical quality" of the system or the number of

reaction acts which lead to the production of population inversion under given experimental conditions. As was the case in Dolgov-Savel'yev's preceding work, the laser pulse duration was much greater than the pumping pulse and was equal to ~10μsec. The energy, power, and duration of the laser pulse retain the same relationship with an increase in the $H_2 + F_2$ pressure to 100 torr.

Figure 7 shows the temporal dependence of v-r transitions $P_{2-1}(4)$ and $P_{2-1}(7)$. A substantial difference from the results described above (Fig. 5), is the simultaneous occurrence of these transitions, observed for all of tne v(2 → 1) transitions.

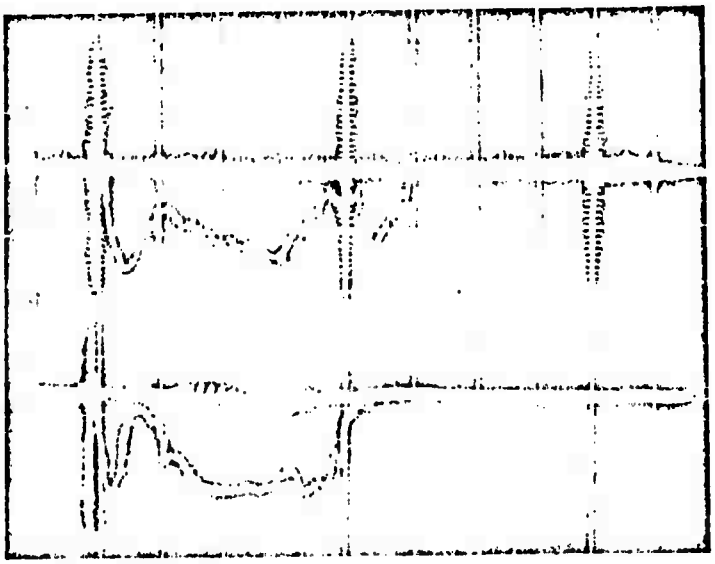

Fig. 7

Oscillograms of $P_{2-1}(7)$ (above) and $P_{2-1}(4)$ (below) transitions. Scan 0.5 μsec/div ($\tau_{pump} \simeq$ 25 nanosec).

c. Photolytic vs. Second Harmonic Excitation

The use of the second harmonic of a ruby laser in the fluorine photolysis experiments appears to open up new possibilities for studying chemical reactions occurring during very short times of 10^{-7} sec and less. It can be seen from Fig. 7 that the $P_{2-1}(4)$ and $P_{2-1}(7)$ transitions coincide to within approximately 0.02 μsec.

Since these transitions occur during times considerably shorter than the vibrational relaxation, the vibrational level distribution is determined by the mechanism of $F + H_2$ reaction. The temperature of the mixture at the onset of generation increases only by several degrees due to the energy evolved in the reaction. If the vibrational relaxation managed to occur in that time, $J_{max} \sim 1$ (i.e., in the laser spectrum the maximum power observed would be due to $P_{2-1}(2)$ transition). One could then safely say that during the $F + H_2$ reaction, all of the vibrational states are populated up to the J = 10 level. The strongest transition is from J = 7 level. This could be explained by the fact that during the photolysis, fluorine atoms are "hot" (0.5 ev) upon entering the reaction. The rate of population of v(1) level is slower than the rate of population of the v(2) level; $k_2/k_1 = 3.5$ (where k_1 and k_2 are the rate constants for the population of v(1) and v(2) levels, and $(k_2/k_1) \approx 2.6$ in the case under consideration). Consequently, at the onset of generation, total inversion occurs, thus causing a simultaneous onset of the laser action due to $v(2 \rightarrow 1)$ transitions. The leading laser peak (Fig. 7) is determined by the initial formation of active centers of atomic fluorine as a result of flash photolysis and its subsequent reaction with molecular hydrogen. The appearance of the second maximum or the onset of a quasi-steady-state regime (Fig. 7) are functions of the chain mechanism of formation of excited HF molecules (v = 2), since the reaction rate of the $H + F_2$ reaction is one order of magnitude smaller than the reaction rate of the $F + H_2$ reaction and the "subsequent portion" of HF(v = 2) molecules is formed at a lower effective rate. The observed processes can be fully explained by solving a system of kinetic equations in which allowance for the relaxation and field inside the cavity are taken into consideration.

A comparison of the spectral composition of the laser pulse with photolytic and second harmonic excitation shows distinct differences. As can be seen in Fig. 5, a number of transitions with different J values occur at different times, unlike in the case of a mixture excited by the second harmonic where they occur simultaneously. The first to occur are transitions with small J,

followed by transitions with J increasing from 5 to 13 for $v(2 \rightarrow 1)$ transitions. This is associated with the different relaxation processes which occur in the gas mixture. The dominant process among these is the rotational and vibrational-vibrational relaxation. Since the rotational relaxation occurs after several collisions, one may reliably expect that at mixture pressures of 20 torr, the distribution of molecules in the rotational level "follows" the mixture temperature (Fig. 5). From the data which the authors obtained, one can evaluate the changes in the rotational temperature of HF molecules with respect to time.

Figure 8 shows the calculated changes in the rotational temperature occurring in the course of generation for an 8 μsec pumping pulse. Toward the end of the process, the rotational temperature becomes comparable with the vibrational thus causing a rapid disruption of generation.

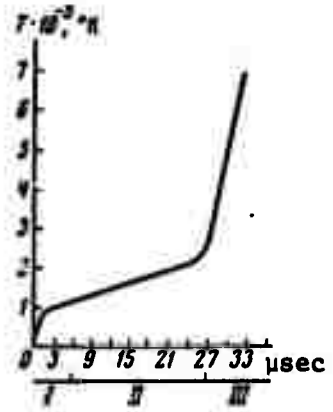

Fig. 8

Rotational temperature variation in the course of generation (see Fig. 5 for Roman numeral notation).

Figure 9 shows the total intensities of $\Sigma_J v_J(2 \rightarrow 1)$ transitions (curve 1) and the remaining transitions $\Sigma_J v_J(n+1 \rightarrow n)$ (curve 2). Time-wise, the sharp maximum in curve 1 coincides with the duration of the pumping pulse. The energy yield calculations

show that during that time, each fluorine atom produced ($F_2 + h\nu \rightarrow 2F$) enters the $F + H_2 \rightarrow HF(v = 2) + H$ reaction and gives rise to a stimulated photon. This confirms that the loss of free fluorine atoms in the volume is small and their effective lifetime is not less than 10 μsec.

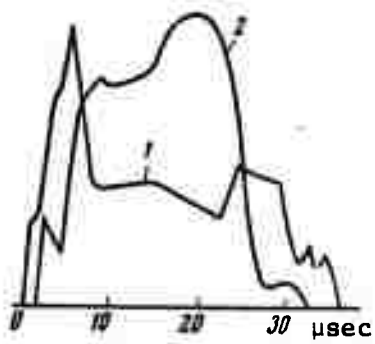

Fig. 9

Cumulative intensities of transitions shown in Fig. 5: 1 -- v-r band $v(2 \rightarrow 1)$; 2 -- v-r bands $v(3 \rightarrow 2) + v(4 \rightarrow 3) + v(5 \rightarrow 4)$.

Figures 5 and 9 indicate that both the reactions $H + F_2 \rightarrow HF^* + F$ and $F + H_2 \rightarrow HF^* + H$ are fairly effective for converting the chemical reaction energy into the stimulated radiation. $\Sigma_J v_J(2 \rightarrow 1)$ transitions contain 40% of the energy while the remaining ones ($\Sigma_J v_J(3 \rightarrow 2)$, $\Sigma_J v_J(4 \rightarrow 3)$ and $\Sigma_J v_J(5 \rightarrow 4)$) contain 30%, 22.3%, and ~7.7%, respectively.

2. HCl Laser

a. $H_2 + Cl_2$ Reaction Kinetics

A comprehensive study of the kinetics of a chemical laser based on $H_2 + Cl_2$ reaction was made by Igoshin and Orayevskiy [5]. The bulk of this study was presented at the Moscow Conference on Chemical Lasers in September 1969. The analysis proceeds from the simultaneous solution of chemical kinetics, vibrational relaxation, and laser field equations.

Chain Reaction Model. The mechanism of a photochemical branched reaction of hydrogen with chlorine in which vibrationally excited HCl molecules are formed can be described in the following form:

$$Cl_2 + h\nu \xrightarrow{ki} 2Cl \qquad \text{initiation} \qquad (1.1)$$

$$Cl + H_2 \xrightarrow{k_1} HCl(v=0) + H \qquad \text{chain stretching} \qquad (1.2)$$

$$H + Cl_2 \xrightarrow{k_2^{(n)}} HCl(v=n) + Cl \qquad \text{laser action} \qquad (1.3)$$

$$H + HCl(v=n) \xrightarrow{k_3^{(n)}} H_2 + Cl \qquad \text{inhibition} \qquad (1.4)$$

$$Cl + Cl + M \xrightarrow{kt} Cl_2 + M \qquad \text{chain termination} \qquad (1.5)$$

The values of reaction constants were borrowed from Western literature and are as follows: $k_1 = 8.3 \times 10^{13} \exp(-5480/RT)\,cm^3/mole.sec$; $k_2 = 4.1 \times 10^{14} \exp(-3000/RT)\,cm^3/mole.sec$; $k_3 = 5.9 \times 10^{13} \exp(-4500/RT)\,cm^3/mole.sec$; $k_t = 10^{15\text{-}16}\ cm^6/mole^2.sec$; $k_3^{(n)}$, where $n \geq 1$, was $5.9 \times 10^{13}\ cm^3/mole.sec$.

In addition to the rate of reaction (1.3), the authors made use of probability α_n of the reaction path along which HCl in the n-th vibrational state was formed. These were taken to be ($\sum_n \alpha_n = 1$):

$$\alpha_0 = 0,\ \alpha_1 = 0.134,\ \alpha_2 = 0.482,\ \alpha_3 = 0.362,\ \alpha_4 = 0.022,\ \alpha_5 = 0.$$

Vibrational Relaxation. The non-equilibrium distribution of vibrationally inverted HCl molecules ($v = 2 \rightarrow 1$) produced in the $H + Cl_2$ reaction, changes rapidly as a result of collisional energy exchange. At temperatures lower than the characteristic vibrational temperature ($T_c = 4140°K$), the basic process responsible for the relaxation of lower levels is energy transfer between vibrational degrees of freedom of the colliding partners.

$$HCl(v=m) + HCl(v=n) \underset{k_{m-1\,m}^{n+1\,n}}{\overset{k_{m\,m-1}^{n\,n+1}}{\rightleftharpoons}} HCl(v=m-1) + HCl(v=n+1). \qquad (1.6)$$

In view of the fact that in the elementary H + Cl_2 reaction v ≥ 4 levels are weakly populated, the authors limit this study "for the sake of simplicity" to the first four vibrational levels. The vibrational energy transfer in this case involves the following "reactions":

$$HCl(v=1) + HCl(v=1) \underset{k_{01}^{21}}{\overset{k_{10}^{12}}{\rightleftharpoons}} HCl(v=0) + HCl(v=2) \tag{1.7}$$

$$HCl(v=1) + HCl(v=2) \underset{k_{21}^{12}}{\overset{k_{10}^{23}}{\rightleftharpoons}} HCl(v=0) + HCl(v=3) \tag{1.8}$$

$$HCl(v=2) + HCl(v=2) \underset{k_{12}^{22}}{\overset{k_{21}^{23}}{\rightleftharpoons}} HCl(v=1) + HCl(v=3). \tag{1.9}$$

The reaction rate of the bimolecular processes (1.6) may be represented in the following form:

$$k_{mm-1}^{nn+1} = z_{nm} P_{mm-1}^{nn+1}, \tag{1.10}$$

where z_{nm} is the specific collisional frequency, P_{mm-1}^{nn+1} is the probability of vibrational transfer. As a result of calculations, the following expressions were obtained:

$$k_{10}^{12} = 2{,}3 \cdot 10^{13} T^{1/2} \exp\left(\frac{435}{T} - \frac{36}{T^{1/3}}\right) \quad \text{cm}^3/\text{mole.sec} \tag{1.11}$$

$$k_{01}^{21} = k_{10}^{12} \exp(-150/T)$$

$$k_{10}^{23} = 1{,}7 \cdot 10^{14} T^{1/2} \exp\left(\frac{510}{T} - \frac{57}{T^{1/3}}\right) \quad \text{cm}^3/\text{mole.sec} \tag{1.12}$$

$$k_{01}^{32} = k_{10}^{23} \exp(-300/T) \tag{1.13}$$

$$k_{21}^{23} = 7 \cdot 10^{13} T^{1/2} \exp\left(\frac{435}{T} - \frac{36}{T^{1/3}}\right) \quad \text{cm}^3/\text{mole.sec} \tag{1.14}$$

$$k_{12}^{32} = k_{21}^{23} \exp(-150/T). \tag{1.15}$$

Temperature Equations. In the nonstationary problems, the normal model is based not on the distribution of temperature of the mixture but on the existence of a certain average temperature. This leads to the following thermal equilibrium equation:

$$V\rho c_v (dT/dt) = W_+ - W_- \tag{1.16}$$

where V is the volume, ρ is the mixture concentration, c_v is the specific heat at constant volume, W_+ is the rate of heat release, W_- is the rate of heat transfer. Allowing for the translational and rotational degrees of freedom, c_v = 5 cal/mole. Neglecting the thermal effects of vibrational relaxation, recombination of atoms in triple collisions, and molecular dissociation, the rate of thermal emission can be written as follows:

$$W_+ = Vq_2k_2[\mathrm{H}][\mathrm{Cl}_2] + \sum_n Vq_3^{(n)}k_3^{(n)}[\mathrm{H}][\mathrm{HCl}(v=n)], \tag{1.17}$$

where q = 45 kcal/mole; $\sum_v \alpha_v E_v$ = 27 kcal/mole is that part of the heat of the reaction H + Cl_2 which is confined to the translational and vibrational degrees of freedom, E_v is the energy of the v-th vibrational level, $q_3^{(0)}$ = 1 kcal/mole, $q_3^{(n)} = q_3^{(0)} + 8.26n$ kcal/mole are the thermal effects of reaction H + HCl(v = n).

The rate of heat transfer is proportional to the mean difference in the temperature of the gas and the walls

$$W_- = \alpha S(T - T_0) \tag{1.18}$$

where T is the mixture temperature, T_0 is the wall temperature, S is a surface parameter, and α is the heat transfer coefficient.

Radiative Processes. The balance equations for populations N'_v and N_v and the number of photons $\rho_{vI}^{v'I'}$ in the resonator are as follows:

$$\begin{aligned}
\frac{dN_{v'}}{dt} &= -A_{v'v}N_{v'} - \frac{\sigma_{vI}^{v'I'}c}{V}\rho_{vI}^{v'I'}\Delta_{vI}^{v'I'} \\
\frac{dN_v}{dt} &= A_{v'v}N_{v'} + \frac{\sigma_{vI}^{v'I'}c}{V}\rho_{vI}^{v'I'}\Delta_{vI}^{v'I'} \\
\frac{d\rho_{vI}^{v'I'}}{dt} &= \frac{\sigma_{vI}^{v'I'}c}{V}\rho_{vI}^{v'I'}\Delta_{vI}^{v'I'} - \frac{\rho_{vI}^{v'I'}}{\tau_p} + \frac{\sigma_{vI}^{v'I'}c}{V}N_{v'I'}
\end{aligned} \tag{1.19}$$

where V is the resonator volume, c is the velocity of light, τ_p is the photon lifetime in the resonator, $\rho_{vI}^{v'I'} = \frac{c^2 A_{vI}^{v'I'}}{8\pi^2\nu^2} g(\nu)$ is the

cross-section of stimulated emission, $g(\nu)$ is the line form factor, $A_{vI}^{v'I'}$ are the Einstein coefficients for a given v-r transition, $\Delta_{vI}^{v'I'}$ is the population inversion for the v'I' → vI transition, $A_{v'v}$ are the Einstein coefficients for the forbidden v-r band.

Integration of Kinetic Equations. The integration of the system of kinetic equations was carried out numerically by means of the Runge-Kutta method on BESM-4 computer. The temporal dependence of the initiating radiation was taken in the following form:

$$k_i(t) = \gamma_1 t \cdot 10^{-\gamma_2 t}, \tag{1.20}$$

where γ_1 and γ_2 are given constants which determine the duration and intensity of the pumping pulse. The basic results of calculations are shown in Figs. 10-13.

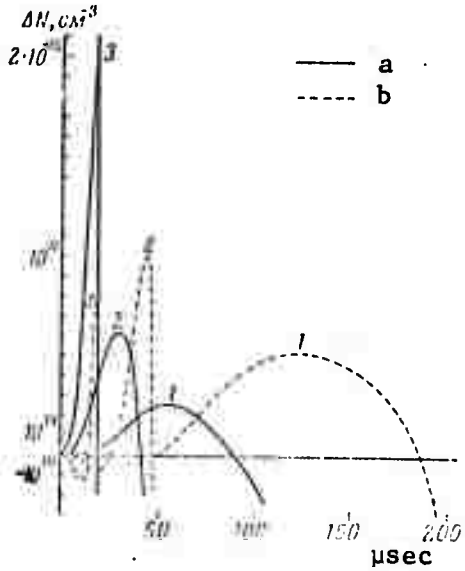

Fig. 10

Temporal variation of population inversion ΔN due to (a) v = 2 → 1 and (b) v = 3 → 2 transitions for $[Cl_2]:[H_2]$ = 1:1; T_o = 300°K, [M] = 2 x 10^{-6} mole.cm^{-3} (total concentration) for various photoinitiation rates k_i in sec^{-1}: 1 -- $k_i = 2 \times 10^7 \times t \times 10^{-2 \times 10^4 t}$; 2 -- $k_i = 2 \times 10^8 \times t \times 10^{-2 \times 10^4 t}$; 3 -- $k_i = 2 \times 10^9 \times t \times 10^{-2 \times 10^4 t}$.

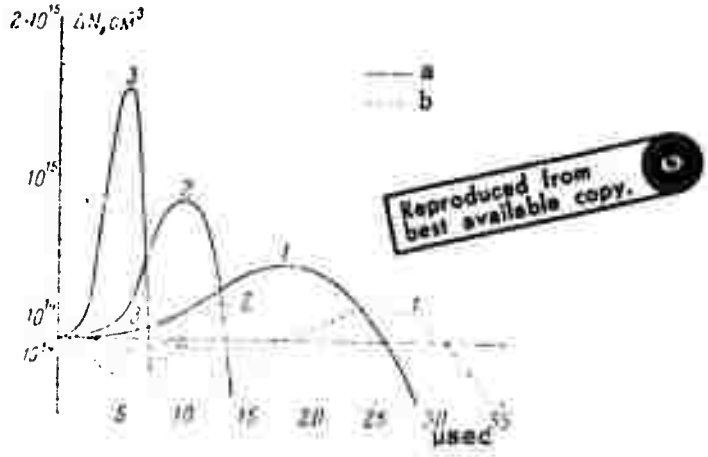

Fig. 11

The same as Fig. 10 except $[Cl_2]:[H_2]$ = 1:9; T_o = 600°K; [M] = 2 x 10^{-6} mole.cm^{-3}. Same photoinitiation rates as Fig. 10.

The equations were integrated for three values of initiating pulse intensities which correspond to 1, 10, and 63% decomposition of Cl_2 due to photodissociation. An increase in the gas temperature in a stage when inversion occurred ($T - T_o \approx 0.1T_o$) was small, although the mixture was heated to a rather high final temperature ($T - T_o \approx (2--20)T_o$). The maximum value of the inversion density increased with the rise in the intensity of initiating radiation and was of the order of 2 x (10^{14}--10^{15}) particles/cm^3. The characteristic feature of the solutions is the fact that the loss of inversion in the v = 2 → 1 transition due to vibrational relaxation is accompanied by an occurrence of inverted v = 3 → 2 states despite the fact that the formation of HCl (v = 2) is more probably in the elementary reaction H + Cl_2 than the formation of HCl (v = 3). This effect becomes less defined when the ratio of concentrations $[Cl_2]:[H_2]$ and the temperature increase. At the same time, an increase in the initial temperature of a mixture containing small amounts of Cl_2 and large amounts of H_2 creates more favorable conditions for the occurrence of v = 2 → 1 inversion, and this is particularly noticeable in the case of weak pumping. This can be seen clearly by comparing curves 1 in Figs. 10 and 11. In the second case, the initial concentration of Cl_2 is 1/5 that in the first case, although the maximum value of inversion had increased by 1.5--2-fold.

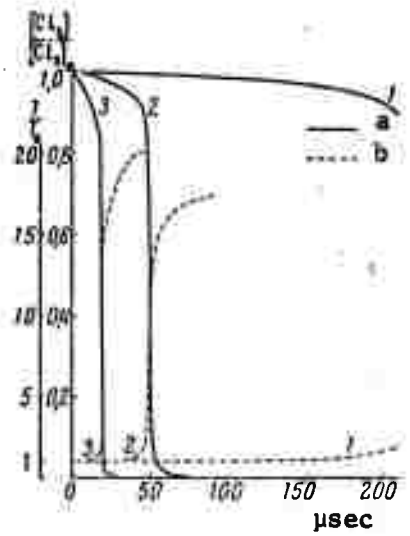

Fig. 12

Kinetics of Cl_2 flow rate (a) and the temperature rise (b) in the course of reaction for $[Cl_2]:[H_2] = 1:1$; $T_o = 300°K$; $[M] = 2 \times 10^{-6}$ mole.cm^{-3}. Same photoinitiation rates as Fig. 10.

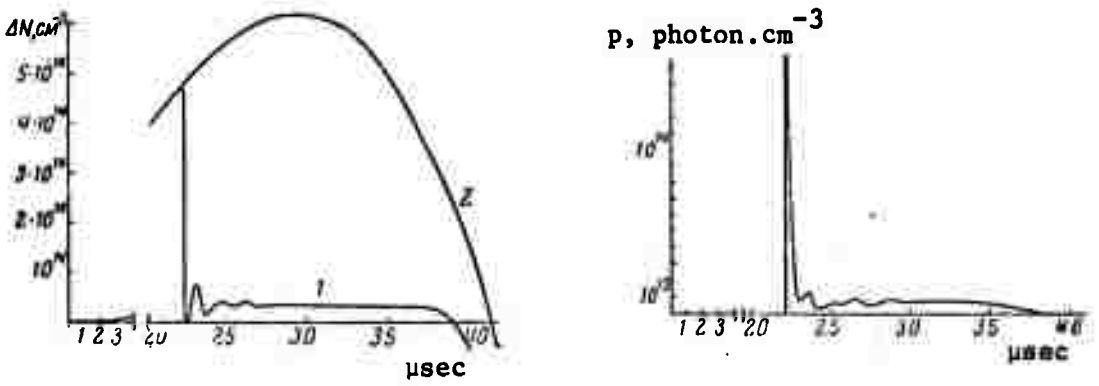

Fig. 13

Generation pulse due to $v = 2 \rightarrow 1$ transition (right) and temporal dependence of inversion ΔN in the presence (1) and absence (2) of laser radiation (left) obtained for the following parameters: $\tau_p = 1.5 \times 10^{-7}$ sec^{-1}; $\Delta\nu = 0.1$ cm^{-1}.atm^{-1}; $\nu = 2782$ cm^{-1}; $\Delta N_{thresh} = 3 \times 10^{13}$ cm^{-3}; $[Cl_2]:[H_2] = 1:1$; $T_o = 300°K$; $[M] = 2 \times 10^{-6}$ mole.cm^{-3}; $V = 300$ cm^3; $k_1 = 2 \times 10^8 \times t \times 10^{-2} \times 10^4 t$ sec^{-1}.

The solutions which describe the generation process due to $v = 2 \rightarrow 1$ transition are shown in Fig 13. The generation is accompanied by transient processes. For the purpose of comparison, Fig. 13 also shows the kinetics of inversion in the absence of generation.

The model under consideration produces laser radiation due to the $v = 3 \rightarrow 2$ transition which occurs with a short delay (on the order of 1 μsec) after the onset of $v = 2 \rightarrow 1$ transition. Moreover, the temporal dependence of $v = 3 \rightarrow 2$ and $v = 2 \rightarrow 1$ transition has a similar form. In the course of experiments, however, laser action due to $v = 3 \rightarrow 2$ transition did not occur with photochemical initiation. This disagreement may be due to the fact that the author's model was somewhat idealized.

The energy output per unit volume of the active substance under the above conditions was 10^{-4}--10^{-5} j/cm^3 and the pulse duration was 10--15 μsec.

Perhaps the most general conclusion which follows from Orayevskiy's calculations is that the population inversion is sustained only in the initial stage of the reaction for a very small depletion of the initial reagents. The instant of maximum inversion (curve 1 in Fig. 10)corresponds to 99.8% H_2 concentration with $[Cl_2]$ being 99.2% of the original concentration. Subsequent progress of reaction is accompanied by a rapid loss of inversion. Physically, this means that the relaxation rate due to HCl collisions begins to considerably exceed the rate of formation of active molecules. This inadvertently inhibits the energy output of the laser.

Another problem which the authors treat qualitatively in this study is the optimization of the temperature and composition of reagents. In the case of a large kinetic length of the chain and short excitation pulses, the number of molecules ν which contribute to the population inversion is given by the following expression:

$$\nu \sim \tau_1/\tau_2 \tag{1.21}$$

where τ_1 is the relaxation of the excited molecule and $\tau_2 = 1/k_1[H_2] + 1/k_2[Cl_2]$ is the average cycle time in the chain. For a given total

mixture concentration, the optimal composition can be found from the conditions of the maximum ν, $[H_2]:[Cl_2] = \sqrt{k_2/k_1}$. Under normal temperatures ($T \approx 300°K$), the optimal composition is $[H_2]:[Cl_2] = 20:1$ and for higher temperatures ($T \approx 3000°K$) it is 3:1. The temperature dependence $\nu(T)$ for the optimal composition is:

$$\nu(T) \sim \tau_1(T) \frac{k_1(T)k_2(T)}{(\sqrt{k_1(T)} + \sqrt{k_2(T)})^2} \qquad (1.22)$$

In the case of $v = 2 \rightarrow 1$ transition, $\tau_1^{-1} \sim k_{01}^{21}(T)$. Equation (1.22) predicts that in the case of $H_2 + Cl_2$ reaction the optimal thermal regime -- which is determined from the conditions of maximum ν -- lies in the range of high temperatures ($T = 2000$--$3000°K$). Although such temperatures can develop in the course of a chemical reaction, population inversion exists only in the initial stage characterized by a low heating up. This has led the authors to conclude that the role of the initial temperature in determining the temporal variation of inversion is exceedingly important.

The usefulness of the Igoshin-Orayevskiy study is limited insofar as their findings pertain to only the initial stage of the reaction, characterized by the v-v relaxation. No consideration was given to the processes of v-t energy transfer. Another serious limitation of the same study is its restriction to the four lower levels of HCl. Yet, despite these simplifications, the results of numerical calculations show that the model is a good facsimile of the $H_2 + Cl_2$ system; it clearly reflects the interrelation of the various kinetic factors and provides a satisfactory quantitative agreement with known experimental observations.

b. O + HCl Reaction Kinetics

Rate constants of the oxygen reaction with hydrochloric acid have not been measured until the recent publication of an experimental work by Balakhanin et al. [6]. The model reaction was $O + HCl \rightarrow OH + Cl$. The atomic oxygen -- produced by a discharge in Ar-doped O_2 -- was fed into the reactor through a nozzle. HCl was obtained from NaCl interacting with concentrated H_2SO_4 which was refined by the fractional distillation method. HCl was fed through an

automatic valve into a large bottle where a constant pressure was maintained. This resulted in a constant linear flow of HCl in the reactor which was measured as a time function of the pressure drop in the large bottle. Also measured was the volumetric rate of Ar kept at the same pressure as HCl. The volumetric rate of HCl was determined from the viscosity rate of Ar and HCl. Reaction time τ was varied by shifting the capillary with HCl along the heated reactor. The pressure was measured directly behind the reaction region. The experiments were conducted at 2 torr pressures in the 295-371°C temperature region. The linear flow velocity was varied correspondingly from 140 to 175 cm/sec. HCl partial pressure was varied from 0.05 torr to 0.1 torr, while [O] was maintained at concentrations always one order of magnitude smaller. The following reaction sequence was assumed:

$$1.\quad O + HCl \xrightarrow{k_1} OH + Cl$$

$$2.\quad O + OH \rightarrow H + O_2$$

$$3.\quad OH + HCl \rightarrow H_2O + Cl$$

$$4.\quad O \rightarrow \text{wall}$$

Large amounts of atomic chlorine were detected which would indicate that the elementary reaction proceeds as in step 1. Another possible reaction $O + HCl \rightarrow H + ClO$ was ruled out due to its high endothermicity (33 kcal/mole).

The experimental data showed that $\log \frac{[O]_{HCl=0}}{[O]_{HCl}}$ was proportional to [HCl] at all the temperatures. The question whether HCl contributes to the heterogeneous loss of O atoms was settled by a number of experiments carried out on an unprocessed quartz surface and also on surfaces processed by fluoric acid and potassium tetraborate. It was found that reaction 1 occurs in the volume and that HCl has a negligible effect on the loss of O atoms. The latter was further evidenced by the fact that when HCl was cut off, the atomic oxygen was instantly restored to a concentration which existed in the absence of HCl.

The final expression which the authors derived for k_1 is as follows:

$$\log \frac{[O]_{HCl=0}}{[O]_{HCl}} = \frac{3}{2} k_1 [HCl] \tau + \frac{3}{2} k_1 [HCl] \tau_1 - \frac{3}{2} \int_{\tau_1}^{\tau_p} k_1 [HCl] d\tau \qquad (1.23)$$

and Fig. 14 shows its solution as a function of l for various temperatures, where l is the length of the reaction region between two different upper positions at a constant flow v, $t = 1/v$ is the reaction time, and τ and τ_1 are, respectively, the times reagents spent in a constant temperature region between the lower and upper positions of the capillary, and the lower capillary position and the variable temperature region. The possibility of the reactions involving O atoms, such as

5. $O + O_2 + M \rightarrow O_3 + M$
6. $O + Cl_2 \rightarrow ClO + Cl$

was ruled out by the experimental findings. Reaction 6 would not give rise to the linear solutions shown in Fig. 14, since unlike [HCl], $[Cl_2]$ is a function of reaction time t. Reaction 5 fails to give rise to Eq. (1.23). The value of k_1 was obtained from the slope of the curves in Fig. 14 for known values of [HCl] and τ. The activation energy E_1 was calculated from Fig. 15 and was 4.5 kcal/mole.

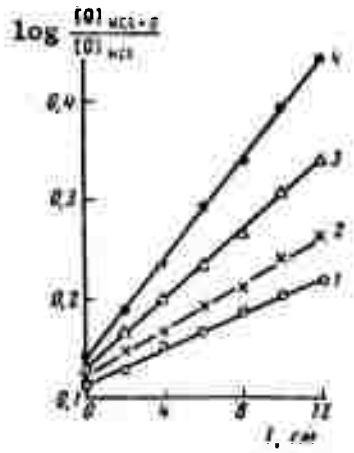

Fig. 14

Dependence of $\log \frac{[O]_{HCl=0}}{[O]_{HCl}}$ on l (P_{HCl} = 0.08 torr) for various temperatures; 1 -- 295; 2 -- 313; 3 -- 335; 4 -- 370°K.

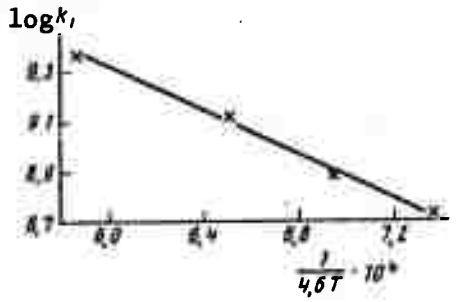

Fig. 15

Dependence of reaction rate k_1 on the temperature.

The expression for reaction rate k_1 can be written as follows:

$$k_1 = (1{,}05 \pm 0{,}35) \cdot 10^{12} \exp(-4500/RT)\ \text{cm}^3/\text{mole.sec} \qquad (1.24)$$

and its dependence on the temperature is shown in Fig. 15.

c. Photodissociation Waves

The photodissociation waves (PW) belong to that category of perturbations which propagate in a gas at supersonic velocities. The velocity of PWs -- determined by the flux density of pumping radiation (I_o) and the concentration of absorbing molecules [A_2] -- may exceed the velocity of an equivalent (with respect to the density jump) shock wave by several orders of magnitude.

A typical medium in which PWs will propagate is a binary gas mixture in which chemical chain reactions are possible. A detailed analysis of the kinetics of this process was made by Orayevskiy and Shcheglov, who also calculated the velocity and profile of a PW for the case of $H_2 + Cl_2$ gas mixture [7,8]. The equations for the wave profile and velocity uniquely and fully characterize the PW. The authors derived these from the system of equations for the radiative transfer and chemical kinetics. In the case of gases with equal component concentrations, the wave profile equations in the zero approximation (with respect to $\mu = \frac{k_1}{k_2} \ll 1$) are:

$$\left.\begin{aligned}
&\frac{\alpha-2}{\alpha} b_{20}^{-\alpha/2}\left\{\left(\frac{b_2}{b_{20}}\right)^{-\alpha/2} F\left(1, \frac{\alpha}{\alpha-2}; \frac{2(\alpha-1)}{\alpha-2}; b_2^{1-\alpha/2}\right) - \right.\\
&\qquad \left. - F\left(1, \frac{\alpha}{\alpha-2}; \frac{2(\alpha-1)}{\alpha-2}; b_{20}^{1-\alpha/2}\right)\right\} = \alpha\eta,\\
&i = \frac{I}{I_0} = \frac{\alpha b_{20}^{-1}}{2-\alpha}(b_2^{\alpha/2} - b_2),\\
&\qquad b = 0, \quad \eta \geqslant 0; \qquad (3.18)\\
&b_2 = b_{20} e^{b_{20}\eta}[2 - e^{b_{20}\eta}]^{-1}, \quad i = 1,\\
&b = \frac{I_0(1-D/c)}{(\beta_2^0)D} - b_2, \quad \eta \leqslant 0,
\end{aligned}\right\} \qquad (1.25)$$

where F is the hypergeometric Gaussian function; $\alpha = \sigma D/k_1(1-D/c) = 2y_o/\xi$, $b_{20} = y_o^{-1}(y_o \neq e)$ and $\alpha \neq 2$, and $\eta = 0$ corresponds to $b_2/u = 1$. The wave velocity is a transcendental equation

$$y = \xi^{\xi/2\xi - y)} \qquad (1.26)$$

and

$$D = D_o = cI_o/(I_o + cN_o) \qquad (1.27)$$

is the velocity of a normal PW. Equation (1.26) has two roots y_0 and $y_1 = \xi$; in the case of a standing wave, the solution obtains with one root only $y = y_0$ which is calculated numerically. In the limiting case, $\xi \to 0$ $y_0 \to 1$, i.e., a normal PW is generated. The analysis showed that taking into consideration chain reactions, leads to an increase in the velocity and to profile broadening of a PW. The numerical example of an $H_2 + Cl_2$ mixture yields the results below. For $\sigma_{Cl_2}(\lambda_{max} = 3300\text{Å}) = 2.6 \times 10^{-19}\text{cm}^{-2}$ at T = 300°K, $k_1 = 1.45 \times 10^{-13}\text{cm}^3/\text{sec}$ and $k_2 = 3.1 \times 10^{-11}\text{cm}^3/\text{sec}(k_1 << k_2)$; when $[Cl_2] = [H_2] = 2 \times 10^{18}\text{cm}^{-3}$ and $I_o = 10^{24}\text{cm}^{-2}\text{sec}^{-1}$, $\xi = 2.25$ and velocity $D \approx 1.2 \times 10^6$ cm/sec while the width of the wavefront at the e^{-1} level is $\Delta x \approx 3$cm.

In the foregoing analysis, the authors assumed implicitly that the chemical reactions proceed under isothermal conditions. In general, this holds for "cold" reactions only. On the other hand, "hot" reactions -- say $H + F_2 \to HF + F$ -- generate a thermal

effect which in principle may lead to the formation of a detonation wave with a considerable velocity ($v_d \leq 10^5$ cm/sec for $Q \leq 50$ kcal/mole). This velocity must be much smaller than the velocity of a PW (i.e., $D >> v_d$) in the presence of chemical reactions, a condition which is readily satisfied in a number of real cases.

In the case when the chain reaction rate substantially exceeds the photodissociation rate, the transcendental velocity equation can be replaced by an approximate analytical equation

$$y_0 \approx \sqrt{\xi}\left[1 - \frac{1}{2}\left(\frac{1}{\sqrt{\xi}} - \gamma\right)\log\left(\frac{1}{\sqrt{\xi}} - \gamma\right)\right] \tag{1.28}$$

for which

$$\gamma < \frac{1}{\sqrt{\xi}} \ll 1, \quad \left|\log\left(\frac{1}{\sqrt{\xi}} - \gamma\right)\right| \ll \sqrt{\xi}. \tag{1.29}$$

Equation (1.28) indicates that breaking of a chain reduces the propagation velocity of a PW. Similarly, if chain breaking occurs, the wave profile equations become

$$\left.\begin{aligned} 2\eta &= \int_{b_{20}}^{b_2} b_2^{-1}\left[\frac{\gamma}{1+\gamma} + C\left(\frac{b_2}{1+\gamma}\right)^{\alpha/2} - \frac{\alpha}{(2-\alpha)}\frac{b_2}{(1+\gamma)}\right]^{-1} db_2, \\ u &= \frac{\gamma}{1+\gamma} + C\left(\frac{b_2}{1+\gamma}\right)^{\alpha/2} - \frac{\alpha}{(2-\alpha)}\frac{b_2}{(1+\gamma)}, \quad b = 0, \quad \eta \geqslant 0; \\ b_2 &= b_{20}e^{b_{20}\eta}[2 - e^{b_{20}\eta}]^{-1}, \quad u = u_0, \quad b = u(1+\gamma) - b_2 - \gamma, \eta \leqslant 0. \end{aligned}\right\} \tag{1.30}$$

B. INDIRECT ENERGY TRANSFER

1. HF(DF) + CO_2 Laser

a. Nonflowing Mixtures

Although the $H_2 + F_2$ branched chain reaction is attractive for use in chemical lasers, it proceeds relatively slowly in comparison

with the duration of the laser pulse. The latter is limited by the deactivation of excited HF molecules by their "cold" HF sisters. In order to overcome this limitation and, yet, to retain the advantages of chain branching and the slow relaxation of the active components, Basov's group resolved to proceed with a $D_2 + F_2 + CO_2$ mixture in which population inversion is accomplished by transfer of excitation from "hot" DF molecules to "cold" CO_2 molecules. In August 1970, the group published a short paper [9] on that subject, based essentially on the earlier results of Gross (J. Chem. Phys., 50, 1889, 1969) and their own experience with $HN_3 + CO_2$ mixtures (see Ref. 19 in [1]). The chemical reaction was excited either optically or electrically in a quartz tube 110 cm long and 10 or 17 mm bore. Laser output from a D_2:F_2 mixture at 0.9 torr equal partial pressures is shown in Fig. 16.

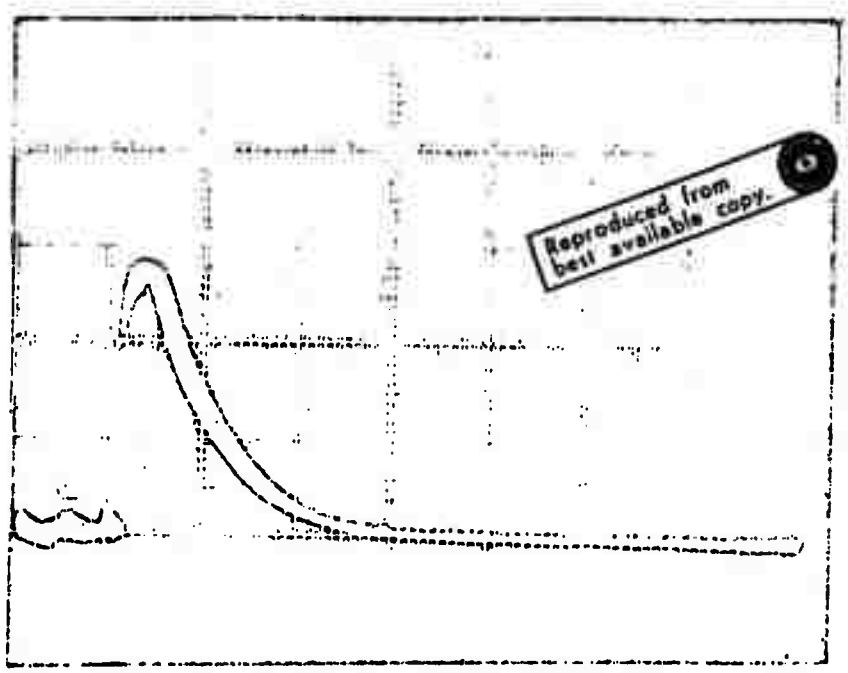

Fig. 16

Laser pulse from a D_2:F = 0.9:0.9 torr mixture at $\lambda \approx 4\mu$. Scan -- 2 μsec/div. origin shows electric trigger pulse (E = 0.25j, τ_{pump} = 1 μsec).

The addition to this mixture of 0.1-torr CO_2 diluent shortened the pulse by a half. At 0.3-torr CO_2 pressures, laser oscillation at $\lambda \approx 4\mu$ was disrupted, giving way to a 10.6μ signal. Subsequent increases in the CO_2 pressure resulted in an increased laser intensity which peaked out (depending on D_2:F_2 concentrations which were not given) at pressures in the 1-2 torr range. The excited CO_2 produced a 400 μsec pulse (Fig. 17), and the authors claim significantly higher (10-fold) per pulse energies than in the DF system without a diluent.

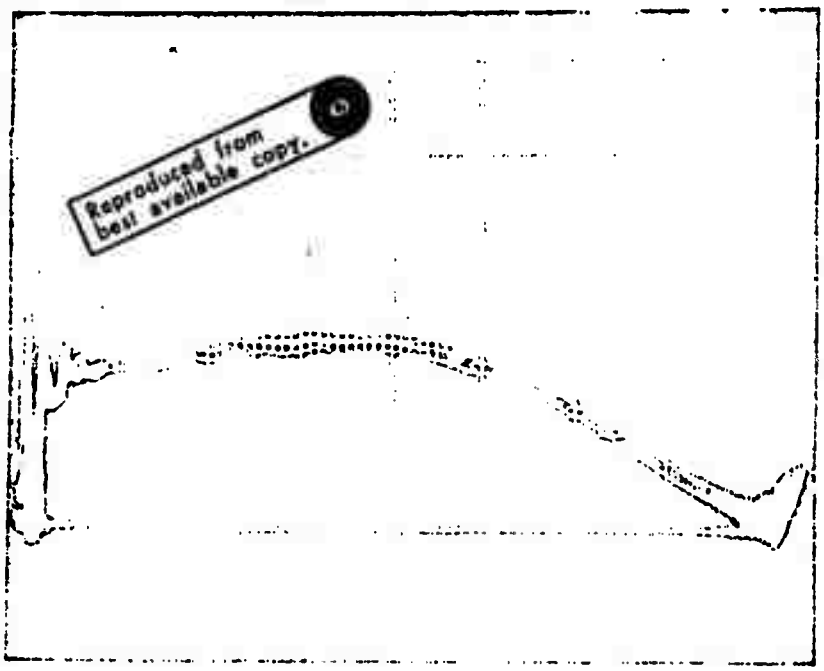

Fig. 17

Laser pulse from a D_2:F_2:CO_2 = 0.9:1.0:0.5 torr mixture at λ = 10.6μ. Scan -- 50 μsec/div.

In the same set of experiments, efforts were made to study energy transfer from vibrationally excited DF to CO_2, for the case of DF molecules obtained in the $NF_3 + D_2$ or $N_2F_4 + D_2$ reactions. Negative results were reported as a result of DF^* deactivation by the NF_2 and N_2F_3 radicals.

The spectroscopy of a nonflowing DF-CO_2 transfer laser at reagent and diluent pressures higher than those above, was carried out in [3]. A typical laser signal at 10.6μ is shown in Fig. 18.

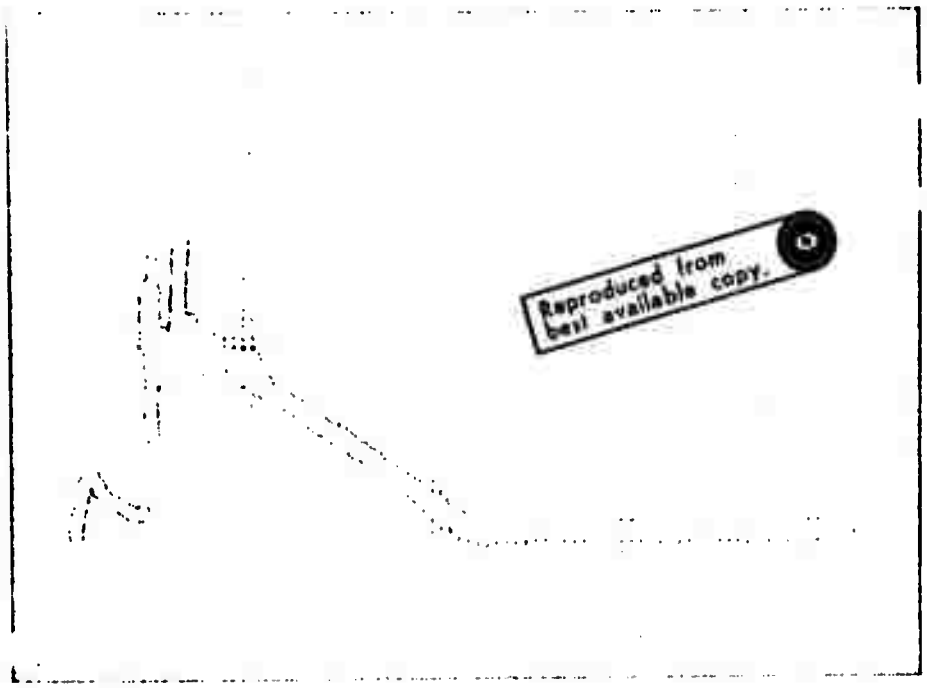

Fig. 18

Laser pulse from a D_2:F_2:CO_2 = 0.5:1.0:8.0 torr mixture at λ = 10.6μ. Scan -- 50 μsec/div. (E = 675j).

The signal has a steep front which is followed by intensity oscillations caused by transients. At fixed F_2 (1 torr) and D_2 (0.5 torr) pressures, laser pulse duration increased with CO_2 pressures from 100 μsec at P_{CO_2} = 3 torr to 190-200 μsec at P_{CO_2} = 8 torr. Subsequent increase in P_{CO_2} to 13 torr sharply reduced pulse duration to 30-40 μsec. Increasing F_2 pressures to 2 torr at a constant P_{D_2} = 0.5 torr, caused laser pulse duration to increase from 30 μsec at P_{CO_2} = 1 torr to 140-150 μsec at P_{CO_2} = 9 torr, and then decreased with increasing CO_2 pressures. The duration of the laser pulse appears to be comparable with the period of the chemical reaction. The decrease in the maximum laser pulse duration with F_2 content is attributable to an increasing reaction rate caused by larger concentrations of atomic fluorine occurring after the triggering.

The laser pulse energy depends largely on the initial reagent and diluent concentrations. The experimental dependence of laser energy on CO_2 pressure for the different mixture compositions (figure not available) shows a maximum; this is qualitatively explained by the dual role played by CO_2 in the chemical laser process. The rate of energy transfer from DF^* to CO_2 increases with increasing P_{CO_2}, resulting in an approximately linear increase of laser energy.

The rate of vibrational energy transfer from DF^* to CO_2 was evaluated by analyzing the measurements of laser pulse delay times with respect to trigger pulse. It was found that the delay time is almost independent of CO_2 pressure, and it is largely determined by F_2 and D_2 content in the mixture. At $P_{CO_2} \leq 3$ torr, the time delay was 24 and 16 μsec for a F_2:D_2 ratio of 1:0.5 and 2:0.5, respectively. The value of the reaction rate constant was found to be $(1.5 \pm 0.5) \times 10^{-12} cm^3 \cdot sec^{-1}$.

b. Subsonic Flow Mixtures

Some 16 months after Cool's introduction of a purely chemical cw DF-CO_2 laser (Appl. Phys. Lett., 16, 55, 1970), Basov announced the development of the first Soviet chemical laser of this type [10]. This device -- clearly identical to Cool's in nearly every design detail -- was operated by the mixing of DF and CO_2 in a subsonic longitudinal flow. The F atoms required to initiate the $F + D_2 \rightarrow DF^* + D$ (1) and $D + F_2 \rightarrow DF^* + F$ (2) chain reactions were directly produced from a reaction of $F_2 + NO \rightarrow ONF + F$ (3). The laser action in this device was due to the standard CO_2 00°1 → 10°0 transition at 10.6μ, produced as a result of $DF^* + CO_2$ (00°0) → CO_2 (00°1) + DF (4). The schematic diagram of the subsonic flow chemical laser with longitudinal optical axis is shown in Fig. 19.

Reaction (3) occurred in the $F_2 + NO_2$ + He flow over a 35 mm section of a sidearm copper tube before this combined flow was introduced into the upstream end of the main flow tube. The secondary mixture of $D_2 + CO_2$ was injected into the main tube a short distance downstream from the primary injection by means of a gas-mixing injector consisting of an array of orifices. Reactions (1), (2) and

(4) took place in the main coaxial Teflon tube of 150 mm length and 8 mm bore.

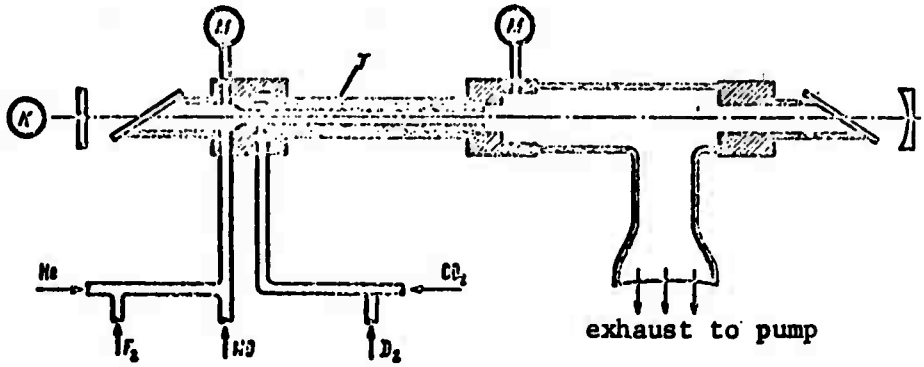

Fig. 19

Experimental setup.

Figure 20 shows the relative variations in purely chemical DF + CO_2 laser output caused by respective variations in each of the partial flow rates. The latter appear to be normalized by the optimum flow rate value for each gas.

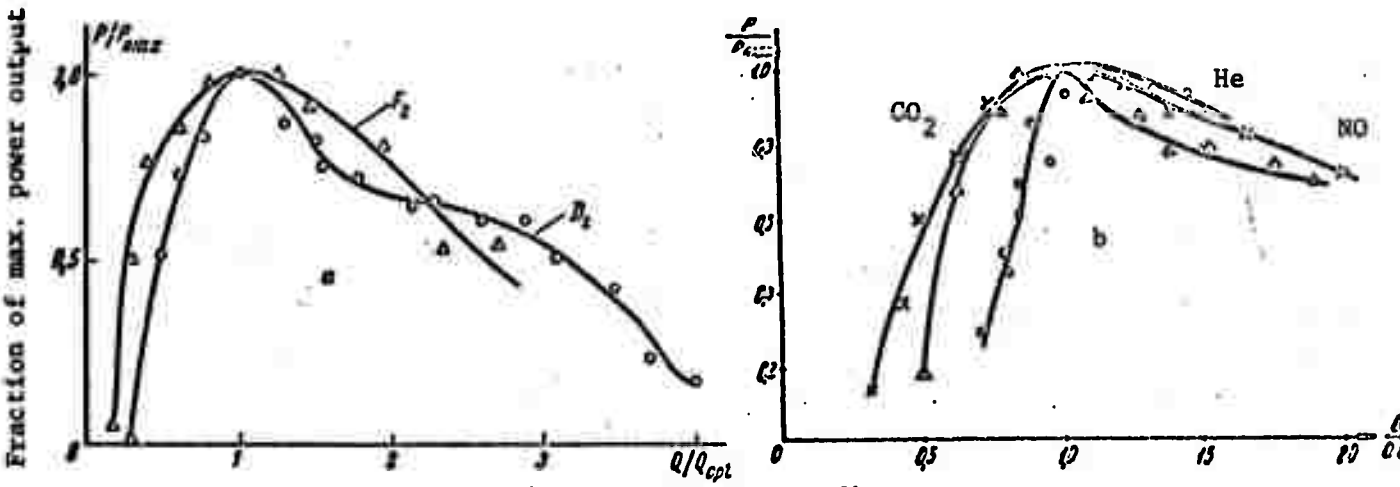

Ratio of flow rate to optimum flow rate

Fig. 20

Dependence of DF + CO_2 laser output on variations in partial flow rates.

A steady maximum power output of 2.1w was observed for the following optimum values of flow rates (in μmoles/sec):

NO	40
F_2	450
D_2	370
CO_2	1650
He	5070

With the flow rates at their optimum values, the pressure at the reaction tube inlet (upstream) was 15--20 torr. The mean flow velocity of the mixture in the Teflon tube was ~200 m/sec. The mixing rate in the experiments was regulated by varying the size of the injector orifices. In the case of d = 1 mm orifices, the pressure drop between the injected gases and the reaction volume was 10--15 torr and for d = 0.35 mm, it was 1 atm (assuming the same flow rates).

A conservative when it comes to disclosing details of his experimental apparatus or discussing the results, Basov nevertheless indicated that his group is interested in scaling of the chemical lasers to higher power outputs. This would imply going over to transverse-flow devices in the 1 kw range with subsonic or supersonic mixing, such as the HF/DF devices reported by the Aerospace Corporation and the United Aircraft groups during March-May 1970. Considering the source of this information, the development of such chemical lasers is undoubtedly well under way at the Lebedev Institute.

In addition to the experiments of Basov at the Lebedev Institute, Tal'roze at the Institute of Chemical Physics is studying processes of the transfer of vibrational energy from HF(DF) molecules to CO_2 molecules [11].

The experimental setup is shown in Fig. 21. Molecular hydrogen (or deuterium) enters discharge tube 4 and CO_2 and fluorine are admitted into reaction chamber 1 directly through calibrated openings with ~100μ diameter. A partial dissociation of $H_2(D_2)$ occurs in the discharge tube. The vibrationally excited HF(DF)

molecules are produced basically in the $H(D) + F_2 \rightarrow HF(DF)^* + F$ reaction. The heart of the experiment was the observation of the changes in the intensity of vibrationally excited HF(DF)(v = 1) molecules as a function of CO_2 concentration in the reactor for a constant $H_2(D_2)$ and F flow and a varying CO_2 flow. The gas flow was determined from the decrease in the pressure in fixed-volume containers and was as follows (in μmoles/sec): H_2 = 170--270, D_2 = 105--210, F_2 = 0.7--1.4, and CO_2 = 0--70. The partial pressures were correspondingly 0.5--0.8, 0.3--0.7, (2--4) x 10^{-3}, and 0--0.2 torr. An average time which the molecules spent in the optical cavity was 9 x 10^{-3} sec, and the temperature in the reactor was ~400°K.

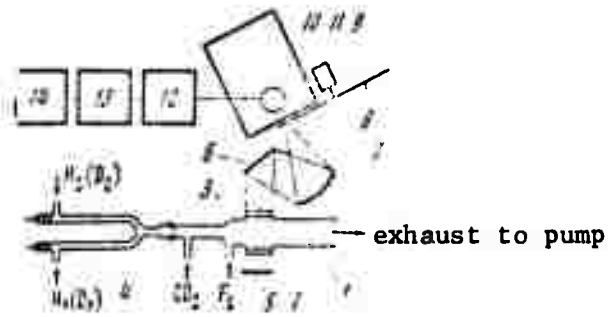

Fig. 21

Experimental setup. 1 -- reaction chamber;
2--optical cavity; 3 -- output windows;
4 -- discharge tube; 5 -- plane mirror;
6-7 --focusing mirrors; 8 -- modulator disc;
9 -- electric motor; 10 -- IKM-1 monochromator;
11 -- AuGe detector; 12 -- amplifier;
13 -- signal detector; 14 -- automatic recorder.

The following conditions were satisfied in the experiments: (1) the concentration of H(D) atoms in the flow was considerably greater than the concentration of F_2 molecules, and the rate of their decomposition was considerably smaller than the rate of their decomposition due to reaction; (2) the rate of vibrational energy transfer from HF(DF) to CO_2 and $H_2(D_2)$ was considerably greater than the rate of reverse processes.

Because of the present-day uncertainty with which the values of the deactivation rate of vibrationally excited HF(DF)

molecules are calculated, the experimental results were processed under the following two assumptions:

(1) the probability of v-v transfer between HF-HF and DF-DF molecules is high while the probabilities of the v-v transfers between HF-H_2 and DF-D_2 are low, and the characteristic time of formation of the excited HF(DF) molecules due to the reaction is considerably smaller than the time of their deactivation as a result of all the processes. Tal'roze claims that this assumption is well supported by the results of Kompa (J. Chem. Phys., 49, 4257, 1968) and a more recent unreferenced data obtained in Tal'roze's laboratory by Chaykin and Arutyunov.

(2) The characteristic time of v-v transfer between HF-H_2 and DF-D_2 molecules is shorter than the time of v-v transfer between HF-CO_2 and DF-CO_2 molecules and it is comparable to or smaller than the time required to produce HF(DF) molecules in the author's reactor. This assumption is supported by the recent experiments of Airey (Chem. Phys. Lett., 8, 23, 1971).

In support of assumption (1)

$$I_{HF,\,v=1} \sim \exp[-k_{HF,CO_2}[CO_2]t] \tag{1.31}$$

and in the case of assumption (2)

$$I_{HF,\,v=1} \sim \exp\left\{-\left[\frac{k_{H_2,HF}}{k_{HF,H_2}}\frac{[HF]}{[H_2]}k_{HF,CO_2} + k_{H_2,CO_2}\right][CO_2]\,t\right\} \tag{1.32}$$

where $I_{HF(v=1)}$ is the measured intensity of radiation of HF molecules; k is the transfer rate of vibrational energy (cm^3/sec.molecule); and [HF], [H_2], and [CO_2] are gas concentrations in the reactor.

Figure 22 shows the dependence of the logarithm of radiation intensity of HF molecules on the concentration of CO_2 and is based on the results of three experiments. The intensities were reduced to a single scale corresponding to the signal in the absence of CO_2 molecules. The experimental points appear to follow a straight line, the slope of which, when condition 1 is satisfied, yields the value of $k_{H,CO_2} = 1.8 \times 10^{-14} cm^3.sec^{-1}.mole^{-1}$, and in the case of condition 2 $k_{HF,CO_2} = 60(1.8 \times 10^{-14} - k_{H_2,CO_2})cm^3.sec^{-1}.mole^{-1}$.

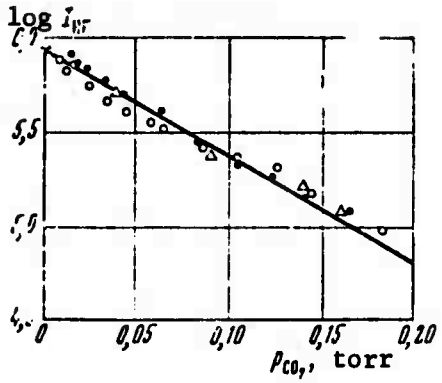

Fig. 22

Variation in the radiation intensity of HF molecules with CO_2 pressure for flow rates in μmoles/sec: ● -- H_2 = 270, F_2 = 1.24; o -- H_2 = 200, F_2 = 0.62; Δ -- H_2 = 170, F_2 = 0.72.

Figure 23 shows the dependence of the logarithm of radiation intensity of DF(v=1) molecules on the concentration of CO_2 in the reactor. From the slope of the line, it was found that when condition 1 was satisfied, $k_{DF,CO_2} = 3.3 \times 10^{-13}$ cm^3.sec^{-1}.molecule^{-1}, and in the case of condition 2, it was $k_{DF,CO_2} = 50 \times (3.3 \times 10^{-13} - k_{D_2,CO_2})$ cm^3 . sec^{-1} . molecule^{-1}. The experimentally determined value of $k_{H_2,CO_2} \ll 1.8 \times 10^{-14}$, i.e., it does not affect the value of k_{HF,CO_2} which is ~1.1 x 10^{-12} cm^3.sec^{-1}.molecule^{-1}. The value of k_{D_2,CO_2} has not yet been determined; if, however, it can be assumed that $k_{D_2,CO_2} \ll 3.3 \times 10^{-13}$, the ratio of $k_{DF,CO_2}/k_{HF,CO_2} \approx 20$ under the conditions of both slow and rapid v-v transfer.

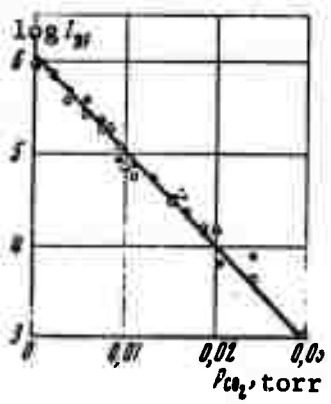

Fig. 23

Variation in the radiation intensity of DF molecules with CO_2 pressure for flow rates in μmoles/sec: ● -- D_2 = 210, F_2 = 1.34; o -- D_2 = 105, F_2 = 1.24; Δ -- D_2 = 185, F_2 = 0.97.

C. REACTION RATE MEASUREMENTS

1. Mass Spectroscopic Method

Highly exothermic reactions of hydrogen and fluorine are particularly interesting in those cases where the reaction proceeds along two or more "channels." The measurement of the absolute and relative values of rates for H and F reacting with CH_3I and CF_3I -- heretofore unavailable -- were recently compiled by Tal'roze et al. [12]. The following reactions were considered:

1. $H + CH_3J \xrightarrow{k_1}$	$\xrightarrow{1a} CH_4 + J^*$	$-\Delta H = 48{,}9$	kcal/mole
	$\xrightarrow{1b} {}^*CH_3 + HJ$	$-\Delta H = 18{,}6$	"
2. $H + CF_3J \xrightarrow{k_2}$	$\xrightarrow{2a} {}^*CF_2J + HF$	$-\Delta H = 13$	"
	$\xrightarrow{2b} CF_3H + {}^*J$	$-\Delta H = 46$	"
	$\xrightarrow{2c} {}^*CF_3 + HJ$	$-\Delta H = 20$	"
3. $F + CH_3J \xrightarrow{k_3}$	$\xrightarrow{3a} {}^*CH_2J + HF$	$-\Delta H = 85$	"
	$\xrightarrow{3b} CH_3F + {}^*J$	$-\Delta H = 68$	"
	$\xrightarrow{3c} {}^*CH_3 + JF$	$-\Delta H = 17$	"
4. $F + CF_3J \xrightarrow{k_4}$	$\xrightarrow{4a} CF_4 + {}^*J$	$-\Delta H = 54$	"
	$\xrightarrow{4b} {}^*CF_3 + JF$	$-\Delta H = 10$	"

Reactions 3a and 3b were the subject of Soviet investigations of methyl iodide fluorination by F_2, in the early '60s. Interest in I-producing reaction with exothermicities in excess of 22 kcal/mole is particularly valid in view of Polanyi's discovery of $^2P_{1/2}$ iodine (in the reaction H + HI = H_2 + I)[#] which offers a possible means for a chemical laser based on electronic transitions. For instance, Andreyeva et al. showed[##] some time ago that in a CF_3I photodissociation laser excited iodine is formed in the secondary reaction $CF_3 + CF_3(hot) = C_2F_6 + I^*$. The production of a stable product IF in these reactions

---

[#] J. Phys. Chem., 72, 3715 (1968).

[##] ZhETF P, Vol. 10, p. 423, 1969.

has not been discovered as yet, although its presence in certain other reactions has been established by optical- and mass-spectroscopy [12].

Tal'roze measurements were carried out by probing the diffusion cloud in a fast helium flow. The F and H atoms were produced by dissociation of F_2 and H_2 in an h-f discharge. He-diluted iodides were passed along a small capillary along the reactor axis to form the diffusion cloud. The purity of all the iodides was better than 99% and was checked by mass spectroscopy. The measurements were carried out at 293 $\pm$ 2°K and the reactor pressure of several torr at relative ~10% reagent concentrations in the carrier gas and ~0.01-0.1% for iodides, during reaction times of ~10^{-3}-10^{-4} sec. The reaction rate measurement was based on the depletion of iodides in the respective reactions, and the existence of reaction paths -- on the product composition.

- $H + CH_3I$. Measurements were made at 2.4 torr He pressure in the reaction region and at the following concentrations: $[H_2] = 3.3 \times 10^{15}$ molecules.cm^{-3}, $[H] = 2.8 \times 10^{15}$ atoms.cm^{-3}, $[CH_3I] \simeq 10^{12}$ molecules.cm^{-3}. The concentration distribution of methyl iodide along the reactor axis is shown in Fig. 24. The calculated rate of reaction was $k_1 = (4 \pm 1) \times 10^{-12}$cm^3/mole.sec.$^{\neq}$

Figure 24 shows changes in the line intensity of the mass spectrometer. The occurrence of HI and the absence of methane lines clearly signifies the predominence of reaction channel 1b, for which $k_{1b} = k_1$, with an accuracy better than 10%. At P = 1 atm, coefficient of diffusion of methyl iodide in He was $D = 0.31 \pm 0.05$ cm^2.sec^{-1}.

- $H + CF_3I$. This reaction was investigated under the same conditions as above. The overall reaction rate was not calculated, however, due to strong variations in [H] caused by instabilities in the capillary surface covered with stable reaction products. Line intensity changes (Fig. 25) point to predominance of channels 2a and 2c.

$^{\neq}$Using the formula derived by Tal'roze et al. [1], viz: $k = \frac{\beta}{[\overline{H}]}(v + D\beta)$ where β = slope, D = coefficient of diffusion of a molecular reagent in He, and v = linear flow rate along the axis.

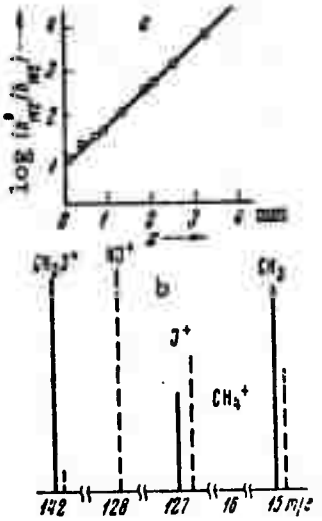

Fig. 24

(a) Concentration distribution of methyl iodide along reactor axis in reacting with H atoms and (b) changes in certain mass-spectral lines of reaction (1) reagents. Here and in Figs. 25-27, solid lines indicate conditions up to reaction, dotted lines -- during reaction.

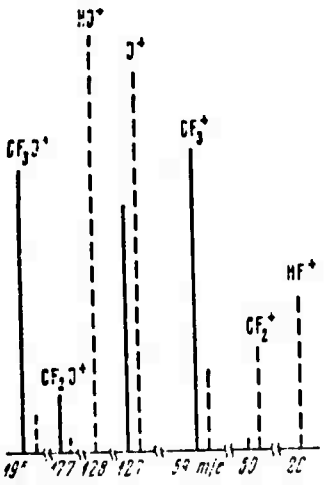

Fig. 25

Variation in certain basic mass-spectral lines of reaction (2) reagents.

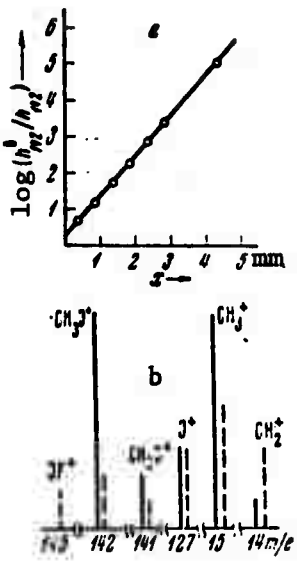

Fig. 26

(a) Concentration distribution of methyl iodide along reactor axis reacting with F atoms and (b) variation in certain basic mass-spectral lines of reaction (3) reagents.

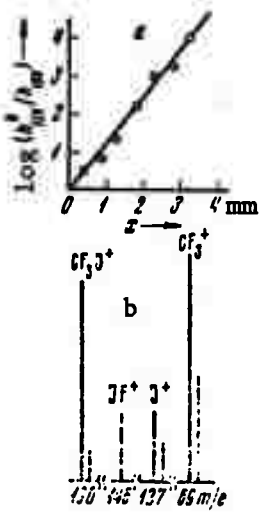

Fig. 27

(a) Concentration distribution of CF_3I along the reactor axis reacting with F atoms and (b) variation in certain basic mass-spectral lines of reaction (4) reagents.

- $F + CH_3I$. This reaction was investigated at a slightly higher pressure in the reaction region, 3.5 torr. The mixture composition in the capillary was as follows: $[F] = 1.3 \times 10^{14}$ atoms.cm^{-3}, $[CH_3I] \approx 10^{12}$ molecules.cm^{-3}. The methyl iodide concentration distribution is shown in Fig. 26a. The reaction rate was $k_3 = (2 \pm 0.7) \times 10^{-10}$ cm^3/mole.sec. Mass-spectrometry of reagent lines (Fig. 26b) favors channel 3c where IF is produced. The CH_3F^+ ion peak (m/e 34) fails to show up and this suggests that CH_3F molecules fail to form in the reaction, and, therefore, channel 3b can be excluded with only a ~30% loss of accuracy, whereupon $k_3 = k_{3a} + k_{3c} > k_{3b}$. The authors have failed to calculate k_{3a} and k_{3c}.

- $F + CF_3I$. This reaction was investigated under the same conditions as the preceding one. The reaction rate was found to be $k = (1.7 \pm 0.6) \times 10^{-10}$ cm^3/mole.sec and $D = 0.32 \pm 0.05$ cm^2.sec^{-1} at P = 1 atm. A rapid drop in the m/e 196 (CF_3I) peak and a reduction in half of the I^+ peak, coupled with the occurrence of a strong IF^+ peak, indicate preference for channel 4b.

The experimental data indicate that in all the reactions, the least dominant -- or totally absent -- path is the one in which atomic iodine is produced, supplying the greatest energy in the majority of cases. In all these cases, therefore, the choice of a reaction path is determined not by the thermal effect but by (1) the inability of an I-producing reaction to approach a molecule from a direction opposite to I and (2) the long-range effect of the electron shell of an I atom in the latter's perpendicular approach to the C-I bond. This also suggests the slowness of reactions involving alkali-iodides and polyatomic radicals in which iodine in the $^2P_{1/2}$ states is produced. If a more rapid path exists, the colliding partners will find it and follow it.

Tal'roze's recent paper [13] deals in much detail with mass-spectroscopic measurement of the $F + H_2$ reaction rate, using methods and procedures identical to those employed in [12].* The temperature and pressure in the reactor were 20°C and 3 torr, respectively, and the carrier gas (He) flow velocity in the reaction region was

*Tal'roze's paper [13] was the subject of brief presentations at the Moscow (chemical lasers) and Kyoto (mass spectroscopy) conferences in 1969.

1160 cm/sec. The mixture composition in the capillary was 30% H_2, 70% He, with H_2 flow rate being 1.1×10^{16} mole.sec^{-1}. The pre-discharge F_2 flow rate was 6×10^{13} mole·sec^{-1} and the reacting F concentrations were 3.8×10^{13} at.cm^{-3} and 5.2×10^{13} at.cm^{-3} with and without H_2 flow, respectively. Figure 28 shows H_2 concentrations along the capillary. The reaction rate was calculated from the equation given in [12] and β and D_{H_2} were assumed to be 0.85 and 350 cm^2/sec, respectively, yielding $k_1 = 3.3 \times 10^{-11}$ cm^3/mole.sec. The calculations of k_1, based on the number of H atoms produced was 2.7×10^{-11} cm^3/mole.sec. The computational error in k_1 is due to the fact that F concentrations in the reaction region can be considered constant to within 10-20% only. Within the overall error, the reaction rate at 293°K was $(3 \pm 1) \times 10^{-11}$ cm^3/mole.sec., i.e., a figure comparable to the one obtained for the same reaction earlier, viz., 1.65×10^{-11} cm^3/mole.sec.[≠]

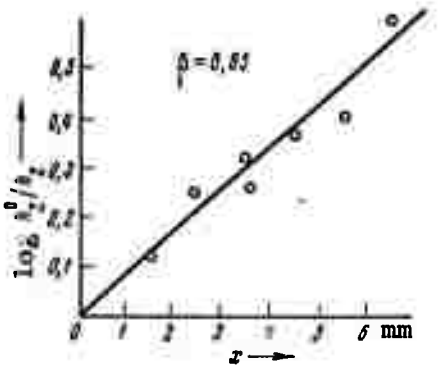

Fig. 28

Distribution of relative concentration of hydrogen along the diffusion cloud axis.

2. Quasi-Steady-State Concentration Method

Kapralova has analyzed kinetics of the following HF reactions at room temperature [14]:

1. $F + H_2 \rightarrow HF^* + H$
2. $H + F_2 \rightarrow HF^* + F$
3. $H_2^* + F_2 \rightarrow HF + F + H$
4. $H_2^* + M \rightarrow H_2 + M$

[≠] Kapralova, G. A., et al., KiK, Vol. 11, 1970, p. 811.

5. $H + O_2 + M \rightarrow HO_2 + M$
6. $HF^* + H_2 \rightarrow H_2^* + HF$

Using the method of quasi-steady-state concentrations of the initial species, she derived the following expression for the reaction rate

$$w = 2w_0 \frac{k_2[F_2]}{k_5[O_2][M]} + 2Sw_0 \frac{k_2^2 k_3 [F_2]^3}{k_5^2 [O_2]^2 [M]^2 \varphi} (e^{\varphi t} - 1), \qquad (1.33)$$

where $\phi = 14\ k_2 k_3 [F_2]^2 / k_5 [O_2][M] - k_4[M]$ and w_0 is the rate of chain production at pressures near the second explosion limit (see Table 2). Using expression (1.33), the experimental partial pressure data and some rate constants of the partial reactions from literature, Kapralova calculated the average rate constants k_3 (branching) and k_4 (H_2^* deactivation). These were, respectively, 2×10^{-20} $cm^3.sec^{-1}$ and 8×10^{-17} $cm^3.sec^{-1}$, and the ratio $k_3/k_4 = 2.5 \times 10^{-4}$ compares favorably with her earlier findings obtained by the explosion limit method (1.4×10^{-4}).[≠] The value of k_4 thus obtained indicates that the branching reaction occurs via the H_2^* molecules and not the HF^* molecules. The lifetimes of the H_2^* and HF^* molecules were found to be $\sim 10^{-1}$ and $\sim 10^{-3}$ sec, respectively.

Table 2

Initial Reagent Pressures and Rates of Chain Production at 300°K

pressure, torr					ϕ, sec^{-1}	$k_3 \times 10^{20}$ $cm^3.sec^{-1}$	$k_4 \times 10^{16}$ $cm^3.sec^{-1}$	$w_0 \times 10^{-6}$ $cm^{-3}.sec^{-1}$
Total	F_2	H_2	O_2	He				
11.7	0.94	0.39	0.15	10.20	7.4	3.9	1.4	6
10.0	0.80	0.33	0.13	8.73	13.7			
5.0	0.70	0.55	0.21	3.52	4.4	0.8	0.7	6
4.8	0.67	0.53	0.20	3.38	4.8			
4.2	0.59	0.46	0.18	2.96	5.2	0.5	0.3	150
3.6	0.50	0.39	0.15	2.50	5.8			
10.3	0.98	0.46	0.18	8.68	6.2	3.4	1.6	45
9.2	0.88	0.41	0.16	7.75	10.9			
11.7	0.94	0.39	0.15	10.20	6.2	1.3	0.4	105
9.8	0.79	0.33	0.13	8.56	7.6			

[≠] Kapralova, G. A., et al., KiK, Vol. 10, 1969, p. 32.

That H_2^* molecules dominate the HF reaction kinetics was further confirmed in Kapralova's subsequent experimental work [15]. The more recent experiments were programmed to glean the effects of temperature, reagent and buffer gas concentrations, reactor vessel diameters and O_2, HF and HD admixtures on the location of the second explosion limit. The experiment with HD was inspired by Kompa[*] and was prompted by the fact that HD and HF transition frequencies -- $v = 1 \rightarrow 0$ and $v = 2 \rightarrow 1$, $J = 5 \rightarrow 4$ -- are coincident. It was argued that if HF^* enhances branching, HD would effectively deactivate HF^*. However, when one half of H_2 was replaced with HD, the explosion limit geometry remained unchanged. This appears to speak convincingly in favor of the functional role of H_2^* in a branched reaction. In the case of branching due to HF^* ($v \geq 4$) molecules, an expected decrease (at least tenfold) in the explosion limit pressure, due to a fast rate of vibrational relaxation of HF^* ($v \geq 4$) by HF collisions, failed to materialize. An addition of hydrogen to HF + F_2 mixture caused an inexplicable uplifting of the explosion limit.

3. Graphical Method

Shumov and Orlova of the Moscow Chemical Engineering Institute have proposed a simple method of determining reaction rates and stoichiometric coefficients based on the initial sections of the kinetic curves of a single reagent [16].

Normally, in order that rate k of second-order reaction may be determined

$$\begin{aligned} & A + C \rightarrow B \qquad \text{(slow)} \\ \rightarrow & \frac{B + (\gamma-1)C \rightarrow D}{A + \gamma C \rightarrow D} \qquad \text{(fast)} \end{aligned}$$

the value of stoichiometric coefficient γ must be known. The latter can be found from the following expression:

---

[*] K. L. Kompa, J. H. Parker and G. C. Pimentel, J. Chem. Phys., 49, 4257 (1968).

$$(1)\quad \gamma = ([C]_0 - [C]_\tau)/([A]_0 - [A]_\tau) \tag{1.34}$$

or

$$(2)\quad \gamma = [[C]_0 - [C]_\infty]/[A]_0 \tag{1.35}$$

The solution of Eq. (1.34) requires data on the changes in the concentration of both reagents. Calculations which employ Eq. (1.35) require nearly 100% conversion which, in the case of slow reactions, presents difficulties. Furthermore, Eq. (1.35) is inapplicable when C reacts rapidly not only with A but also D. In order to avoid these disadvantages, the authors propose a simple graphical method.

The reaction rate equation

$$\frac{d[C]}{d\tau} = k_c[A][C] = k_c[[A]_0 - ([C]_0-[C])/\gamma][C] \tag{1.36}$$

is transformed into

$$-\frac{d[C]}{d\tau}\ \frac{1}{[C]} = k_c[A]_0 - \frac{k_c}{\gamma}([C]_0 - [C]) \tag{1.37}$$

Equation (1.37) can be solved by graphical differentiation as a result of which a straight line is constructed, whose slope is γ and intercept is reaction rate k_c. If 1 and 2 are two close points along the locus $[C] = f(\tau)$, Eq. (1.36) can be represented as follows:

$$-\frac{\Delta[C]}{\Delta\tau} = k_c\frac{[A]_1+[A]_2}{2}\cdot\frac{[C]_1+[C]_2}{2} = \\ = k_c\frac{\left([A]_0-\frac{[C]_0-[C]_1}{\gamma}\right)+\left([A]_0-\frac{[C]_0-[C]_2}{\gamma}\right)}{2}\cdot\frac{[C]_1+[C]_2}{2}. \tag{1.38}$$

After certain transformations, Eq. (1.38) becomes

$$\frac{[C]_1-[C]_2}{(\tau_2-\tau_1)([C]_1+[C]_2)} = \frac{k_c}{4\gamma}([C]_1+[C]_2)+\frac{k_c}{2}\left([A]_0-\frac{[C]_0}{\gamma}\right) \tag{1.39}$$

from which k_c and γ can be determined. Similar first- and third-order reactions can be described by the following equations:

$$\frac{[C]_1 - [C]_2}{\tau_2 - \tau_1} = (k_c/2\gamma)([C]_1 + [C]_2) + k_c\left([A]_0 - \frac{[C]_0}{\gamma}\right). \tag{1.40}$$

$$([C]_1 - [C]_2)/(\tau_2 - \tau_1)([C]_1 + [C]_2)^2 = \\ = (k_c/8\gamma)([C]_1 + [C]_2) + (k_c/4)([A]_0 - [C]_0/\gamma). \tag{1.41}$$

The proposed method has further advantages, particularly in those cases where the accuracy of initial concentrations $[A]_0$ and $[C]_0$ is comparatively low (e.g., in the early stages of the reaction reagents are used up more rapidly than dilutent C). When initial concentrations $[A]_0$ and $[C]_0$ are totally unknown, this method further yields a useful parameter $k_A = k_e/\gamma$.

4. Explosion Limit Method

The explosion limit method is commonly used in the study of the reaction kinetics of atomic hydrogen with various substances. Normally, the reaction rate is determined from data on the effect of the substance on the upper and lower self-explosion limits of the hydrogen-oxygen mixtures. However, the reactions occurring between oxygen atoms and OH radicals with an inhibitor are seldom -- mistakenly -- taken into consideration when determining the reaction rates. Examples of such reactions -- where RH is inhibitor and R radical -- are as follows:

$$O + RH = OH + R$$

$$OH + RH = H_2O + R$$

In order to avoid making this mistake, Azatyan and Romanovich of the Chemical Physics Institute have carried out an experimental study using ethane as an example and have determined the rates of its reaction with the atomic hydrogen by the explosion limit method allowing for the inhibiting reactions of the above type [17].

At temperatures considerably in excess of the self-explosion temperature and at pressures close to the lower explosion limit, the reaction mechanism in the presence of ethane may be represented by the following system:

0. $H_2 + O_2 = 2OH$
1. $OH + H_2 = H_2O + H$
2. $H + O_2 = OH + O$
3. $O + H_2 = OH + H$
4. $H + \text{wall} \rightarrow \text{termination}$
5. $H + C_2H_6 = H_2 + C_2H_5$
6. $O + C_2H_6 = OH + C_2H_5$
7. $OH + C_2H_6 = H_2O + C_2H_5$

As can be seen from the above mechanisms, reactions 6 and 7 -- whose rates are proportional to the RH concentration -- compete considerably with reactions 3 and 1 whose rates are proportional to concentrations of H_2. This means, that if the amount of RH added to the initial mixture is varied so that the ratio of concentrations of RH to H_2 remains constant, changes in the inhibiting effect (changes in the magnitude of the explosion limit) with corresponding changes of RH content should be a function of reaction 5 only.

The experiments were performed using ethane obtained by the electrolysis of a sodium acetate solution which was acidified with acetic acid and purified so as not to contain olefin impurities by way of passing it through concentrated sulfuric acid and bromine water. Subsequently, the ethane was vacuum distilled. The experiments were carried out in the temperature range from 567-665°C. The ethane content in the $H_2 + O_2$ mixture was varied from 0.37-0.58% and the H_2 content, from 48.1 to 75.2%. The ratio of ethane to H_2 concentrations in all the mixtures was 7.7×10^{-3}.

The temperature dependence of the explosion limits of the various mixtures is shown in Fig. 29. The rate of reaction 5 was calculated from the curves shown in Fig. 30 for various temperatures. The reaction rate was found to be 7.4×10^{13} $cm^3.mole^{-1}.sec^{-1}$, and the

activation energy was 9.6 kcal/mole. The value of k_5 obtained by the present method was only 25-30% lower than that which one of the authors had obtained previously by the EPR method (DAN SSSR, Vol. 184, 625, 1969). The authors criticize a number of works on k_5 calculation which consider the effect of the admixture not on the explosion limit but on the combustion regime. In these works, apparently no account was taken of the $O + OH \rightarrow O_2 + H$ reaction. This reaction appears to play an important role inside the explosion "peninsula." The explosion limit method appears to be within the accuracy limit of the EPR method, and it confirms the validity of the mechanism of inhibited combustion of hydrogen. In particular, this agreement points to the fact that nearly all the ethyl radicals which are formed in reactions 5-7 lead to the breaking of the chains.

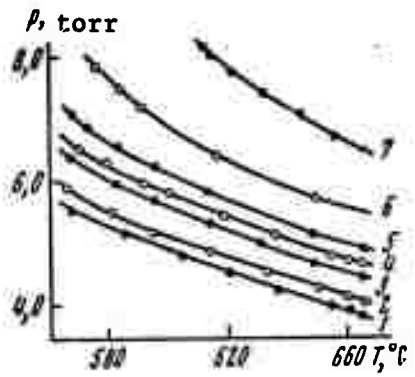

Fig. 29

Lower self-explosion limits of $H_2 + O_2$ mixtures with various ethane content (%): 1 -- 0.37; 2 -- 0.40; 3 -- 0.44; 4 -- 0.0 stoichiometric mixture; 5 -- 0.48; 6 -- 0.52; 7 -- 0.58.

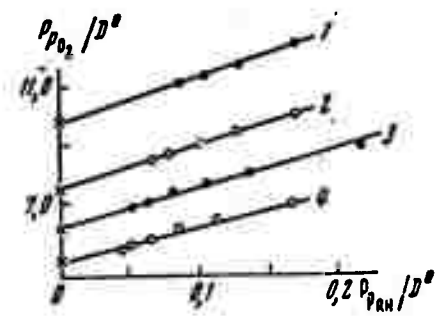

Fig. 30

Dependence of $P_{P_{O_2}}/D^\circ$ on $P_{P_{RH}}/D^\circ$ at temperatures (°C): 1 -- 567; 2 -- 600; 3 -- 630; 4 -- 665.

D. VIBRATIONAL RELAXATION

1. Harmonic Oscillators

The theory of thermal dissociation of diatomic molecules has been studied rather well in the temperature region where the characteristic dissociation time τ_d and vibrational relaxation τ_v differ from each other by an order of magnitude ($\tau_v \ll \tau_d$). The dissociation occurs essentially when the vibrational relaxation is practically completed. However, as the temperature increases, the rates of dissociation and vibrational relaxation become comparable and their combined effects considerably increase and require further studies. Very little has been done in this direction until now. Admittedly, the effect of vibrational relaxation on dissociation has been studied for pure molecular gases in which vibrational energy transfer between molecules produces a rapid build-up of Boltzmann distribution. Dissociation of diatomic molecules in an inert gas at high temperatures has also been studied. In the opinion of Safaryan and Stupochenko, the bulk of research on this subject contains assumptions which have not been verified physically so far. In a recent paper, the two Soviet authors [18] use the diffusion theory to study the processes of thermal dissociation and vibrational relaxation of diatomic molecules in an inert gas at high temperatures ($7 \gtrsim D/kT \gtrsim 1$) taking into account interaction between them. An approximate analytical description is given for the dissociation at times $t > \tau_v$ ($\tau_v/\tau_d < 1$). A complete ($0 < t < \infty$) numerical calculation is carried out for a Morse oscillator and truncated harmonic oscillators.

Adkhamov's calculations of the vibrational relaxation of several harmonic oscillators were based on theoretical or experimental values of transition cross section and were compared with those obtained experimentally and cited by Cotrell and McCoubrey (Molecular Energy Transfer in Gases, London 1961) [19]. Adkhamov used the following equation in his calculations:

$$\tau_{vib}^{-1} = ZP_{10}(1-e^{\frac{-h\nu}{kT}}) \qquad (1.42)$$

where $P_{10} = e^{h\nu/kT}\bar{Q}_{01}/Q_{elastic}$ is the cross section of the $1 \rightarrow 0$ transition with respect to a single collision; $Z = 4nQ_{elastic}(kT/\pi m)^{1/2}$ is the number of elastic collisions which one molecule sustains per 1 sec. Adkhamov's data are shown in Table 3. Data agreement appears to be better at higher temperatures.

Table 3

Vibrational Relaxation Times for Several Harmonic Oscillators

Gas	T°K	$\tau_v \times 10^6$ sec	
		Experimental (after Cotrell)	Calcul.
Cl_2	298	4.9	1.1
I_2	385	0.11	0.34
Br_2	301	0.85	1.52
	331	1.8	1.36
	373	0.76	0.98
Cs_2	273	0.54	0.90
	296	0.53	0.88
	303	0.40	0.65
	308	0.51	0.81
	341	0.45	0.60
	390	0.41	0.51

2. Effect of Anharmonicity

Studies [20] of the vibrational relaxatation behind a shock wave front in oxygen and nitrogen were made and it was found out that the value of relaxation τ of average vibrational energy $\bar{\varepsilon}$ of a gas can be defined by the following equation:

$$d\varepsilon/dt = (\bar{\varepsilon} - \varepsilon)/\tau \tag{1.43}$$

where $\bar{\varepsilon}$ is the average vibrational energy in an equilibrium, and that this quantity (τ) does not remain constant in a vibrational excitation region. Earlier, one of the authors (Losev) observed a growth in the relaxation rate behind the shock wave front in an undiluted oxygen which he attributed to the decrease in the gas temperature. Subsequently, the author also observed a considerable reduction in the relaxation toward the end of the relaxation period. His present study [20] deals with a more detailed investigation of changes in the relaxation rate in a 10% O_2 + 90% Ar mixture and in undiluted nitrogen. His experiments were carried out using a shock tube and a method of absorption uv spectroscopy which was described in earlier references.≠

The experimental results -- obtained under almost isothermal conditions -- are shown in Fig. 31, where the value of τ behind the shock front decreases at all times; in the case of an undiluted molecular gas, the value of τ begins to decrease after a certain time after the passage of the shock front regardless of the temperature drop. Under these conditions, the relaxation time ceases to be a single-valued function of the gas temperature; this considerably complicates the conduct of the experiment, theoretical calculations, and the comparison of the results of the various authors. In essence, this means that Eq. (1.43) describes the process of vibrational relaxation with insufficient accuracy since it holds for a model of a molecule in the form of a harmonic oscillator only. This work [20] is, therefore, an attempt to apply a correction for anharmonicity of molecules.

≠Losev, S.A. et al. (KhVE, Vol. 4, p. 269, 1970; ZhPS, Vol. 10, p. 229, 1969).

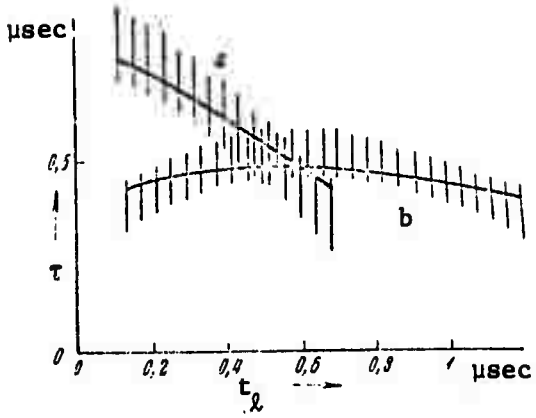

Fig. 31

Examples of changes in the vibrational relaxation τ behind a shock wave front in (a) 10% O_2 + 90% Ar mixture at T = 6000°K and (b) undiluted nitrogen with temperature changing from 6500 to 6000°K. Vertical lines indicate experimental region. Solid lines -- calculated changes in τ using Eq. (1.44). τ is normalized with respect to gas density (scale for (a) magnified 5-fold). t_l is time in the laboratory frame of reference.

To illustrate this effect, an expression was found for the relaxation τ/τ_0 ratio where τ_0 is relaxation in a system of harmonic oscillators. In the case of single quantum transitions in a system of harmonic oscillators, the vibrational relaxation is described by the Boltzmann distribution of molecules. The ratio τ/τ_0 can then be expressed as follows

$$\tau/\tau_0 = [(1 - \gamma\exp(-\theta/T_v))/(1-\exp(-\theta/T_v))]^2 \qquad (1.44)$$

where T_v is the instantaneous value of vibrational temperature. The above relationship most likely corresponds to the process of vibrational excitation in a gas behind a front of a somewhat weak shock wave. Clearly, Eq. (1.44) indicates that immediately behind the shock wave front ($T_v \approx 0$), $\tau \approx \tau_0$; as the vibrational relaxation process develops, τ/τ_0 decreases, an event clearly observable in the experiments (see Fig. 31). Evidently, the role of anharmonicity is reduced to the acceleration of the vibrational excitation. The above equation

appears to be in good agreement with the result of an exact solution of a system of kinetic equations of the balance type

$$dx_k/dt = P_{k+1,k}x_{k+1} - P_{k,k-1}x_k + P_{k-1,k}x_{k-1} \qquad (1.45)$$

since the Boltzmann distribution in the process of vibrational excitation of anharmonic oscillators is disturbed only in the upper levels whose contribution to the total vibrational energy is negligibly small due to a very small population. Therefore, Eq. (1.44) also describes changes in the relaxation rate in the case of a slow deactivation of vibrational energy (in the case of preservation of Boltzmann distribution of the lower levels). In this case, in the process of relaxation, τ will increase remaining smaller than τ_0 (Fig. 32). The critical value of τ_∞ in the case of total statistical balance (shown by a dotted line in Fig. 32, where $T_v = T$) is always smaller than τ_0 for an anharmonic oscillator.

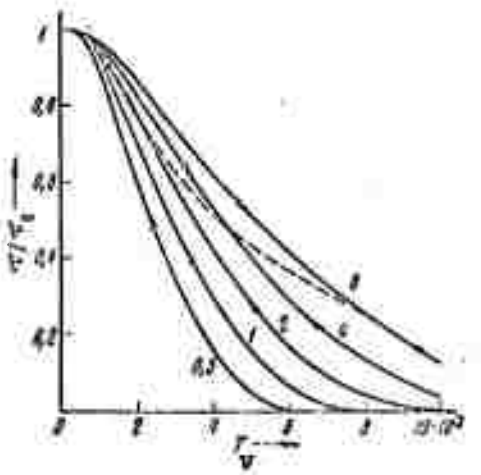

Fig. 32

Ratio of instantaneous value of vibrational relaxation of O_2 and τ_0 for a harmonic oscillator as a function of vibrational temperature T_v. Numbers near curves indicate gas temperature in thousands of °K. Arrows indicate direction of motion of relaxing system under isothermal excitation (down) and deactivation (up). Dotted line is the critical value of τ for $T_v = T$.

However, in the case of rapid cooling of a gas in the process of deactivation, a considerable departure from the Boltzmann distribution occurs on the lower vibrational levels and even the population inversion is possible. The corresponding values of τ/τ_0 for nitrogen are shown by dotted lines in Fig. 33. Finally, in the case of δ-distribution for which all the molecules are on the m-th level, this ratio is as follows:

$$\frac{\tau}{\tau_0} = \frac{1}{\gamma^{m-1}} \frac{m(e^{\theta/T}-1) - 1}{m(e^{\theta/T}-\gamma) - \gamma} \tag{1.46}$$

This is indicated by solid lines in Fig. 33. Both Figs. 32 and 33 indicate that an allowance for anharmonicity may lead to a considerable reduction of the vibrational deactivation time. This appears to be at variance with the results obtained in shock tubes. Researchers (e.g., Hurle and Russo) measuring τ of a gas cooled in a nozzle observed the same effect. Consequently, quantitative comparison of results of experiments which investigate deactivation should also take into consideration the effect of anharmonicity.

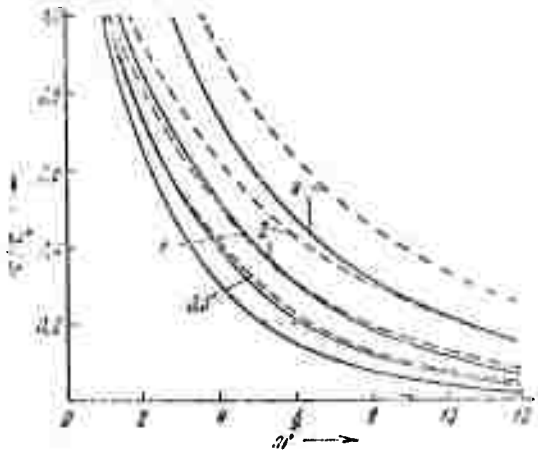

Fig. 33

Ratio τ/τ_0 for N_2 under conditions of strong deviation from Boltzmann distribution, m is level number. Solid lines indicate δ-distribution of m-th level. Numbers near curves indicate gas temperature in thousands °K.

Equation (1.44) can be used to find τ_0 for the dependence of τ on T_v and T obtained in shock tube experiments. Values of τ_0 for nitrogen in a 10% O_2 + 90% Ar mixture are shown in Fig. 34 in Landau-Teller coordinates. The value of τ_0 exceeds the values published earlier by tens of percent for $T \approx \theta$ and by more than 100% for much higher temperatures. Thus, the refined value of vibrational relaxation clearly shows its dependence on the temperature. Unfortunately, the temperature region shown in Fig. 34 is insufficiently wide in order to make a comparison between the experimental and theoretical results. Equation (1.44) provides only the first approximation of τ. In experiments, particularly at high temperatures, toward the end of the relaxation period, the value of τ changes more steeply than it would follow from Eq. (1.44). On the other hand, under these conditions, the effect of multiphoton processes and the onset of dissociation of molecules may have some bearing.

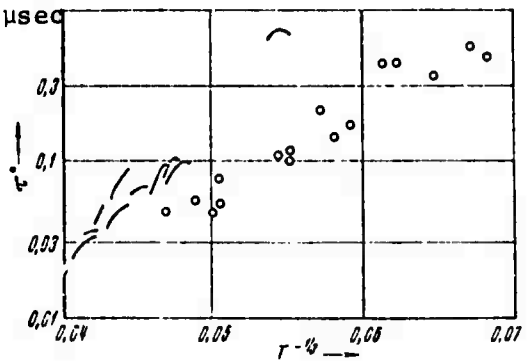

Fig. 34

Dependence of τ_0 (at normal gas density) on temperature in Landau-Teller coordinates for 10% O_2 + 90% Ar mixture (circles) and N_2 (lines).

E. FLUORINATION OF ORGANIC COMPOUNDS

1. Dichloromethane ($CHCl_2$)

The kinetics of a number of highly exothermic chain branching reactions involving organic compounds and molecular fluorine have been studied by Medvedev et al. at Tal'roze's laboratory. The branching mechanism in the following reactions:

$$1.\quad CHCl_2 + F_2 \rightarrow CHFCl_2^* + F + 73 \text{ kcal/mole}$$

$$2.\quad CHFCl + F_2 \rightarrow CHF_2Cl^* + F + \sim 78 \text{ kcal/mole}$$

was considered to be the monomolecular decomposition of vibrationally excited $CHFCl_2$ [21] and CHF_2Cl [22]. The authors have determined experimentally the composition of the reaction products as a function of the inert gas (nitrogen) pressure. The results of a sample run are shown in Table 4.

Table 4

% Product Composition of Reaction $CHCl_2 + F_2$ at Different N_2 Pressures

P_{N_2}, torr	CF_3Cl	$C_2F_4Cl_2$	CF_2HCl	$CHFCl_2$
60	55,90	27,23	9,85	7,02
200	32,60	38,60	10,30	18,50
400	20,90	39,50	7,90	31,70
700	14,50	31,84	9,46	44,20
1900	13,15	21,35	9,40	56,10
3800	6,75	16,03	10,17	67,00
19000	2,38	5,61	2,51	89,50
38000	1,30	3,30	1,40	94,00
76000	0,80	2,10	0,10	97,00

In the case of $CHFCl_2^*$, the excited molecules were found most likely to decompose into CFCl and HCl.

In addition to the 4 basic reaction products shown in Table 4, small amounts of CO_2 were observed. The formation of CF_3Cl and $CHCl_2F$ is evident from reaction 3 through 6

3. $CHCl_2F^* \rightarrow CFCl + HCl$
4. $CHCl_2F^* \rightarrow CHCl_2F + Q$
5. $:CFCl + F_2 \rightarrow \cdot CF_2Cl + F$
6. $\cdot CF_2Cl + F_2 \rightarrow CF_3Cl + F$

$C_2F_4Cl_2$ was formed clearly by way of the recombination of CF_2Cl radicals, and the appearance of CO_2 was apparently associated with the addition of oxygen to the initial fluorine. In order to explain the formation of CHF_2Cl by way of the following two mechanisms:

A. $:CFCl + HF \rightarrow CHF_2Cl$

B. $\begin{cases} \cdot CHCl_2 + \cdot F \rightarrow \cdot CHFCl + \cdot Cl \\ \cdot CHFCl + F_2 \rightarrow CHF_2Cl + F\cdot \end{cases}$

the authors have carried out experiments on the fluorination of CH_2FCl which proceeds apparently in the following manner:

7. $CH_2FCl + \cdot F \rightarrow CHFCl + HF$
8. $\cdot CHFCl + F_2 \rightarrow CHF_2Cl^* + F\cdot$
9. $CHF_2Cl^* \rightarrow$ decomposition products
   $CHF_2Cl^* \xrightarrow{[M]} CHF_2Cl$

It turned out that at nitrogen pressures of 60 torr, CHF_2Cl was practically nonexistent.

Experiments carried out at small pressures (5 torr) in which the surface to volume ratio of the reaction vessel was increased four-fold,

have shown that the CHF_2Cl content sharply increases (approximately twenty-fold) which points to a heterogeneous nature of its formation at the walls.

When the reagent pressure was varied in the 0.6-5 torr range, for a fixed value of nitrogen pressure, the product composition remained unchanged. This points to the absence of self-heating of the reacting mixture or to its effect on the product composition. Thus, CF_3Cl and $C_2F_4Cl_2$ are the products of decomposition of chemically activated $CHFCl_2$ molecules; $[D] = [CF_3Cl] + 2[C_2F_4Cl_2]$ and $CHFCl_2$ is the stabilizing product; $[S] = CHFCl_2$. The ratio $[S]/[D]$ as a function of pressure is shown in Fig. 35.

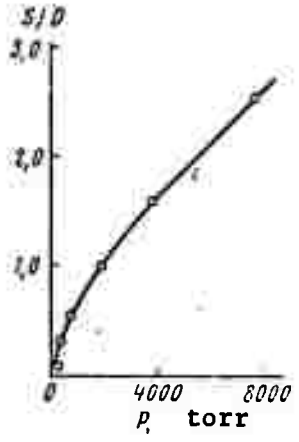

Fig. 35

Dependence of [S]/[D] on pressure.

Knowing the values of these concentrations, the average rate of reaction was found from the following expression

$$k_{av} = \omega[D]/[S] \qquad (1.47)$$

where ω is the frequency of deactivating collisions which was calculated from the elementary kinetic theory without corrections for non-ideal gases at high pressures. It was assumed that $\sigma_o(N_2) = 3.7\text{Å}$ and $\sigma_o(CHCl_2F) = 4.9\text{Å}$. The extrapolation of the reaction rate for high and low pressures yields the corresponding values of k_{a_∞} and k_{a_0} (Fig. 36).

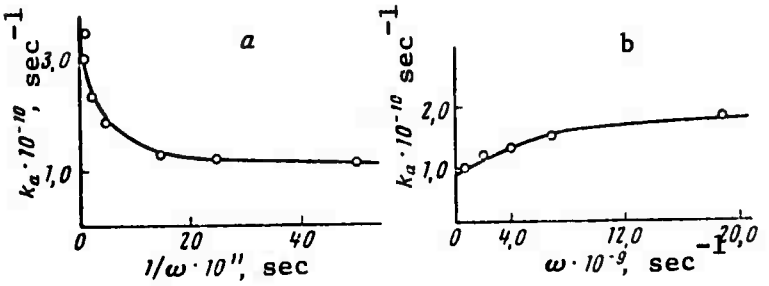

Fig. 36

Dependence of k_{av} on (a) $1/\omega$ and (b) ω.

The proposed mechanism fully confirms that with an increasing nitrogen pressure, the relative content of CHFCl increases and the $CF_3Cl + C_2F_4Cl$ content decreases (see Table 4).

In the calculation of k_a using Eq. (1.47), the authors have proceeded from the mechanism of strong collisions, assuming that the deactivation occurs with every collison. The mechanism of gradual deactivation leads to enormously high values of k_a at low pressures. Normally, this effect is noticeable at [S]/[D] values of 0.1. In the authors' case, this effect was not observed, although low [S]/[D] ratios down to 0.06 were obtained. The authors speculate that the absence of this effect is associated with a comparatively large energy scattering of the hot molecules and the step-like deactivation may become noticeable at even lower values of [S]/[D]. Conceivably, the departure from the strong collision mechanism has no practical value under Medvedev's conditions. The assumption concerning the deactivation of activated molecules with each collision leads possibly to some error in the calculation of k_a. The ratio k_{a_∞}/k_{a_0} is approximately 3.8 which is somewhat higher than the same ratio normally observed for the case of chemical activation in the addition reactions. The minimum excess energy was 6-10 kcal/mole.

At this stage, the result of the Soviet work and those of Clark and Tedder (Trans. Faraday Soc., 62, 399, 1966) appear to be at variance with each other concerning the dependence of the product yield and deactivation of $CHFCl_2^*$ on pressure. The Clark-Tedder experiments involved the following systems:

10. $CFCl_3 + H \rightarrow CFCl_2 + HCl$

11. $\cdot CFCl_2 + \cdot H \rightarrow CHFCl_2^* + 97$ kcal/mole

In the Clark-Tedder experiments, [S]/[D] was ~1.8 at the pressure of 0.23 torr. In the Medvedev experiments, the same ratio was ~0.06 at 60 torr pressure. The exothermicity of reaction 1 was approximately 73 kcal/moles whereas the Clark-Tedder experiments indicate that the excited $CHFCl_2^*$ molecules have considerably higher energies.

In order to evaluate the rate of $CHFCl_2^*$ decomposition, it was necessary to know the critical energy of this reaction. Evidently, the activation energy of thermal decomposition of dichlorofluoremethane which proceeds along the following mechanism:

12. $CHFCl_2 \rightarrow :CFCl + HCl$

lies between the values of the energy of activation of a thermal decomposition of difluorochloromethane:

13. $CHClF_2 \rightarrow :CF_2 + HCl$

and of chloroform:

14. $CHCl_3 \rightarrow :CCl + HCl$

The study of thermal decomposition of the above reactions was made by one of the authors (Shilov) elsewhere in the Soviet literature where it was assumed that the activation energies for the decomposition of $CHFCl_2$ was ~50 kcal/mole. Assuming that this value may be somewhat low, Medvedev carried out computations for the specific rate of decomposition assuming two arbitrary values of critical energies ε_o = 60 and 75 kcal/mole. The calculation showed that the decomposition rate of $CHFCl_2$ molecules with activation energy of 97 kcal/mole was ~7×10^{10} sec^{-1} for ε_o = 60 kcal/mole and ~3×10^9 sec^{-1} for ε_o = 75 kcal/mole. The deactivation rate was assumed to be equal to

the number of collisions of the excited molecules which at a pressure of 0.23 torr was ~7 x 10^5 sec^{-1}. This indicates that at the indicated pressure, the decomposition rate of $CHFCl_2^*$ molecules with activation energy of 97 kcal/mole exceeds their deactivation rate by several orders of magnitude.

As far as the Soviet authors are concerned, there is one way only in which the decomposition of $CHFCl_2^*$ proceeds:

15. $CHFCl_2^* \rightarrow :CFCl + HCl$

However, they admit that the Clark-Tedder experiments are valid with respect to the alternative decomposition of the same excited molecule into

16. $CHFCl_2^* \rightarrow CCl_2 + HF$

It is possible that the activation energy of reaction 16 is greater than that of 15. For this reason, $CHFCl_2^*$ formed in reaction 11 (activation energy 97 kcal/mole) may be decomposed along two channels while $CHFCl_2^*$ obtained in reaction 1 -- and possessing considerably smaller energy -- decomposes along one channel only.

2. Chlorofluoromethane (CHFCl)

In the case of CHF_2Cl^* [22], the formation of all the products (with the exception of trifluoromethane (CHF_3)) and the changes in their relative content with pressure can be explained by the following branching system:

1. $CH_2FCl + \cdot F \rightarrow \cdot CHFCl + HF$
2. $\cdot CHFCl + F_2 \rightarrow CHF_2Cl^* + F\cdot + \sim 78$ kcal/mole
3. CHF_2Cl^* branches to $:CFCl + HF$ (a); $:CF_2 + HCl$ (b); and, with $[N_2]$, CHF_2Cl (c)

4. $:CFCl + F_2 \rightarrow \cdot CF_2Cl + F\cdot$

5. $:CF_2 + F_2 \rightarrow \cdot CF_3 + F\cdot$

6. $\cdot CF_2Cl + F_2 \rightarrow CF_3Cl + F\cdot$

7. $\cdot CF_3 + F_2 \rightarrow CF_4 + F\cdot$

8. $\cdot CF_2Cl + \cdot CF_2Cl \rightarrow C_2F_4Cl_2$

9. $\cdot CF_3 + \cdot CF_3 \rightarrow C_2F_6$

10. $\cdot CF^3 + \cdot CF_2Cl \rightarrow C_2F_5Cl$

The composition of the reaction products as a function of inert gas (nitrogen) pressure is shown in Table 5. The authors favor reaction 3a as the basic channel through which the decomposition occurs. They appear to stress the point developed earlier by Clark and Tedder, which postulates that the decomposition of a molecule may depend on the nature of its activation.

Table 5

% Product Composition of Reaction $CHFCl + F_2$ at Different N_2 Pressures

P_{N_2}, atm	CF_4	C_2F_6	CF_3Cl	C_2F_5Cl	$C_2F_4Cl_2$	CHF_2Cl	CF_3H
3,3	0,2	1,6	52,3	13,2	10,4	2,7	19,6
5	1,1	1,8	64,5	10,5	12,4	4,4	5,3
20	0,7	2,2	62,5	8,8	7,9	11,5	6,4
30	0,5	1,6	47,6	9,7	6,5	28,5	5,6
40	0,6	1,2	43,5	6,9	5,6	32,2	10,0
50	0,1	1,4	50,5	6,9	2,5	33,6	5,0
70	0,3	1,0	30,1	6,6	2,8	52,0	7,2
83	0,1	0,6	[illegible]	3,9	7,2	58,0	2,7
90	—	0,9	[illegible]	4,9	4,6	60,5	7,0
100	0,1	0,6	20,5	4,4	4,7	61,7	8,0

3. Difluoromethane (CH_2F_2)

In addition to the group led by Tal'roze, the Chemical Physics Institute supports another group which works in an area associated with chemical lasers. Literature published by this group does not reveal an explicit connection with Tal'roze's group either through co-author relationships or salutatory remarks, yet its efforts appear to be if not directly pertinent to Tal'roze's experiments, at least adjunct to them. This work is being done by Vedeneyev and Pariyskaya, and it concerns the measurement of the rate of fluorination of methane and some of its derivatives under identical conditions. All the three works [23-25] were submitted for publication in late 1969 and did not appear in print until January 1971.

The experimental kinetic data indicates that fluorination of CH_2F_2 is a chain branching reaction. The following reactions occur:

1. $CH_2F_2 + F \rightarrow CHF_2 + HF$
2. $CHF_2 + F_2 \rightarrow CHF_3 + F - H$

The exothermicity of reaction 2 is greater than 80 kcal/mole which exceeds the energy of activation for the decomposition of CHF_3 into CF_2 and HF (60--70 kcal/mole). This would lead one to expect that a certain portion of CHF_3 molecules would decay shortly after their formation, leading to chain branching. In fact, difluoromethane was shown to fluorinate considerably faster than methane and some of its fluorine derivatives [24].

The basic products of fluorination of difluoromethane were CHF_3 and CO_2. The production of the latter is associated with the presence in the system of small amounts of oxygen which exists in fluorine as an admixture. In addition to the two basic products, other products were also formed, one of which was CF_4. The analysis of products carried out immediately after formulation of mixture reagents showed that in many cases, the reaction proceeded to some degree already in the process of mixing.

If fluorination of difluoromethane is indeed a branched chain reaction, one should be able to observe in this reaction certain critical phenomena. The results of certain experiments are shown in Table 6.

Table 6

Effect of Mixture Composition and Temperature on Reaction Time

Mixture composition (F_2:CH_2F_2: inert gas)	T°K	Reactor vessel	Reaction time
0.2:0.04:70 (He)	170	Molybdenum glass d = 6cm	Complete reaction < 30 sec
0.15:0.03:50 (He)	170	same	No reaction 12 min.
0.2:0.07:125 (N_2)	143	same	Complete reaction < 2 min.
0.1:0.07:125 (N_2)	143	same	No reaction 30 min.
0.44:0.08:140 (N_2)	143	Copper cylinder d = 4cm, L = 10cm	Complete reaction < 2 min.
0.33:0.06:100 (N_2)	143	same	No reaction 8 min.

The data in the above table show that small changes in the concentration of initial components have strong effects on the reaction rate. The same phenomena were observed also when temperature was changed. The presence of critical phenomena, however, does not prove explicitly the chain branching nature of the process. These are characteristic also for systems in which thermal explosions may occur. Reagent concentrations in Pariyskaya's experiments were too small to permit the latter to occur.

In order to settle the problem concerning the two mechanisms of fluorination of difluoromethane, the authors studied the reaction kinetics on the basis of product analysis and thermal balance of

mixture heating. The study of product kinetics showed that the reaction goes through a certain period of induction after which a jump-like conversion of initial materials into reaction products occurs. The duration of the induction period strongly depends on the concentration of reaction materials, mixture composition, temperature, the condition of the reacting vessel surface, and fluorine purity. The parameters which appear to control this process are concentration, composition, and temperature, and they were selected in such a way as to cause the induction period to be from one to several minutes long.

The study of fluorination kinetics is hindered by poor reproducibility. However, if short series of experiments are undertaken -- having first "processed" the vessel with fast reactions -- one may obtain kinetic data as shown in Figs. 37 and 38 [23]. The greater the number of experiments (carried out during the induction period) the longer are the induction periods. This is clearly visible in Fig. 39, where results of two short series are shown. The induction periods can be reduced again by increasing the number of fast reactions in the vessel. Figure 40 shows the results of an effort to plot the kinetics of a fast reaction stage. The figure shows that the reaction time is short and amounts to ~ 10 seconds.

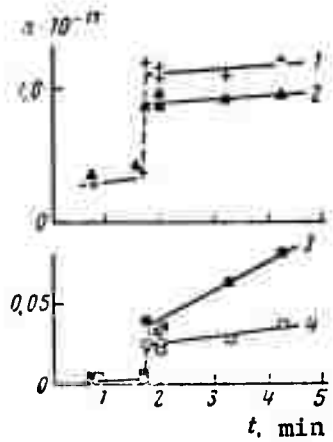

Fig. 37

Kinetics of product formation in CH_2F_2 + F reaction at 173°K (F_2:CH_2F_2:N_2 = 0.35:0.05:100) 1 -- CHF_3; 2 -- CO_2; 3 -- C_2F_6; 4 -- C_2F_4.

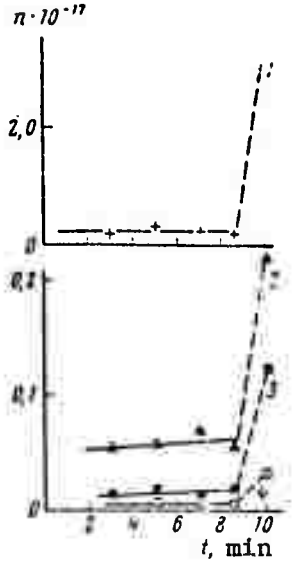

Fig. 38

Kinetics of product formation in CH_2F_2 + F reaction (induction period) at 158°K (F_2:CH_2F_2:He = 0.33:0.1:90). Numbers as in Fig. 37.

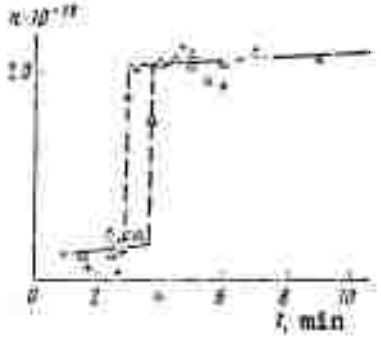

Fig. 39

Kinetics of formation of CHF_3 in the CH_2F_2 + F reaction at 143°K (F_2:CH_2F_2:N_2 = 0.4:0.07:125).

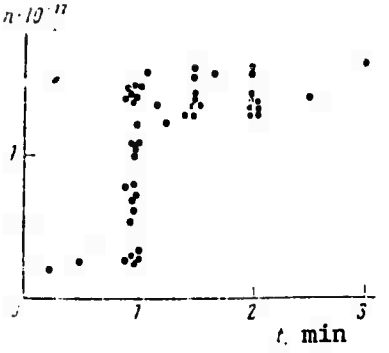

Fig. 40

Kinetics of formation of CHF_3 in the CH_2F_2 + F reaction at 173°K (F_2:CH_2F_2:N_2 = 0.33:0.05:100).

The study of reaction kinetics of heated up mixtures showed that the induction periods determined by thermal balance analysis and the product analysis coincide. A series of experiments was undertaken in which the reaction was studied simultaneously by thermal balance and product analyses; these showed that at the peak of heating difluoromethane was practically fully used up. Thus, the period during which the heating peak occurred coincided with the period of rapid reaction. Under the experimental conditions, this period was 5-10 seconds. The maximum heating up was not more than 1° and normally was measured in fractions of a degree. The foregoing would seem to indicate that after the induction period, the reaction self-accelerates under practically isothermal conditions. This uniquely proves the authors' claim that the fluorination of difluoromethane is a chain branching process.

It was indicated above that chain branching can occur in the following reaction:

$$3.\quad CHF_3^* \rightarrow CF_2 + HF$$

where CHF_3^* is a vibrationally excited molecule whose energy exceeds the activation energy when it decays into CF_2 and HF. Another explanation is possible for the self-acceleration of the reaction:

chain branching occurs not along reaction 3 but is due to some product of reaction which is formed during the period of induction. It was shown that the basic reaction product in the induction period were trifluoromethane and carbon dioxide and also hexafluoroethane and tetrafluoroethane whose content was not more than 5-7% and 1%, respectively, of the CHF_3 content. Trifluoromethane, carbon dioxide, and tetrafluoroethane cannot be responsible for self-acceleration of the reaction since under the experimental conditions they do not react with fluorine. C_2F_4 may, in principle, interact with fluorine radicals in the course of the following reactions:

4. $F_2 + C_2F_4 = F + C_2F_5$
5. $F_2 + C_2F_5 \rightarrow C_2F_6^* \rightarrow 2CF_3$

The concentration of tetrafluoroethane during the induction period is, however, too small to be responsible for the self-acceleration reaction.

The following scheme of fluorination of difluoromethane could be proposed. The production of radicals at low temperatures occurs most probably at the walls of the reacting vessel. The nascent radicals undergo stretching of chains (reaction 1 and 2), producing vibrationally excited CHF_3^* molecules. The decomposition of the excited CHF_3^* molecules leads to chain branching (reaction 3).

The excited molecules CHF_3^* can also be deactivated as a result of collisions with molecules of an inert gas. The authors have not made a special effort to study the effects of the inert gas on the conduct of the reactions; however, its concentration was changed in a number of experiments without any noticeable effects being observed. It is possible that much higher pressures are necessary in order to cause a noticeable deactivation of CHF_3^*. The following reactions may occur in the footsteps of reaction 3:

6. $CF_2 + F_2 = CF_3 + F$
7. $CF_3 + F_2 = CF_4 + F$

The formation of C_2F_6 and C_2F_4 may be explained in terms of the recombination of radicals CF_3 and CF_2:

8. $CF_3 + CF_3 = C_2F_6$
9. $CF_2 + CF_2 = C_2F_4$

The decomposition of radicals may also occur at the vessel walls or in reactions with an addition of oxygen. In this connection, it should be noted that the duration of induction periods is clearly determined by the reaction of the radicals and oxygen molecules. The self-acceleration reaction may begin only when an effective branching factor exceeds the effective decomposition which also includes the decomposition of the active particles by oxygen. Thus, small additions of oxygen strongly influence the duration of the induction period.

4. Fluoromethyl (CH_3F)

In the case of fluorination of CH_3F [25], the reaction mechanism is somewhat different to those of difluoromethane [23] and methane [24]. The self-acceleration of reactions may be explained in terms of two possible mechanisms.

(1) Branching occurs in the fluorination chain of CH_3F. The chain consists of two stretching reactions:

1. $CH_3F \rightarrow CH_2F + HF$
2. $CH_2F + F_2 \rightarrow CH_2F_2^* + F - \Delta H_2$

where $\Delta H_2 = 72 + E_2$ kcal/mole (where E_2 is the activation energy). A slight excess of ΔH_2 over activation energy of CH_2F_2 decomposition may, in principle, lead to branching

3. $CH_2F_2^* \rightarrow CHF + HF$

where $CH_2F_2^*$ are vibrationally excited molecules with energies equal to or greater than 72 kcal/mole. Clearly, the number of such molecules

is small. Thus, although branching reaction 3 may occur in principle, one should seek a more effective means of branching reactions.

(2) As was indicated in [23] and [24], the fluorination of CH_2F_2 is a branching reaction which occurs effectively. Since CH_2F_2 is an original product of fluorination of CH_3F, the fluorination mechanism of the latter may be treated as a chain degenerate-branched process in which the role of the branching product is played by CH_2F_2. In this connection, one would expect the production of large amounts of CH_2F_2 during the period of induction fluorination of CH_3F. That this indeed occurs can be seen in Figs. 41 and 42, where the origin coincides with the amount of product formed during the mixing of reagents. In addition to CH_2F_2, there also occur during the period of induction small quantities of CHF_3 and CO_2. Neither one of these can be held responsible for the rapid acceleration of reaction.

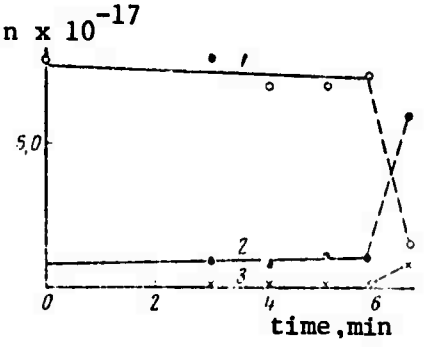

Fig. 41

Kinetics of product formation in the induction period of CH_3F fluorination at 173°K; (F_2:CH_3F:He ≅ 0.15:0.13:180); 1 -- CH_3F; 2 -- CH_2F_2; 3 -- CHF_3.

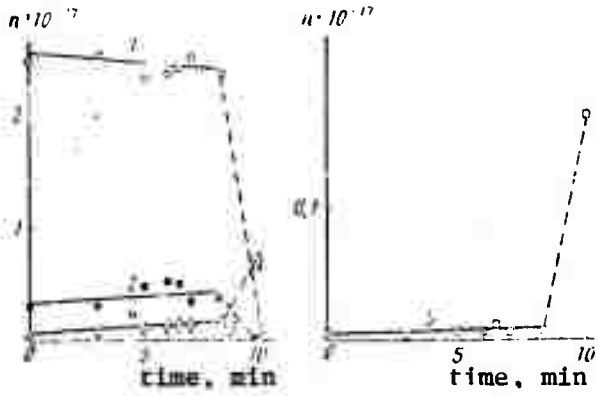

Fig. 42

Kinetics of product formation in the induction period of CH_3F fluorination at 213°K. (F_2:CH_3F:He = 0.25:0.04:60); 1 -- CH_3F; 2 -- CH_2F_2; 3 -- CHF_3; 4 -- CO_2; 5 -- C_2F_6.

The experimental data indicate that CH_2F_2 fluorinates slower than CH_3F in the sense that reaction rates k_4 and k_5

4. $CH_2F_2 + F \rightarrow CHF_2 + HF$

5. $CHF_2 + F_2 \rightarrow CHF_3 + F$

could be lower than rates k_1 and k_2 of reactions 1 and 2 which comprise the elements of the CH_3F fluorination chain. The fact that branching occurs in the CH_2F_2 fluorination chain has little meaning in this case since branching leads only to an increase in the total concentration of active centers in the system and, consequently, equally affects the rates of reactions 1 and 2 as it does reactions 4 and 5. The location of the concentration maximum for CH_2F_2 is only determined by relations between k_1, k_2, k_4, and k_5.

All these considerations have led the authors to believe that they are encountering for the first time a new type of chain branching which is degenerate in nature. In this type of reactions, branching occurred as a result of decomposition of the excited product molecule into radicals. In the case of fluorination of CH_3F, such an excited molecule is the CHF_3 molecule. It should be pointed

out that thermalized CHF_3 molecules under these conditions are absolutely inert and, consequently, do not lead to branching. These molecules may acquire energy sufficient for decomposition only at the time of formation due to the chemical energy of the reaction. Since such vibrationally excited molecules CHF_3 are formed in the fluorination of CH_2F_2, the latter can be considered in the kinetic sense as an intermediate branching product. In this type of branching, the requirement that molecule CH_2F_2 be chemically less stable than the initial materials is completely waived. The only important condition is that the fluorination chain for CH_2F_2 contains a sufficiently exothermic component and that the excited molecules produced in this process have a channel for decaying into radicals. The deactivation energy of the latter ought to be smaller than the exothermicity of the elementary act in which those products were formed.

The following mechanism for the fluorination of CH_3F can now be considered. The production of active centers occurs probably as a result of heterogenous decay of fluorine molecules.

$$6.\quad (F_2)_{ad} = (F)_{ad} + (F)_{gas}$$

where $(F_2)_{ad}$ and $(F)_{ad}$ are particles absorbed on the surface of the reaction vessel. The production of radicals also may occur along a different channel

$$7.\quad (F_2)_{ad} + (CH_3F)_{gas} = (F)_{ad} + (CH_2F)_{gas} + HF$$

in an exothermic reaction with a small activation energy. The basic products of reaction are formed in the chain stretching reactions 1, 2, 4, and 5. A certain portion of excited CHF_3 molecules decays leading to chain branching

$$8.\quad CHF_3^* = CF_2 + HF$$

$$9.\quad CF_2 + F = CF_3 + F$$

$$10.\quad CF_3 + F_2 = CF_4 + F$$

It is natural for the vibrationally excited CHF_3 and other molecules to lose their energy as a result of various collisions. Pariyskaya thinks that CF_4 was formed as a result of fluorination of CH_3F, although this has not been established experimentally. As before [23], the formation of C_2F_4 and C_2F_6 was attributed to the following recombination reactions:

11. $CF_3 + CF_2 = C_2F_4$
12. $CF_3 + CF_3 = C_2F_6$

The active particles may also be destroyed as a result of heterogenous reactions or in reactions with admixtures.

The new type of mechanism is not entirely clear to the authors. Presumably work will be done to further explain the nature of this mechanism. At the present, the authors have looked only at means of formation of basic products which essentially determine the kinetics of fluorination of CH_3F.

II. PHOTODISSOCIATION LASER

No effort was made to review the Soviet work on photodissociation lasers in the previous paper [1]. The volume of Soviet literature in this area has been steadily increasing since the development of the first photodissociation laser by Pimentel in 1964. In this paper, only some of the more recent (1970-1971) Soviet papers are emphasized.

A. REACTION KINETICS

A highly formal study of the reaction kinetics of photodissociation lasers was compiled by Skorobogatov of the Leningrad State University [26]. This work serves as a basis for the mathematical analysis of the various chemical reactions which appear to inhibit the stimulated emission of CF_3I and C_3F_7I lasers [27].

1. C_3F_7I

On the experimental side, Belousova et al. studied the kinetics of the quenching of the $^2P_{1/2}$ state of I by molecular iodine in a C_3F_7I laser [28]. The technique used there involved a simultaneous recording of the laser pulses and the absorption of the 4900Å and 2700Å radiation focused on a cell containing C_3F_7I at 45-torr pressure. The study showed (Fig. 43) that I_2 concentration in the active volume increases with time and pressure. The temporal dependence of the degree of dissociation of the working molecules is shown as curve 4 in Fig. 43. The laser action was terminated after 160 μs by large quantities of I_2 quenching the $^2P_{1/2}$ state. This was confirmed by the fact that only ~60% of the C_3F_7I molecules were dissociated at the time laser action terminated in the working substance at a pressure of ~90 torr.

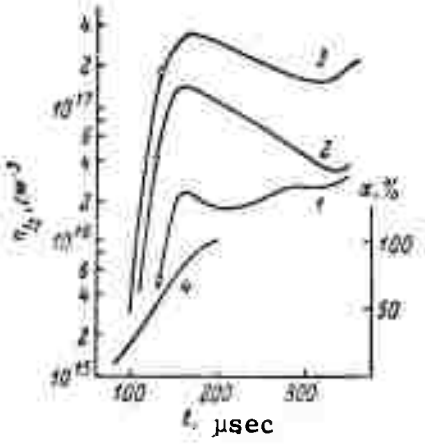

Fig. 43

Temporal dependence of concentration I_2 for different pressures of working gas (1--3) and the temporal dependence of dissociation degree of working molecules (4); circles indicate instant of generation disruption.

2. CF_3I

In another experimental work, Andreyeva et al. postulate the use of a CF_3I photodissociation laser as a convenient tool for studying the reaction kinetics of atomic iodine [29]. In view of the relatively long lifetime of the $^2P_{1/2}$ state of the excited iodine atom (~0.1 sec), it was possible to select conditions (low pressures or weak pumping) for which all of the atomic iodine remained in the excited state for a relatively long period of time ($\Delta t \approx 10^{-3}$ sec). However, at the onset of the laser action, the working volume contained both excited and stable atomic iodine. Thus, a study of CF_3I photolysis in the laser and non-laser regimes enabled the authors to separate the reactions involving the excited and stable iodine atoms.

The main thrust of the experiment was the study of the temporal dependence of formation of I_2 in the process of CF_3I photolysis as a function of absorption at $\lambda = 4650$Å. The pressure was $P_{CF_3I} = 0.1$ atm and the working substance decomposition for a given pumping did not exceed 1.5%. Under these conditions, the temperature remained practically constant ($\Delta T \leq 100°C$). Two series of experiments were performed for each value of pumping: (1) in the laser regime

and (2) without laser action, i.e., under the conditions of ordinary photolysis. The final quantity of I_2 molecules was determined by iodometric methods. In addition to this, measurement of the final amount of I_2 in CF_3I mixtures with NO in concentrations of 1:0.3, 1:1, and 1:2 was made at a constant partial pressure $P_{CF_3I} = 0.1$ atm. The NO molecules were added in order to preclude interaction between the atomic iodine with CF_3 radicals. The experimental results are shown in Fig. 44. The curves for the production of $I_2(t)$ are sharply different in the two regimes. The basic feature is the intersection of curves a and b. In the interpretation of experimental data, the following reactions of I, I^*, CF_3 radicals, and I_2 molecules were considered:

$$I + I + M \xrightarrow{k_1} I_2 + M$$

$$I + I^* + M \xrightarrow{k_1'} I_2 + M$$

$$I^* + I^* + M \xrightarrow{k_1''} I_2 + M$$

$$I^* + CF_3I \xrightarrow{k_2} I_2 + CF_3$$

$$CF_3 + I \xrightarrow{k_3} CF_3I$$

$$CF_3 + I^* \xrightarrow{k_3'} CF_3I$$

$$CF_3 + CF_3 \xrightarrow{k_4} C_2F_6$$

$$I^* + I_2 \xrightarrow{k_5} I + I_2$$

$$I^* + CF_3I \xrightarrow{k_6} I + CF_3I$$

$$CF_3 + CF_3I \xrightarrow{k_7} C_2F_6 + I$$

$$CF_3 + CF_3I \xrightarrow{k_7'} C_2F_6 + I^*$$

where M is the third component.

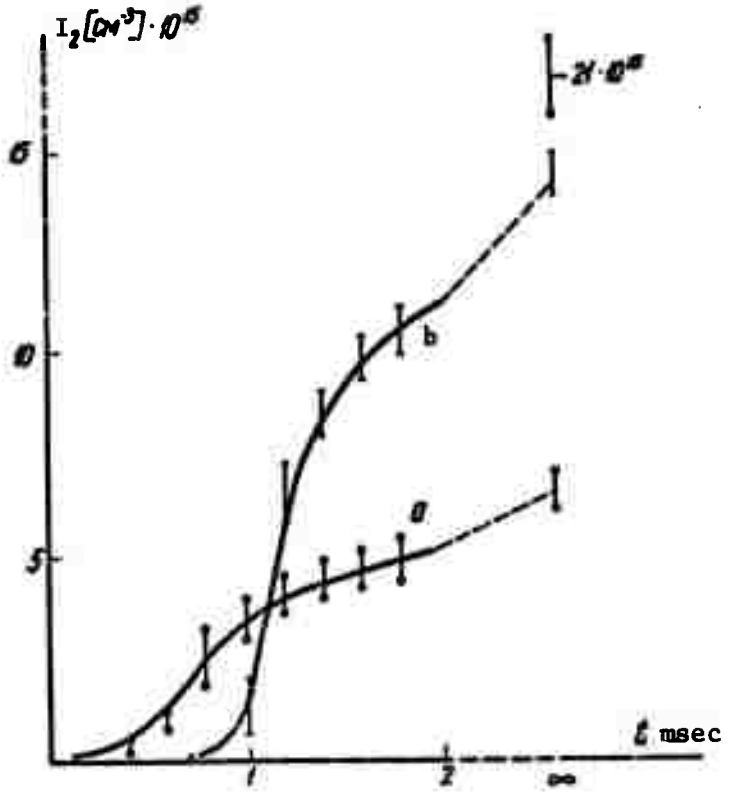

Fig. 44

Temporal dependence of I_2 formation. E_{pump} = 445j, P_{CF_3I} = 0.1 atm. (a) with laser action and (b) without laser action. Solid curves denote calculated data using the following constants: $k_1 = 5 \times 10^{-32}$ cm^6·sec^{-1}; $k_3 = 6.5 \times 10^{-11}$ cm^3·sec^{-1}; $k_3' = 3 \times 10^{-12}$ cm^3·sec^{-1}; $k_6 = 4.3 \times 10^{-17}$ cm^3·sec^{-1}.

A number of reaction rates in the above reactions are known from literature: $k_4 = 3.9 \times 10^{-11}$ cm^3 x sec^{-1}, $k_5 = 5 \times 10^{-12}$ cm^3 x sec^{-1}, $k_6 = 3.5 \times 10^{-16}$ cm^3 x sec^{-1}. The remaining constants were either calculated or measured in the experiment. Thus, when I_2 is starting to form, the working volume does not contain any free radicals CF_3. This excludes the reaction $CF_3 + I_2 \rightarrow CF_3I + I$ which under other conditions may play a considerable role. In the ordinary photolysis case (2), the upper value of the rate of reaction involving the excited iodine atoms (k_1'', k_2, k_6, k_7) can be obtained from the value

of Δt_0 (Δt_0 is time from extinction of pumping). A portion of $I_2(t)$ curve can be singled out ($t > t_{cr}$ and $[I_2]$ is greater than a certain critical value) for which all of the atomic iodine is in the ground state; k_1 can be evaluated from this section. The singular points where the curves in the laser and non-laser regimes intersect can be explained only by means of inverse recombination reactions (constants k_3 and k_3'), under the condition that $k_3 >> k_3'$. The value of the latter is determined by the difference in the final concentrations of molecular iodine in pure CF_3I in the non-laser regime and in mixtures with NO; constant k_3 can be determined by the difference in $[I_2]^{\infty}$ for the two regimes. Actually, in the non-laser regime, I atoms appear only after the disappearance of CF_3 radicals.

The final values of constants were found by machine integration of the corresponding systems of equations for the concentration. The results are:

$$k_1 = 5 \times 10^{-32} cm^6 \times sec^{-1}$$

$$k_1' \leq 2 \times 10^{-33} cm^6 \times sec^{-1}$$

$$k_1'' \leq 2 \times 10^{-33} cm^6 \times sec^{-1}$$

$$k_2 \leq 10^{-17} cm^3 \times sec^{-1}$$

$$k_3 = (4\text{--}6.5) \times 10^{-11} cm^3 \times sec^{-1}$$

$$k_3' = (3\text{--}4) \times 10^{-12} cm^3 \times sec^{-1}$$

$$k_6 = (4.3\text{--}7) \times 10^{-17} cm^3 \times sec^{-1}$$

$$k_7 \leq 3 \times 10^{-16} cm^3 \times sec^{-1}$$

Constants k_3 and k_3' were evaluated on the assumption that the corresponding reactions were binary; however, it is conceivable that these occur with the participation of the third component. The authors were unable to calculate the value of constant k_7'.

B. DYNAMICS OF CF_3I LASER

The dynamics of CF_3I photodissociation lasers were also studied by Andreyeva et al. [30]. Q-switching the CF_3I laser -- one of the few gas lasers in which output power can be scaled up in this manner -- the authors were able to determine the depth and duration of population inversion of the atomic iodine at various pumping energies and CF_3I pressures at all times. An example of the experimental results obtained for a pumping energy of 1.84 kj is shown in Table 7. The table shows that the peak power attained was 0.6 Mw at a CF_3I pressure of 0.15 atm.

Table 7

Output Characteristics of CF_3I Laser at Different Pressures

Pressure atm	Pulse energy, j			Peak power, kw			Pulse duration		
	E_1	E_2	$\frac{E_1}{E_2}$	W_1	W_2	$\frac{W_2}{W_1}$	τ_1	τ_2	$\frac{\tau_1}{\tau_2}$
0.05	0.14	0.05	2.5	7	500	70	20 μsec	100 nanosec	200
0.15	0.42	0.06	7.0	21	600	30	20 μsec	100 nanosec	200

*Subscripts 1 and 2 denote free running and giant pulse regimes, respectively.

The temporal dependence of pulse energy at various CF_3I pressures and pumping energies (delivered in ~100 μsec pulses) is shown in Figs. 45-47.

The graphical data show that changes in the pumping energy lead to substantial quali- and quantitative changes in the physicochemical processes in the iodine laser. The population inversion lifetime is not merely limited by the quenching of the excited I atoms by CF_3I, but it is dependent on the secondary reactions involving

the photolytic products of CF_3I. The data appear to be also useful in determining the range of working gas pressures, and the duration and the energy of pumping pulses within which a CF_3I laser can be operated in a giant pulse mode.

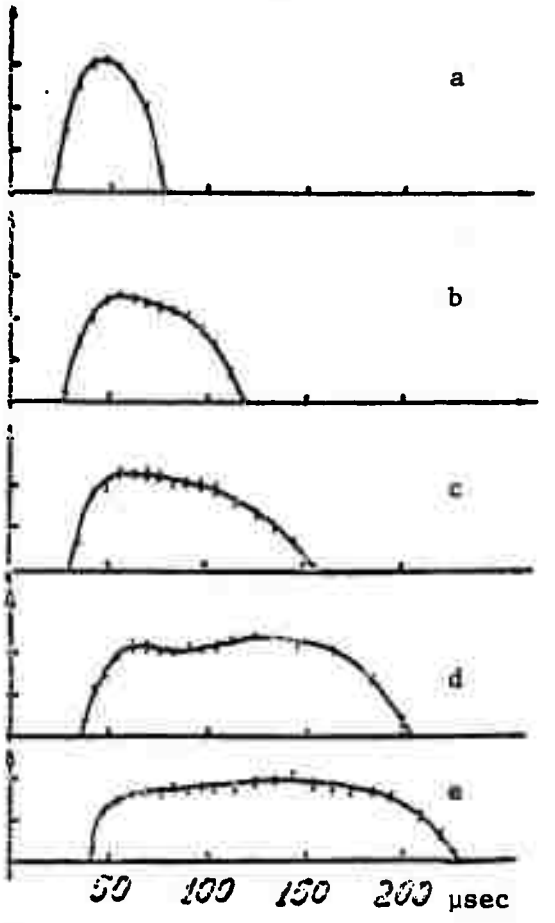

Fig. 45

Dependence of total output energy (proportional to the magnitude of population inversion) on Q-switching time for P_{CF_3I} = 0.15 atm and various pumping energies. E_{pump}: a -- 1840j; b -- 1360j; c -- 1140j; d -- 940j; e -- 760j.

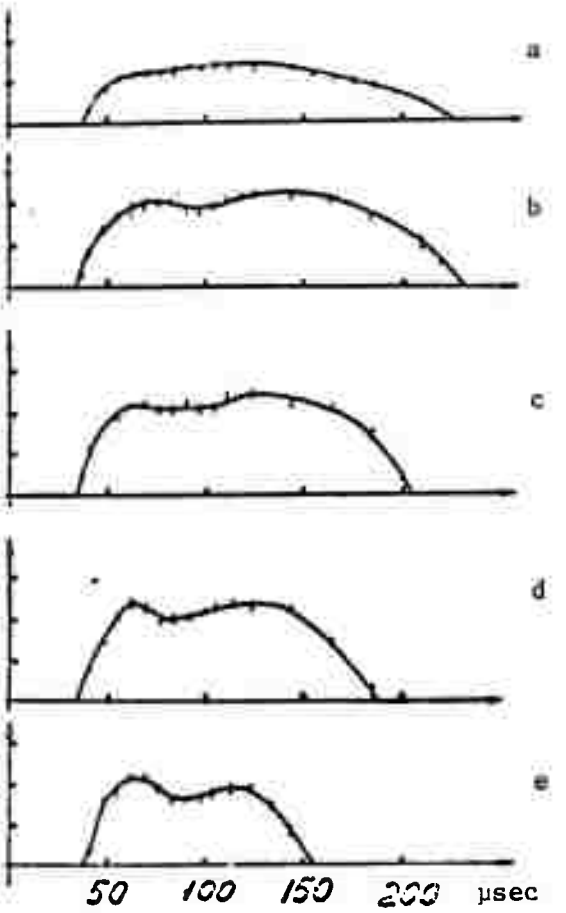

Fig. 46

Dependence of total output energy on Q-switching time for E_{pump} = 940j and various P_{CF_3I} pressures in atm:
a -- 0.05; b -- 0.10; c -- 0.15; d -- 0.20; e -- 0.25.

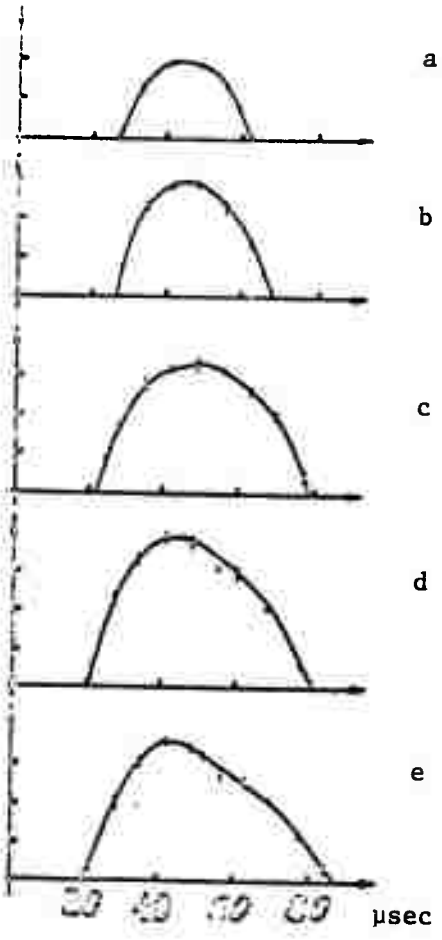

Fig. 47

Dependence of total output energy on Q-switching time for E_{pump} = 1840j and various P_{CF_3I} pressures in atm:
a -- 0.05; b -- 0.10; c -- 0.15; d -- 0.20; e -- 0.25.

C. REPETITIVELY PULSED LASER

One of the inherent limitations of photodissociation lasers is the irreversibility of the chemical processes occurring in them. Before the second pulse can be obtained, the reaction vessel has to be flushed out and recharged. This disqualifies such lasers for physical studies. On the other hand, lasers in which the dissociated products readily recombine into the original fuel are highly desirable since periodic (and, in principle, cw) operation is possible in a sealed-off tube. Giuliano and Hess were the first

to show this for the case of NOCl and IBr.[≠] Their work was picked up recently by Dudkin et al. [31], although not without criticism that the Giuliano-Hess experiments were carried out under single pulse conditions.

The Soviet experiments were carried out at relatively low pumping pulse repetition frequencies (6--7 pps). The pumping and laser pulses are shown in Fig. 48.

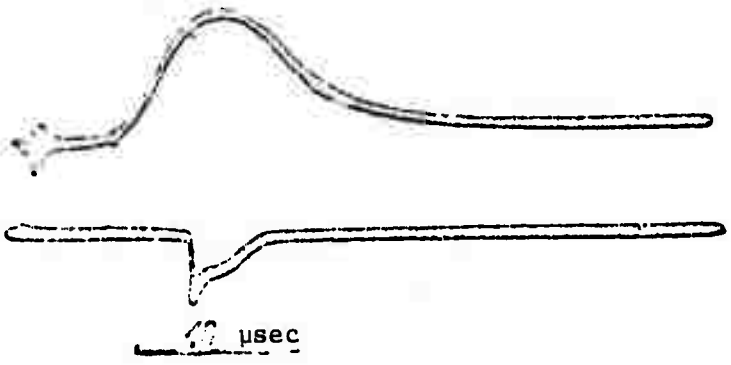

Fig. 48

Pumping and laser pulses.

Operating a sealed-off laser in a repetitive pulse regime without changing the fuel causes a gradual decrease in the output energy. This is shown in Fig. 49, where average data are shown for 5 laser pulses and tube temperatures are indicated for 0, 10, and 55 pulses. When the tube was cooled, the output energy returned to the previous level. The experimental data shows a 25-30% decrease in the pulse energy with an increase in the tube temperature from 20° to 60° C. This decrease appears to be associated with the periodic operation of the laser itself, if one assumes that IBr recombines partially before the onset of the next pumping pulse. The authors further assume that the recombination of IBr is a 2-step process, consisting of rapid formation of IBr, I_2, and Br_2 molecules

[≠] J. Appl. Phys., 38, 4451, 1967 and 40, 2428, 1969.

followed by a slower formation of IBr in the reaction $I_2 + Br_2 \rightarrow 2IBr$. Depending on the pump-pulse repetition rate, IBr concentration falls off with increasing I_2 and Br_2 concentrations which, in turn, may intensify the quenching of Br^*. The rise in the cell temperature prevents I_2 from collecting on the tube walls.

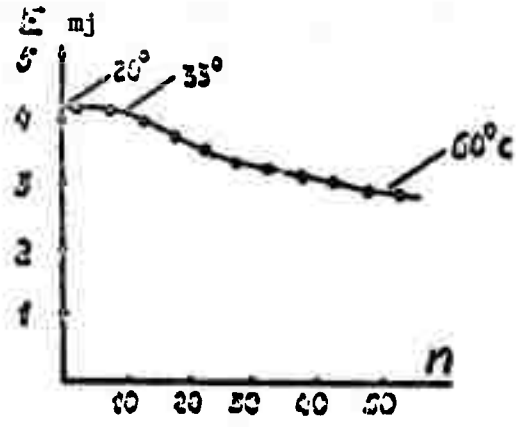

Fig. 49

Dependence of output energy on the number of pulses. E_{pump} = 900j, period 7 sec.

The maximum output energy for a 900j pumping was 3--4 x 10^{-3}j and the peak power in a 4--5-μsec pulse was on the order of 1 kw.

D. LINEWIDTH MEASUREMENTS

One of the important laser parameters is the spectral width of the stimulated transition line $\Delta\lambda$ which is directly related to the gain cross section σ by the following expression:

$$\sigma = \lambda^4/4\pi^2 c\ \tau\Delta\lambda \qquad (2.1)$$

where c is the speed of light, λ is the wavelength of the line center and τ is the lifetime of the excited level.

Linewidth measurements of the $^2P_{1/2} - {}^2P_{3/2}$ transition of the atomic iodine were made by Volkov and Zubarev using the second harmonic of the C_3F_7I photodissociation laser [32]. At the time of

publication (October 1970), this was claimed to be the first attempt to obtain the stimulated linewidth of the excited iodine atom. The experimental setup is shown in Fig. 50.

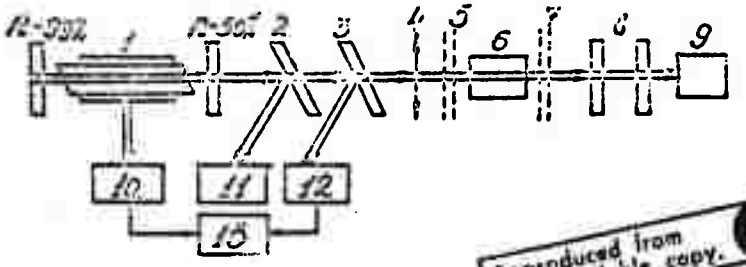

Fig. 50

Experimental setup; 1 -- photodissociation laser; 2,3 -- glass plates; 4 -- f = 33 cm optics; 5 -- 1KS-2 ir filter; 6 -- KDP crystal; 7 -- S3S-14 filter; 8 -- Fabry-Perot etalon; 9 -- camera in SP-51 spectrograph; 10 -- F-7 photocell; 11 -- calorimeter; 12 -- photodiode; 13 -- OK-17M oscillograph.

The bore of the coaxial flashlamp (15 mm) served as the discharge tube (250 mm long), a technique which neutralized the effect of an uncontrolled magnetic field on the active medium. The magnetic field was < 10 oe. The working medium was either pure or Xe-doped C_3F_7I. The flashlamp was fed from a 300-μf 2-kv condenser bank. The cavity consisted of two 100%- and 50%-reflective mirrors, 30 cm apart and parallel to within 10^{-4} rad. The duration of the quasi-cw laser pulse was ~25μsec and the energy 0.02--0.15j. The experiments were carried out in the pressure range from 5 to 120 torr for pure C_3F_7I and at $P_{C_3F_7I}$ = 5 torr and P_{Xe} = 700 torr for the mixture. The second harmonic conversion of the C_3F_7I laser pulse was made by means of a KDP crystal with 1% efficiency. The converted signal was fed into the slit (2 mm) of a Fabry-Perot etalon. The experimental results are shown in Fig. 51.

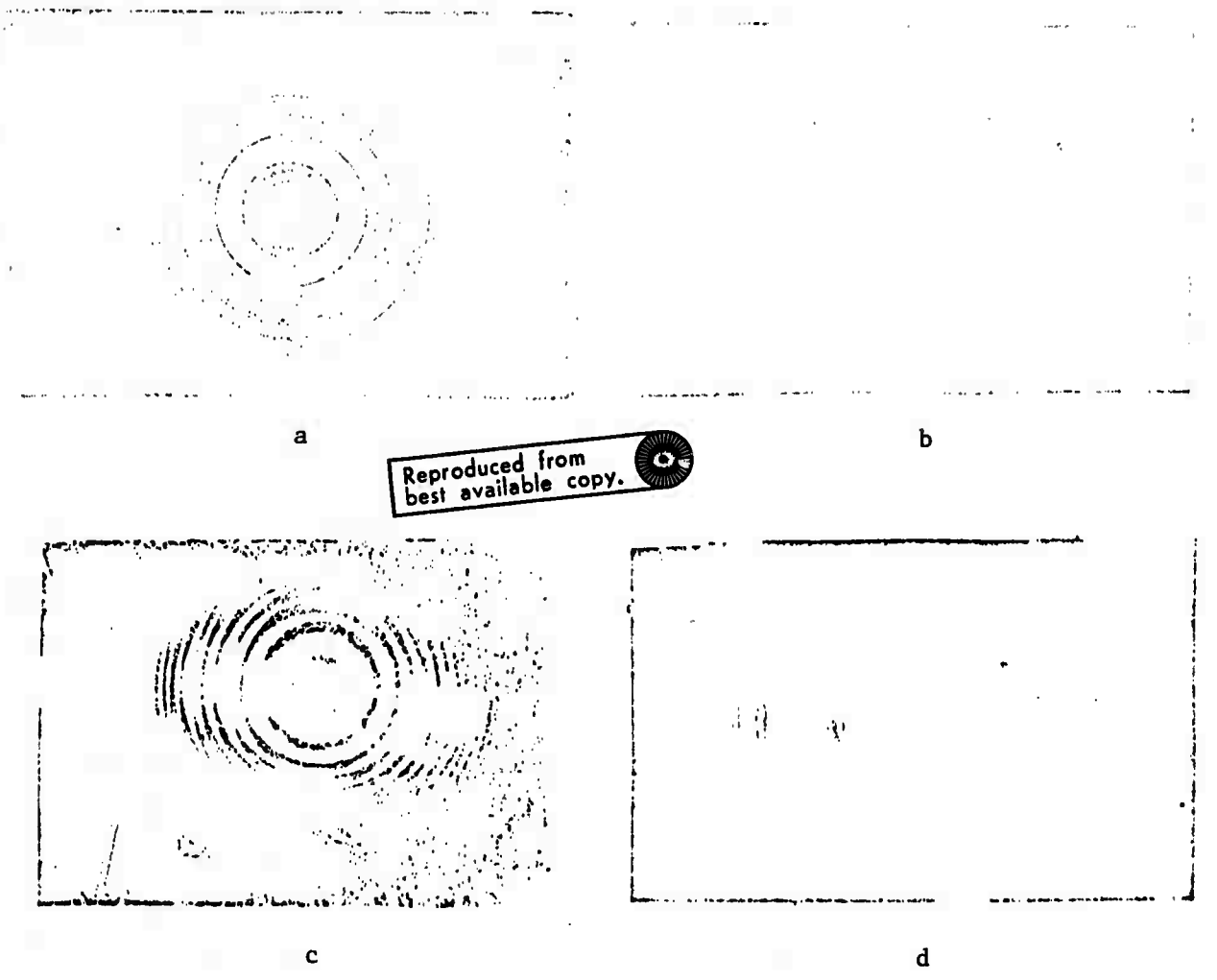

Fig. 51

Fabry-Perot interferograms of the second harmonic of C_3F_7I laser. a -- C_3F_7I at 40 torr pressure, slit width 2 mm; b -- C_3F_7I at 40 torr pressure, slit width 30 mm; c -- $P_{C_3F_7I}$ = 5 torr P_{Xe} ~ 700 torr; d -- interferogram obtained by means of an image converter; $P_{C_3F_7I}$ = 40 torr, slit width 2 mm.

The upshot of the experiments was the detection of two highly intense fine-structure components of the $P_{1/2} \rightarrow P_{3/2}$ transition with an 0.47 cm^{-1} separation for a pure C_3F_7I at pressures from 5 to 120 torr. In the case of a C_3F_7I-Xe mixture at the corresponding partial pressures of ~5 and ~760 torr, only one spectral line

was observed. The latter result is attributable to the piling up of the fine structure components -- which at working-substance pressures of ~1 atm are shock broadened -- which are observed as a single homogeneously broadened line. The measured width of the spectral line was $< 5 \times 10^{-3} cm^{-1}$.

Velikanov's measurement of the $5^2P_{1/2} \rightarrow 5^2P_{3/2}$ linewidth of C_3F_7I emission was carried out at $\lambda = 1.315\mu$ and at lower (than Volkov's) C_3F_7I pressures (38 and 50 torr) [33]. The interferograms are shown in Figs. 52 and 53. The laser linewidth was ~0.04Å for both values of pressure. Also measured was the intermode spacing in a 1-m cavity which was 0.0086Å and the mode width -- in the case of 99 and 8% reflective mirrors -- was 0.0035Å. This would indicate that the laser spectrum consists of 4--5 modes. However, the authors were unable to resolve the latter due to photodiode and F-P etalon limitations. The observed linewidth value yields (from Eq. (2.1)) the upper limit for σ which is $\leq 5 \times 10^{-18} cm^2$.

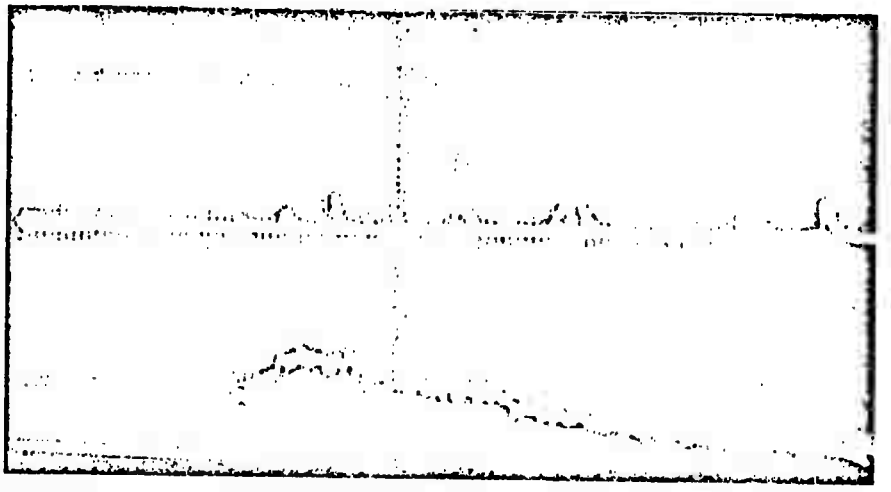

Fig. 52

Upper beam shows at RHS two spikes which correspond to interference maxima of control ring. Lower beam is the laser pulse. Scanning (duration 100 μsec) begins with the onset of pumping.

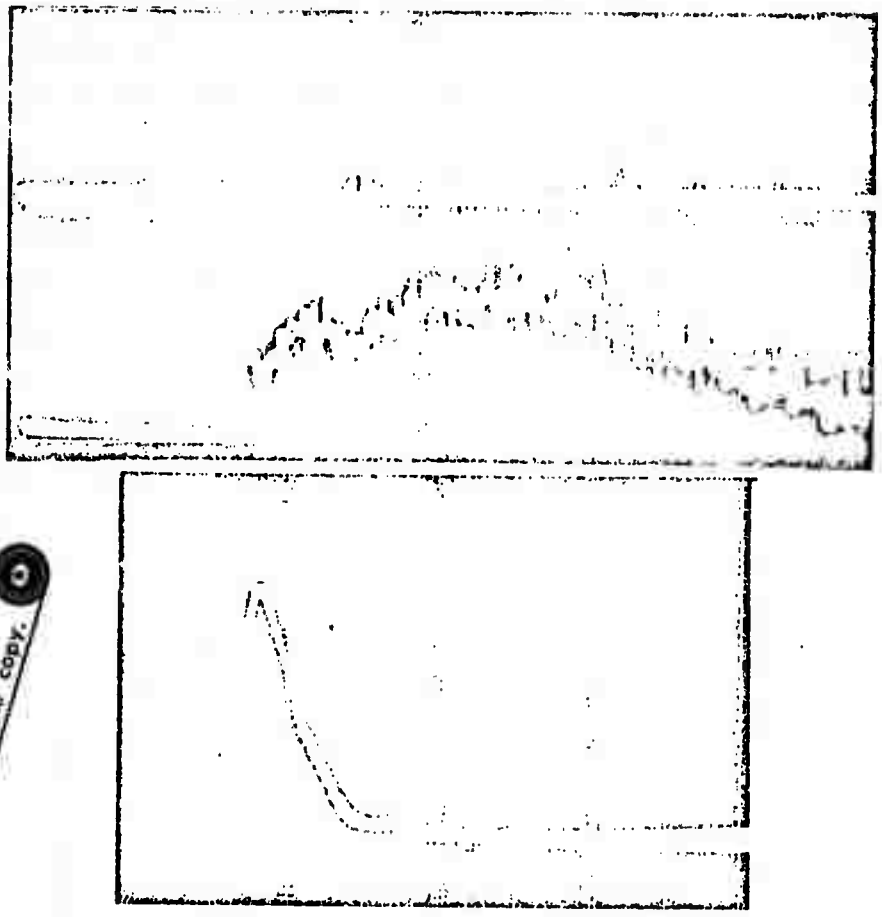

Fig. 53

Photodiode signal also fed to oscillogram (lower figure) which shows the first maximum (upper trace) of central ring. Scanning 8 μsec.

The study of the width and form of the stimulated (or spontaneous) transitions of atoms and molecules can be used in calculating the relaxation rates of individual levels. The method proposed by Beterov, Matyugin and Chebotayev [34] involves measuring the linewidth of stimulated (or spontaneous) resonance scattering in a gas with a three-level structure (see Fig. 54).

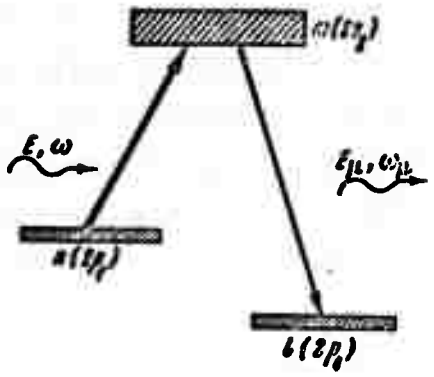

Fig. 54

System of levels for observing stimulated resonance scattering

In such a system, the difference between the widths of forward- and back-scattered radiation yields the width of the total level (γm), i.e.,

$$\Gamma_0 - \Gamma_- = 2\gamma_m \qquad (2.2)$$

which, in the case of "strong" collisions -- such as those associated with resonant transfer -- can be expressed as follows

$$\Gamma_0 - \Gamma_- = (2\gamma_m + 2\nu) \qquad (2.3)$$

where ν is the collisional frequency of an atom or molecule in the m-th state.

Beterov's experiments were carried out using the $2s_2$-$2p_1$ (λ=1.52μ) and $2s_2$-$2p_4$ (λ=1.15μ) Ne transitions with the common $2s_2$ level. The experimental apparatus was the same as that described earlier (ZhETF P, Vol. 10, p. 296, 1969, and ZhETF, Vol. 58, p. 1243, 1970), where the diffusion of excitation was studied in the case of resonant radiation capture. The significant difference between the present [34] and past experiments was a provision made for recording the line shape without the effect of Doppler "cushioning" which the resonant

capture entails. This procedure had facilitated the observation and processing of measurements of the form of a scattered line in that portion where narrow resonances occur with widths Γ_0 and Γ_-. Under the experimental conditions, the S/N ratio was greater than 20 db (Fig. 55). The measured linewidth of the $2s_2$ level was (27.5 + 14p) $\pm$ 5 MHz (where p is neon pressure in torr). This favorably compares with the values obtained by alternate methods used by the authors and others (Lawrence and Listt, Phys. Rev., 178, 122, 1969). Although the value itself is irrelevant, its coincidence with values obtained by other methods highly underscores the utility of this method as a tool in linewidth measurements.

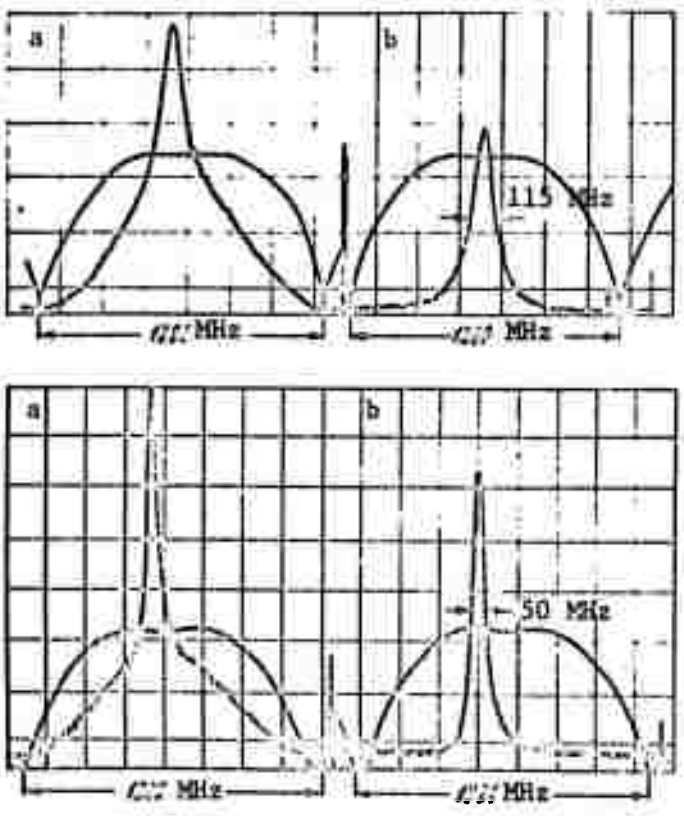

Fig. 55

Line shape of shifted stimulated resonance scattering a -- without Doppler cushioning, b -- pure scattering line. Upper curves -- back scattering (P_{Ne} = 0.5 torr); Lower curves; forward scattering (P_{Ne} = 0.9 torr). Broadening due to field was 11 MHz and 6 MHz for forward- and back-scattering, respectively.

III. PHOTORECOMBINATION LASER

In the preceding note [1], a new type of chemical laser was described in which the stimulated transition of electrons occurred at the very instant of contact between two unexcited reagents (atoms, molecules, radicals), the event coinciding with the elementary act of a chemical reaction:

$$1.\quad A_2 + B_2 \rightarrow 2AB + \{_{Q}^{h\nu}$$

In such a laser, the increasing radiation intensity speeds up not only the stimulated transitions but also the reaction itself. The latter thus ceases to be a factor which limits the rate and strength of the laser process. Proposed by Pekar and dubbed a "high-pressure chemical laser," this device was studied in detail theoretically in a number of articles [35-37].*

A. REACTION KINETICS

A detailed study of the kinetics of the photorecombination laser described in [1] was made by Kochelap and Pekar as a single mode approximation for the steady-state regime under the conditions of spatially homogeneous pumping density, radiation intensity, and concentrations of initial molecules and the reaction products [35]. Calculations were made for two cases: recombination or addition reactions in which the product of the elementary act is a single molecule, and exchange or substitution reactions in which two unbound molecules are produced.

---

*Under a relatively low gas pressure, an excited molecule will lase before being deactivated by collisions with other molecules, without producing a chemical reaction. Pressure limitations will limit the optical yield.

1. Recombination or Addition Reaction

Let the reaction equation have the following form:

2. A + B = AB

Let the concentrations remain equal at the time of the reaction $n_A = n_B = n$. Also, let m be the concentration of the AB molecule. There are two ways in which molecules A and B will come in contact with each other: (1) simple elastic gas-kinetic collision in which the contact time is on the order of 10^{-13} sec and which is normally achieved in the case of simple monoatomic molecules; and (2) gas-kinetic collision, where the kinetic energy is first transferred into the energy of the internal degrees of freedom of these molecules, as a result of which they appear bound for a considerably long period of time. In a resultant quasi-molecule of this sort, atoms continue their conservative motion until such time when the energy stored in a specific degree of freedom is sufficient to dissociate the quasi-molecule into A and B. The converging molecules A and B may form a quasi-molecule in several electron states. For the sake of simplicity, the authors assume that the principal role is played by two electron states only with concentrations n' and n".

The kinetic equations for case (2) are given below. Case (1) can be considered as a special case of (2) to which these equations are also applicable. If q is the photon flux density and V is the resonator volume, the kinetic equations can be written in the following manner:

$$\frac{dn}{dt} = W - (r' + r'')n^2 + d'n' + d''n'' + a''n''q = 0, \tag{3.1}$$

$$\frac{dn'}{dt} = r'n^2 - (d' + k')n' - b\left(\frac{1}{V} + q\right)n' + aqm = 0, \tag{3.2}$$

$$\frac{dn''}{dt} = r''n^2 - (d'' + k'' + a''q)n'' = 0, \tag{3.3}$$

$$\frac{dm}{dt} = b\left(\frac{1}{V} + q\right)n' - aqm + k'n' + k''n'' - g_1m - g_2m^2 = 0, \tag{3.4}$$

$$\frac{dq}{dt} = b\left(\frac{1}{V} + q\right)n' - aqm - a''qn'' - \gamma q = 0. \tag{3.5}$$

where W is the density of pumping radiation, i.e., the number of pairs of initial molecules A and B per unit volume per second; $r'n^2$ and $r''n^2$ are terms for the recombination of molecules A and B per unit volume per second corresponding to the formation of quasi-molecules in the first and second electron states; d'n' and d"n" are the numbers of thermal dissociations of these quasi-molecules into molecules A and B, a"qn" is the number of absorbed photons by quasi-molecules in the second electron state, the absorption being accompanied by dissociation of quasi-molecules; $b(1/V + q)n'$ is the number of spontaneous and stimulated photons in the working mode, i.e., the number of phototransformations of quasi-molecules in the first electron state into the reaction products (stable molecules AB); aqm is the number of inverse phototransitions; k'n' and k"n" are the numbers of elementary acts of chemical reaction due to other mechanisms (normal thermal chemical reaction, radiative chemical reaction with spontaneous emission of photons other than those of the working mode); g_1m and g_2m^2 are the rates at which the reaction products are removed (linear and quadratic with respect to concentration); γq is the rate of loss of working-mode photons per unit volume, i.e., volumetric scattering of photons, partial reflection by mirrors, etc.

It should be pointed out that the rate of normal thermal chemical reactions may be determined by collisions of quasi-molecules with third bodies (original molecules, reaction products, molecules of an impurity gas). Thus, coefficients k' and k" may depend on the concentration of these substances. The remaining coefficients r', r", d', d", g_1, g_2, a, a", b, and γ are independent of concentration and depend on the temperature if one assumes that for each electron state of a molecule and quasi-molecule a thermal equilibrium is attained for the vibrational, rotational and translational degrees of freedom with one and the same temperature for all. If, however, such thermal equilibrium is not achieved, the above coefficients will depend on the rate of the entire laser process, i.e., on W. The last four coefficients also depend on the frequency of the working mode photons.

It should be pointed out that Eqs. (3.1-3.5) can also describe the kinetics of a normal chemical laser in which the elementary chemical reaction of addition --- in which a stable excited molecule is formed -- precedes the stimulated emission. In this case, term $r'n^2$ should be interpreted as the rate of chemical reaction in which molecule AB is formed in such an excited electron state from which a stimulated phototransition preeceds. Term $r''n^2$ corresponds to a chemical reaction in which the same product is formed but in a different electron state. Coefficients d' and d" are both trivial, which corresponds to neglecting of the reverse chemical processes. Coefficient a" is also trivial. Terms k'n' and k"n" should be interpreted as rates of deactivation of the excited reaction products.

Clearly, terms $r''n^2$ and k'n' correspond to a process which decreases the quantum yield of the laser. For the sake of simplicity, the authors first considered a laser with a quantum yield equal to 1. In this case, the number of photons emitted per unit volume of gas per unit time is W. Subsequently, they explained under what conditions W can be increased in the steady state regime.

It obtains from Eq. (3.1) that $W \leq r'n^2$. Consequently, large laser power is principally associated with a large value of r' and a high gas pressure. In this connection, it is interesting to compare the capabilities of a "normal" chemical laser and the Pekar laser. In the case of an ordinary chemical addition reaction -- which occurs in the course of triple molecular collisions -- $r'_{chem} \leq uv^{5/3}n_3$, where v is the gas-kinetic volume of a molecule, u is its average thermal velocity, and n_3 is the concentration of the "third body" molecules. In the Pekar laser, $r'n^2$ is the number of simple gas-kinetic paired collisions per unit volume per second, so that $r' = uv^{2/3}$. Thus,

$$\frac{r'_{chem}}{r'} \leq vn_3 \qquad (3.6)$$

when $v = 10^{-23}\text{cm}^3$ and $n_3 = 10^{19}\text{cm}^{-3}$, $r'_{chem}/r' \leq 10^{-4}$. This shows that the power limit of the Pekar laser considerably exceeds the power limit of "normal" chemical lasers.

After certain transformations, Eqs. (3.1-3.5) can be written in the following form:

$$Aq^3 + Bq^2 - Cq - \frac{W\delta}{V} = 0 \tag{3.7}$$

$$m = \frac{g_1}{2g_2}\left[\sqrt{1 + \frac{4g_2}{g_1^2}W} - 1\right] \tag{3.8}$$

where the following notations are introduced:

$$b_0 \equiv \frac{a''r''d'}{r'd'' + k''(r' + r'')}, \quad \delta \equiv \frac{r'(d'' + k'')}{r'd'' + k''(r' + r'')},$$

$$A \equiv \gamma\frac{r'b_0}{r''d'}, \quad B \equiv W\frac{b_0}{d'}\left(1 - \frac{r'}{r''}\right) + \frac{amb_0}{b}\left(1 + \frac{r'k'}{r''d'}\right) + \gamma\left(1 + \frac{r'b_0}{Vd'r''} + \frac{k'r'b_0}{d'r''b}\right)$$
$$C \equiv \left(1 - \frac{b_0}{b}\right)(W\delta - kn_0) - \frac{Wb_0}{d'V}\left(1 - \frac{r'}{r''}\right) - \frac{\gamma}{V}, \tag{3.9}$$

$$k \equiv \frac{(d' + k')k''r'' + (d'' + k'')k'r'}{r'd'' + k''(r' + r'')}, \quad n_0 \equiv \frac{am + \gamma + b_0\frac{W}{d'}}{b - b_0}.$$

It could be shown by a numerical calculation that terms proportional to 1/V and corresponding to the spontaneous emission in the expressions for B and C, can be neglected.

In the region of small q's, which include the below-threshold, threshold, and even above-threshold regimes of the laser, term q^3 can be neglected in Eq. (3.7). As a result of this, a quadratic equation for q is obtained

$$q = \frac{1}{2B}\left[C + \sqrt{C^2 + 4B\frac{W\delta}{V}}\right] \tag{3.10}$$

where $4B\frac{W\delta}{V}$ is several orders of magnitude smaller than C^2. Expressions for q in the below- and above- threshold regions are as follows:

$$q = -\frac{W\delta}{CV} \tag{3.11}$$

$$q = \frac{C}{B} \tag{3.12}$$

The threshold value of W, for which the sign of C changes and the onset of laser regime begins, can be calculated for the two limiting cases:

Case 1:

$$\frac{4g_2}{g_1^2} W << 1 \tag{3.13}$$

where in accordance with Eq. (3.8), $m = W/g_1$. In this case, the above-threshold regime occurs when

$$[W > \gamma \left[\frac{b - b_0}{k} \delta - \frac{a}{g_1} - \frac{b_0}{d'} \right]^{-1} \tag{3.14}$$

and the following condition is necessary

$$\frac{b - b_0}{k} \delta - \frac{a}{g_1} - \frac{b_0}{d'} > 0 \tag{3.15}$$

and

Case 2:

$$\frac{4g_2}{g_1^2} W >> 1, \quad m = \sqrt{\frac{W}{g_2}} \tag{3.16}$$

the above-threshold regime occurs when

$$W > \left\{ \frac{\frac{a}{\sqrt{g_2}} + \sqrt{\frac{a^2}{g_2^2} + 4\gamma\left[\frac{\delta}{k}(b - b_o) - \frac{b_0}{d'}\right]}}{2\left[\frac{\delta}{k} b - b_0) - \frac{b_0}{d'}\right]} \right\}^2 \tag{3.17}$$

and when the following condition is necessary:

$$\frac{\delta}{k} (b - b_0) - \frac{b_0}{d'} > 0 \tag{3.18}$$

The case for large q's (when in Eq. (3.7) the cubic term is preserved and $\frac{W\delta}{V}$ is neglected) is considered subsequently. In this case

$$q = \frac{1}{2A} [-B + \sqrt{B^2 + 4AC}] \tag{3.19}$$

The above solution coincides with Eq. (3.12) when $4AC << B^2$. The quantum yield of a laser is

$$\eta = \frac{\gamma_0 q}{W} \tag{3.20}$$

where $\gamma_0 q$ is the number of photons per unit volume of resonator which pass through the mirror per unit time ($\gamma_0 \leq \gamma$).

The above analysis shows that the rate of the laser process both in the pulsed and steady-state regimes is governed by recombination rate $r'n^2$. In the case of the Pekar laser, this rate is on the order of $2.5 \times 10^{27} cm^{-3} \times sec^{-1}$ for $u = 5 \times 10^4 cm \times sec^{-1}$, $v = 10^{-23} cm^3$, and $n = 10^{19} cm^{-3}$. In the case of $\eta = 1$ and the emitted photon energy of 2 ev, this corresponds to a power of 8×10^8 watt$\cdot cm^{-3}$. In the steady-state regime, $r'n^2$ constitutes the upper limit for W.

In Eqs. (3.1-3.5), terms $g_1 m$ and $g_2 m^2$ are the linear and quadratic (with respect to concentration) rates of removal of the reaction products. The linear dependence is realized, for example,

(1) when the products are pumped out from the working volume or when they are removed by a continuous flow of gas, (2) when the reaction products are destroyed by means of a chemical reaction with a third gas, (3) in the course of spontaneous transitions and thermal transition of electrons in the reaction products if the latter are excited, etc. In the case of the removal of reaction products by continuous gas flow, $g_1 = U/l$, where U is the gas flow rate and l is the optical length of the working gas volume in the direction of the flow. Assuming that $U = 10^5 cm \cdot sec^{-1}$ and $l = 1$ cm, g_1 yields $10^5\ sec^{-1}$.

The reaction products are removed at a nonlinear (quadratic) rate when they react with each other during collisions. If the reaction occurs in the presence of molecules of the third gas whose concentration is $10^{19}\ cm^{-3}$, $g_2 \sim 5 \times 10^{-5} cm^3 \times sec^{-1}$.

In verifying Eqs. (3.13 and 3.16), it should be noted that $\frac{4g_2}{g_1^2} \cdot W = 1$, when $W = 5 \times 10^{23}\ cm^{-3} \times sec^{-1}$.

The thermal dissociation rates of quasi-molecules d' and d" in case 1 were on the order of the inverse time of the gas-kinetic contact between the two molecules, and in case 2, one or two orders of magnitude smaller. It was assumed that $d' \sim d'' \sim 10^{11}$--$10^{13}\ sec^{-1}$.

The rate of the thermal chemical reaction k' was determined assuming that a quasi-molecule undergoes an elementary act of reaction for nearly every collision. As a result of this, $k \sim k' \sim 2.5 \times 10^8\ sec^{-1}$.

2. Exchange or Substitution Reaction

The chemical reactions considered in this section pertain to those reactions whose products are two unbound molecules. These reactions are of the type:

3. $AB + C = AC + B$

4. $AB + CD = AC + BD$

For the sake of simplicity, Kochelap and Pekar discuss only a case where in colliding, the initial molecules form quasi-molecules in one electron state only. The concentration of such quasi-molecules is n'. As a result of stimulated phototransition or thermal transition of electrons, such a quasi-molecule is transformed into an unstable quasi-molecule of the reaction product, whose concentration is m' Each of the latter decays into two molecules which form the final reaction product, with concentration m.

The kinetic equations have the following form:

$$\frac{dn}{dt} = W - r'n^2 + d'n' = 0 \tag{3.21}$$

$$\frac{dn'}{dt} = r'n^2 - d'n' - k'n' - b(\frac{1}{V} + q)n' + aqm' = 0 \tag{3.22}$$

$$\frac{dm'}{dt} = r''m^2 - d''m' + k'n' + b(\frac{1}{V} + q)n' - aqm' = 0 \tag{3.23}$$

$$\frac{dm}{dt} = -r''m^2 + d''m' - g_1m - g_2m^2 = 0 \tag{3.24}$$

$$\frac{dq}{dt} = b(\frac{1}{V} + q)n' - aqm' - \gamma q = 0 \tag{3.25}$$

The majority of terms in these equations has the same sense as in the case of the recombination reaction. The only difference with Eqs. (3.1--3.5) is the fact that the absorption of the working mode photons represented by term aqm' is due to unstable quasi-molecules in the terminal electron state, whose concentration rn' is small.

Equations (3.21--3.25) also yield a type Eq. (3.8) formula, with critical case equations (3.13) and (3.16). Furthermore, from the above equations, it follows that

$$n^2 = \frac{1}{r'}\left[W(1 + \frac{d'}{k'}) - \frac{d'\gamma}{k'}q\right] \tag{3.26}$$

$$n' = \frac{1}{k'}(W - \gamma q) \tag{3.27}$$

$$m' = \frac{1}{d''}(W + r''m^2) \tag{3.28}$$

As before, equations for q are obtained except that the expressions for coefficients are simpler than those in Eq. (3.9):

$$B \equiv \gamma,\ \delta = 1,\ C = \xi W + \frac{k'ar''g_1^2}{2bd''g_2^2}\sqrt{1 + \frac{4g_2W}{g_1^2}} - \frac{k'\gamma}{b} - \frac{\gamma}{V} \tag{3.29}$$

$$\xi \equiv 1 - \frac{ak'}{bd''}\left(1 + \frac{r''}{g_2}\right)$$

The laser regime occurs in the case of Eq. (3.12) when q is several orders of magnitude greater than in the case of Eq. (3.11). In accordance with Eq. (3.29), when $\xi > 0$, C increases monotonically with W, and goes from negative to positive values. The change in the sign of C occurs in the region determined by Eq. (3.16). The corresponding threshold value of W is determined by the expression below:

$$W > \frac{k'\gamma}{\xi b} \tag{3.30}$$

In this case, for large values of W, the quantum yield is:

$$\eta \to \frac{\gamma_0}{\gamma}\,\xi \tag{3.31}$$

For $\xi < 0$, with increasing W, C goes through a maximum and then decreases to $-\infty$. If at the maximum $C > 0$, there exists a region of values of W bounded on both sides in which laser regime is realized (Eq. (3.12)). Condition $\xi < 0$ is not compatible with Eq. (3.16). In the critical case, Eq. (3.13), the limits of the laser regime region are determined by the following formulas:

$$W_1 < W < W_2, \quad W_{1,2} = \frac{g_1^2 bd''}{2ak'r''}\left[1 - \frac{ak'}{bd''} \pm \sqrt{\left(1 - \frac{ak'}{bd''}\right)^2 - \frac{4k'^2 ar''\gamma}{b^2 d'' g_1^2}}\right] \quad (3.32)$$

It is essential that the maximum value of C is positive

$$C_{max} = \frac{g_1^2 bd''}{4ak'r''}\left(1 - \frac{ak'}{bd''}\right)^2 - \frac{k'\gamma}{b} > 0 \quad (3.33)$$

When $\xi = 0$, the threshold condition has the following form:

$$W > \frac{\gamma^2 g_2^3 d''^2}{a^2 r''^2 g_1^2}\left[1 - \left(\frac{ar'' g_1^2}{2\gamma d'' g_2^2}\right)^2\right] \quad (3.34)$$

and $\eta \to 0$ when $W \to \infty$.

3. Thermal vs. Photostimulated Reaction Comparison

The analysis of Eqs. (3.1--3.5) and (3.21--3.25) shows that these describe not only the kinetics of chemical lasers but also the kinetics of self-photostimulated chemical reactions which occur in the resonator. The chemical reaction may occur simultaneously in two ways: "normal" thermal and with stimulated emission of light. When the pumping power W is less than a certain threshold value, the first mechanism predominates; when W is greater than the threshold value, the second mechanism takes over.

In the chemical laser, both in the steady-state and pulsed regimes, the rate of the entire laser process is controlled by the rate of the bimolecular recombination of the initial molecules $r'n^2$. In an ordinary chemical laser, such recombination constitutes an elementary act of a chemical reaction. In the Pekar laser, however, the rate of recombination is the number of simple gas kinetic collisions per unit volume per second which considerably exceeds the rate of bimolecular reaction in a "normal" chemical laser. Correspondingly, also the peak power in a recombination laser can be greater than in an ordinary laser.

In the case of the addition reaction, if $b_0 \neq 0$ when $\beta > 0$, the photon density in the resonator q tends to a constant value with increasing W, and $\eta \to 0$. In the case when $\beta < 0$, q increases proportionally with W, and η tends to a constant value. When $\beta = 0$, q changes proportionally to the $\sqrt{W}$ and $\eta \to 0$. The greatest interest is presented by the case when $\beta < 0$. In this case, the greatest quantum yield is obtained when $g_2 > 0$, i.e.,

$$\eta \to \frac{\gamma_0}{\gamma} \begin{cases} 1 - \frac{r''}{r'} - \frac{a}{g_1 b}\left(k' + \frac{r''d'}{r'}\right) & \text{for } g_2 = 0 \\ 1 - \frac{r''}{r'} & \text{for } g_2 > 0 \end{cases} \tag{3.35}$$

when the rate of removal of reaction products is proportional to the square of their concentration.

However, the most favorable case is when $b_0 = 0$ (the absorption of laser radiation by quasi-molecules in the second electron state does not exist). Then, the greatest quantum yield is obtained also when $g_2 > 0$:

$$\eta \to \frac{\gamma_0}{\gamma} \begin{cases} \delta - \frac{ak}{bg_1} & \text{for } g_2 = 0 \\ \delta & \text{for } g_2 > 0 \end{cases} \tag{3.36}$$

It should be pointed out that the competing thermal chemical reaction is characterized by coefficient k' and it does not decrease the quantum yield in the region of large W's, since in this case the rate of photostimulated reaction increases by such an amount that the concurrent thermal reaction is not substantial. Conversely, a chemical reaction during which quasi-molecules in the second electron state are formed and which is characterized by the product r"k", decreases the quantum yield since even in the limit W, $q \to \infty$, and the reaction rate in which quasi-molecules in the first electron state are formed is not infinite but is bound by the value $r'n^2$.

In the case of exchange or substitution reaction, according to Eqs. (3.29) and (3.31), when $\xi > 0$, density q increases proportionally to W and the quantum yield tends to a constant value. The case where $\xi > 0$ is realized for sufficiently large values of g_2. In the case where $\xi < 0$, laser regime is realized for the values of W bound on both sides when the necessary condition -- Eq. (3.33) -- is satisfied. This region broadens with an increase in g_1. When $\xi = 0$, q increases proportionally to $\sqrt{W}$, and $\eta \to 0$. The most favorable is the case of positive values of ξ near the unity. It should be pointed out that in the case of exchange or substitution reactions, the converging initial molecules fail to form quasi-molecules in the terminal electron state, unlike in the case of the addition reaction. For this reason, in the case of exchange reaction, quantities n", a", and k" are not shown in the kinetic equations.

B. USE OF THERMAL METHODS FOR INCREASING MOLECULE CONCENTRATION

According to Kochelap, a photostimulated chemical reaction will take place provided the concentration of chemically active molecules in the reactor is sufficient [36]. The latter can be achieved by means of known thermal methods (rapid heating or cooling). An example of this can be the recombination reaction A + B = AB, which involves a partly dissociated equilibrium gas at an initial temperature T_0. When such a gas is cooled in a time $\tau_{cool} \leq \tau_{rec}$ (where τ_{rec} is the recombination relaxation), equilibrium is disturbed and recombination begins. Given a rapid relaxation of the vibrationally excited reaction products AB (τ_{relax}), a chemical reaction will ensue. The conditions necessary to achieve the latter are:

$$\tau_{rec} \gtrsim \tau_{cool}, \quad \tau_{rec} \gg \tau_{relax} \tag{3.37}$$

In effect, $\tau_{rec}^{-1} = z_{rec}\, uv^{5/3} n^2$ and $\tau_{relax}^{-1} = z_{relax}\, uv^{2/3} n$, where z_{rec} and z_{relax} are the efficiencies of collisions which lead to recombination and relaxation, respectively, u is the mean thermal velocity of particles in a gas, v is the volume occupied by one atom,

and n is the concentration of particles in a gas. Assuming $z_{relax} = 0.1$, $z_{rec} = 0.001$, $u = 10^5$ cm·sec^{-1}, $v = 10^{-23}$ cm^3 and $n = 10^{18}$ cm^{-3}, both τ_{rec} and τ_{relax} are ~3 x 10^{-6} sec. Since cooling of a gas can be achieved in times $\tau_{cool} \sim 10^{-4}$--10^{-6} sec, condition (3.37) can be easily satisfied.

The optical gain due to the partially dissociated gas can be expressed as follows [37]:

$$\alpha = \frac{(2\pi)^{3/2} e^2 |u_{xgg'}(r_j)|^2 \omega_0 \mu^{1/2} r_j^2}{c\omega T_k^{1/2} |F_g(r_j) - F_{g'}(r_j)|} \left| \frac{(2\pi)^{3/2} r_0^2 T_k^{1/2} p_g(r_j)}{\omega_0 \mu^{1/2}} n_A n_B - n_{AB} e^{\frac{U_{g'}(r_0) - U_{g'}(r_j)}{T_k}} \right| \tag{3.38}$$

where the phototransition is assumed to occur from $U_g(r)$ to $U_{g'}(r)$ electronic states at a frequency ω; r_j is the internuclear distance whereby, $U_g(r_j) - U_{g'}(r_j) = \hbar\omega$, $F_g(r) = \partial U_g/\partial r$, ω_o and r_o are, respectively, the vibrational frequency and equilibrium distance between nuclei in state g', $u_{xgg'}(r)$ is the matrix element of the electron velocity operator, and $p_g(r_j)$ is

$$p_g(r) = \frac{1}{G} \begin{cases} e^{-\frac{U_g(r)}{T_k}}, & U_g(r) > 0, \\ 2\sqrt{\frac{-U_g(r)}{\pi T_k}} + e^{-\frac{U_g(r)}{T_k}} \left[1 - \Phi\left(\sqrt{\frac{-U_g(r)}{T_k}}\right)\right], & U_g(r) < 0 \end{cases} \tag{3.39}$$

where G is the number of overlapping states for $r \to \infty$, $\Phi(x) \equiv \frac{2}{\sqrt{\pi}} \int_0^x e^{-t^2} dt$ and T_k is the terminal gas temperature. Equations (3.38) and (3.39) are derived under the assumption that T_0 and $T_k >> \hbar\omega$.

Given that Eq. (3.37) is satisfied, it can be assumed that

$$n_A n_B = \frac{\mu^{1/2} \omega_0 n_{AB}}{(2\pi)^{3/2} r_0^2 T_0^{1/2}} e^{-\frac{D}{T_0}} \tag{3.40}$$

where D is the dissociation energy of molecule AB and $D >> T_0$.

The gain equation for $\alpha > 0$ is, therefore,

$$p_g(r_j)\sqrt{\frac{T_k}{T_0}}e^{-\frac{D}{T_0}} > e^{\frac{U_{g'}(r_0)-U_{g'}(r_j)}{T_k}}. \qquad (3.41)$$

The above clearly shows that in the case of phototransitions which occur at frequencies corresponding to $r_j \neq r_o$, a sufficiently deep cooling of a gas may result in a positive gain. Thus, when T_k is sufficiently small so that the above inequality intensifies, the absorption by AB molecules may be neglected in Eq. (3.38), and the condition for the occurrence of a photostimulated chemical reaction becomes:

$$n_{AB} > \frac{1-\varkappa}{L}\frac{c\omega r_0^2 T_0^{1/2}|F_g(r_j)-F_{g'}(r_j)|e^{D/T_0}}{(2\pi)^{3/2}e^2|v_{xgg'}(r_j)|^2 r_j^2\omega_0\mu^{1/2}p_g(r_j)}, \qquad (3.42)$$

where $\varkappa$ is the mirror reflectivity and L is the reactor length.

An example of the above analysis is the recombination of Br + Br atoms into $Br_2 + \hbar\omega$. Assuming in this case $\omega_0 = 10^{13}\,sec^{-1}$, $r_o = 2.28\text{Å}$, $D = 2.88 \times 10^{-12}$ erg, and $\omega = 10^{15}\,sec^{-1}$, Kochelap obtained $r_j = 2.6\text{Å}$, $|F_g(r_j) - F_{g'}(r_j)| = 2.5 \times 10^{-4}\,erg\cdot cm^{-1}$, $|v_{xgg'}(r_j)| = 10^7\,cm\cdot sec^{-1}$, $U_{g'}(r_j) - U_{g'}(r_o) = 1.4 \times 10^{-12}$ erg and $p_g(r_j) \approx 0.5$. When these were substituted into Eq. (3.41), it became evident that the gain could be produced for $T_0 \geq 2T_k$. If $T_0 = 2000°K$, a chemical reaction would proceed at $T_k \leq 1000°K$ and $n_{Br_2} \geq 5.6 \times 10^{18}\,cm^{-3}$.

C. GAIN CALCULATIONS AND POPULATION INVERSION CRITERIA

The gain calculations made in [35-37] are far too general and based on a fragmentary knowledge of several parameters for the reacting molecules, such as electron wave functions, dipole moment matrix elements, potential energies, etc. A new quasi-thermodynamic method proposed by Pekar and Kochelap appears to greatly simplify laser gain calculations [38]. The new method radically avoids the above parameters and requires only the knowledge of the chemical equilibrium constant for the given reaction and the coefficient of light absorption by the reaction products. The latter is known for a number of gases. In addition to gain measurements, the

proposed method appears to define more precisely the criteria for the population inversion for a broad class of substances.

1. Radiative Recombination

In a thermodynamically balanced radiative recombination reaction of the type $A + B = AB + \begin{cases} \hbar\omega \\ Q \end{cases}$ -- an exothermal reaction which emits $\hbar\omega$ photons and generates Q heat --

$$\mu(\omega, T, p_M)\bar{p}_{AB}\bar{q}(\omega)c = k(\omega, T, p_M)\bar{p}_A\bar{p}_B[1 + V\bar{q}(\omega)] \tag{3.43}$$

where p_A, p_B, p_{AB}, and p_M are partial gas pressures in atm[≠], $q(\omega)$ is the photon density in a given mode in cm^{-3}, V is the resonator volume and μ is the coefficient of absorption per unit pressure in AB gas in the presence of third gas M, c is the velocity of light, k ($cm^{-3}\cdot atm^{-2}\cdot sec^{-1}$) is the rate of spontaneous recombination. reaction, and $V\bar{q}$ corresponds to stimulated transitions.

In the case of a thermal equilibrium, $V\bar{q} = [e^{\hbar\omega/T}-1]^{-1}$. Also, based on the law of mass action

$$\bar{p}_A\bar{p}_B/\bar{p}_{AB} = K_{eq}(T) \tag{3.44}$$

where K_{eq} is the chemical equilibrium constant (in atm). The expression for the Einstein relationship for the stimulated chemiluminescence is obtained from Eqs. (3.43) and (3.44)

$$k(\omega, T, p_M) = \\ = c\mu(\omega, T, p_M)e^{-\hbar\omega/T}/VK_{eq}(T) \tag{3.45}$$

When k and μ are known, optical gain in the mixture α can be expressed as follows:

$$\alpha(\omega, T) = \mu(\omega, T, p_M)\left[\frac{e^{-\hbar\omega/T}}{K_{eq}(T)}p_Ap_B - p_{AB}\right] \tag{3.46}$$

[≠]Parameters designated with bars pertain to thermal equilibrium conditions.

where the first term represents gain due to stimulated chemiluminescence and the second, absorption of light by the reaction products. It is further assumed that the majority of reaction products AB has become thermalized.

Equation (3.46) yields the following criterion for the population inversion of the reacting mixture:

$$\frac{e^{-\hbar\omega/T}}{K_{eq}(T)} p_A p_B > p_{AB}. \tag{3.47}$$

The power of Eq. (3.47) is reduced with a decreasing ω; yet, in reality, a decrease in ω is limited by the requirement that the initial phototransition state and the dissociated states are in a thermal equilibrium with each other.

The applicability of the Pekar-Kochelap method is demonstrated on the example of a reaction $NO + O = NO_2 + \hbar\omega$ at the room temperature and $\lambda = 4047$Å. In this case, the photodissociation quantum yield of NO_2 is on the order of 1 and $\mu = 7.6\ cm^{-1} \cdot atm^{-1}$. Assuming $K_{eq} = 1.73 \times 10^{-47}$ atm, Eq. (3.46) yields a value for $\alpha = 4.5 \times 10^{-4} p_{NO} p_O cm^{-1}$. Although the selected wavelength is in the violet region, spontaneous chemiluminescence in the observed reaction exhibits the highest intensity in the green region. This indicates that a move in the longwave direction could enhance the gain.

In the case of $I + Cl = ICl + \hbar\omega$ reaction at $T = 300°K$ and $\lambda = 6000$Å, $\mu = 0.475\ cm^{-1} \cdot atm^{-1}$ and $\eta = 1$. Assuming $K_{eq} = 1.69 \times 10^{-32}$atm, from Eq. (3.46) $\alpha = 4.5 \times 10^{-4} p_I p_{Cl} cm^{-1}$.

2. Radiative Substitution

In the case of a thermodynamically balanced reaction of the type $AB + C = AC + B + \begin{cases} \hbar\omega \\ Q \end{cases}$, Eq. (3.43) becomes:

$$a(\omega, T, p_M) \bar{p}_{AC} \bar{p}_B c \bar{q}(\omega) = k(\omega, T, p_M) \bar{p}_{AB} \bar{p}_C [1 + \bar{q}(\omega)] \tag{3.48}$$

where the left-hand side represents the number of photons of a given mode (ω) absorbed per unit volume per second by the contacting molecule pairs AC and B, and $\underline{a}$ is the coefficient of absorption at equal partial pressures $p_{AC} = p_B = 1$ atm. From Eq. (3.48)

$$k = \frac{\alpha c}{KV} e^{-\hbar\omega/T}, \tag{3.49}$$

where $K(T) = \bar{P}_{AB}\bar{P}_C/\bar{P}_{AC}\bar{P}_B$ is the chemical equilibrium constant. Subsequently, the expressions for the optical gain and the population inversion criterion are, respectively,

$$\alpha = a[K^{-1}e^{-\hbar\omega/T}P_{AB}P_C - P_{AC}P_B] \tag{3.50}$$

$$K^{-1}e^{-\hbar\omega/T}P_{AB}P_C > P_{AC}P_B \tag{3.51}$$

In the case of atmospheric partial pressures of the initial gas, the strength of Eq. (3.51) is less than that of Eq.(3.47). Thus, k and α can be determined when a is measured experimentally. The measurement of a ought to be highly sensitive since Eq. (3.50) clearly indicates that very high values of α correspond to small values of a.

Formulas similar to Eqs. (3.48 -- 3.51) can be derived for the exchange reaction of the type AB + CD = AC + BD + $\begin{cases}\hbar\omega \\ Q\end{cases}$.

IV. CONTROLLED CHEMICAL REACTIONS

Several major categories of chemical reactions can be induced by a laser: photoexcitation, photopolymerization, pyrolosis, fog induction, and dissipation, etc. The basic justification for using a laser to induce chemical reactions is based on its selectivity, penetrability, focus ability, rapid applicability of beam, coherence, and tunability. Dramatic recent examples of laser induced reactions are isotope separation (Gross, U.S.), synthesis of polymer fuels (Asmus, U.S.), and fog nucleation (Yamanaka, Japan).

In the Soviet Union, a number of theoretical and experimental works on controlling chemical processes have been undertaken. One of the important problems gleaned in this area concerns the determination of criteria which govern the mechanism of production of the reaction products. The control over the reaction in the form of resonant coupling of radiation to a given vibrational degree of freedom of a molecule followed by the selective heating is another important problem. The effect of molecular anharmonicity on the progress of a chemical reaction was also reviewed as was the selective breaking of chemical bonds by way of two-step photodissociation.

A. MODEL PROBLEM

The absorption of laser radiation is inadvertently accompanied by the heating of the medium, and it becomes interesting to find the criteria which would enable one to decide which of the two competing processes -- thermal or photochemical -- is responsible for the transformation of a substance in the laser field. This problem was treated in much detail by Barashev and Tal'roze, who looked on the effect of the laser pulse duration τ on the nature of chemical reactions occurring in condensed media [39]. Particular attention was paid to the determination of the critical laser pulse duration τ_{cr} for which the role of thermal processes leading to the formation of the same reaction products as in the case of photochemical reactions was negligible.

B. THERMAL AND PHOTOCHEMICAL MECHANISMS

The thermal mechanism problem was solved for the case in which the optical pulse acts on the medium for which the coefficients of absorption k, thermal conductivity $\varkappa$, and thermal diffusivity a are assumed to be constant and independent of the temperature. Unlike in a number of works where the thermal mechanism of laser interaction with highly absorbing media (metals, $k \simeq 10^5$--10^6 cm^{-1}) was considered, the Tal'roze work [39] examines the thermal problem in a much broader sense; it holds that the bulk absorption of the incident radiation may occur and that the coefficient of absorption k is a function of density of the pumping radiation I ($[I] \sim cal \cdot cm^{-2} \cdot sec^{-1}$). Assuming the dependence of k on I is useful as it permits one to evaluate the role of heating in the process of multiphoton absorption in transparent media for a case when the optical flux densities become so great that nonlinear absorption occurs in the medium. In view of the fact that 2- and 3-photon absorption cross-sections σ_2 and σ_3 are exceedingly small, the experimentally observed values of phenomenological coefficient of absorption k seldom exceed 10 cm^{-1}, even for large flux densities ($J \simeq 10^9 \cdot cm^{-2}$). In Tal'roze's opinion, this prohibits the assumption (made in a number of other works) that the entire laser energy is deposited on the surface of the irradiated substance. Instead, one must allow for the fact that the energy is liberated over the entire length which the laser beam traverses through the substance

In analytical terms, Tal'roze has derived a solution for the following one-dimensional heat equation for temperature field T(x,t) inside the irradiated substance in a semispace $x \geq 0$

$$(\partial T / \partial t) = a(\partial^2 T / \partial x^2) + f(x, t) \tag{4.1}$$

with the initial and boundary conditions in the following form:

$$[\partial T(\infty, t) / \partial x] = 0; \quad [\partial T(0, t) / \partial x] = 0; \qquad T(0, x) = T_0; \quad T(\infty, t) = T_0$$

$$f(x,t) = \begin{cases} f_0(x) & \text{for } 0 \leqslant t \leqslant \tau \\ 0 & \text{for } t > \tau. \end{cases} \tag{4.2}$$

for which function f(x,t) takes into consideration spatial distribution of the optical flux density in a medium. In the case when $I(x) = I_0 \exp(-kx)$, $f(x,t) = (a/\varkappa)kI(x,t)$, where I_0 is the intensity of the optical flux at the boundary x = 0. This picture changes for the case of the nonlinear multiphoton absorption in a medium, whereby

$$dI/I = -\beta_n I^{(n-1)} \tag{4.3}$$

where β_n = const for a fixed value of I and n is the number of photons absorbed in the elementary act of interaction. The solution of Eq. (4.3) under the assumption that $I = I_0$ when x = 0 is

$$I(x,t) = I_0(t)[1 + (n-1)\beta_n x\{I_0(t)\}^{n-1}]^{-1/(n-1)} = \\ = I_0(t)[1 + (n-1)k_n x]^{-1/(n-1)}. \tag{4.4}$$

The quantity $k_n = \beta_n I_0^{(n-1)} = \sigma N I_0^{(n-1)} \text{cm}^{-1}$ can be called the phenomenological coefficient of n-photon absorption (where N is the number of absorbing molecules per unit volume).

The expression for the distribution function of equivalent thermal sources f(x,t) for a medium with n-photon absorption and assuming Eq. (4.4) has the following form:

$$f_n = (a/\varkappa)k_n I = (a/\varkappa)k_n I_0[1 + (n-1)k_n x]^{-1/(n-1)}, \quad (n \geqslant 2). \tag{4.5}$$

In the case of relatively weak absorption, when $|k_n x| < 1$, the expression for f(x,t) becomes

$$f_n(x,t) = (a/\varkappa)k_n I_0 e^{-k_n x} \tag{4.6}$$

The solution of Eq. (4.1) -- with boundary and initial conditions (Eq. (4.2)) for source functions given in Eq. (4.6) -- is relatively easy. Because the expression for the temperature distribution T(x,t) is exceedingly awkward, the authors provide only the value for the surface temperature of the sample at the time when the laser pulse τ had been switched off:

$$T(0,\tau) = T_0 + (I_0/\varkappa k_n)\{\exp(k_n^2 a\tau)[1-\Phi(k_n\sqrt{a\tau})] - \exp(-k_n^2 a\tau) + (2/\sqrt{\pi})k_n\sqrt{a\tau}\}, \quad (4.7)$$

where $\Phi(z)$ is the probability integral. They then used this expression to evaluate critical pulse length τ_{cr}, since it is evident that the maximum temperature in a medium is attained on the surface of the sample toward the end of the laser pulse.

In looking at Eq. (4.7), the first and second terms become negligible compared to the third term for media with large coefficients of absorption; therefore,

$$(\Delta T)_{max} = T(0,\tau) - T(0,0) = \frac{2(1-r)}{\varkappa} I\sqrt{\frac{a}{\pi}}\tau^{1/2}, \quad (4.8)$$

The authors introduce a correction (1-r) which allows for the fact that the coefficient of reflection of the medium is r. Equation (4.8) coincides with solutions obtained elsewhere, where assumptions were made that the entire laser energy is transformed into heat on the surface of the sample (thus, Eq. (4.8) is independent of the coefficient of absorption k). In the case of media with small coefficients of absorption and poor thermal diffusivity, i.e., in the case when $|k_n\sqrt{a}| < 1$, Eq. (4.7) becomes

$$(\Delta T)_{max} = \frac{2(1-r)I}{\varkappa} ak\tau\left[1 - \frac{2}{3\sqrt{\pi}} k\sqrt{a\tau}\right]. \quad (4.9)$$

In subsequent considerations, the second term in Eq. (4.9) is considered by the authors negligibly small in comparison with the first. This approximation holds for pulses with durations $\tau < 10^{-3}$ sec, including when $|k^2 a| < 7 \times 10^3$, i.e., it holds practically always for multiphoton absorption in a medium with flux densities $J \leq 10^{30}$ photon$\cdot$cm$^{-2}\cdot$sec^{-1}.

Having first derived the temporal dependence of temperature in an absorbing medium (Eqs. (4.8) and (4.9)), the authors then solved the following model problem for determining the value of τ_{cr}. They assumed that the product of a chemical reaction A can be formed either in the process of photochemical reactions or as a result of thermal reductions caused by the heating of the medium in the course

of absorption of laser radiation. The question which arises at this stage is: What should be the laser pulse parameters (τ and I) for which the concentration of products of the photochemical reaction $[A]_{photo}$ considerably exceeds the concentration of the same products arising in the process of a thermal reaction $[A]_{thermal}$?, i.e., whether $[A]_{photo} >> [A]_{thermal}$ at the end of the laser pulse. Simple reasoning suggests that by increasing the intensity of the optical flux while reducing the pulse length, one may achieve such experimental conditions for which the role of thermal effect will be small in comparison with photochemical, and the value of the flux density will be sufficient for multiphoton reactions to occur.

The kinetic equation for an n-photon photochemical reaction is

$$(d/dt)[C_A] = - \sigma_n J^n [C_A] \tag{4.10}$$

and its solution is

$$([C_A]/[C_A^{(0)}]) = \exp[-\sigma_n J^n t] \tag{4.11}$$

In Eqs. (4.10) and (4.11), $[C_A^0]$ is the original concentration of component A and J is the optical flux density in terms of photons per unit area per unit time. In order to find the conditions for determining τ_{cr} for a given value of J, the authors solved the kinetic problem of the production of reaction products under the effect of heating of the medium for which the following condition must be fulfilled:

$$([C_A]/[C_A^{(0)}])_{photo} \ll ([C_A]/[C_A^{(0)}])_{thermal} \tag{4.12}$$

which means that the mechanism for transformation is basically a photochemical one. This is done for the case of reactions of the first and second order:

$$A \xrightarrow{k_a} \ldots \quad \text{and} \quad A + A \xrightarrow{k_a'} \ldots \tag{4.13}$$

In comparing the monomolecular thermal and photochemical reactions, the authors had in mind the dissociation or isomerization reactions of particle A.

A thermal bimolecular reaction may compete with a photochemical reaction in two respects. First, a thermal bimolecular reaction -- which may be predominantly association or disproportionation -- may compete with a photochemical reaction not only in the sense of the mechanism, but also in the sense of directions which produce different products. Second, a photochemical reaction may also be bimolecular: excited particle A^* is introduced to react with stable particle A. In such a case, in principle, the products will remain identical to those produced in a thermal reaction. However, the rate of such a reaction is, naturally, equal to the rate of formation of the original exciting particles only in the critical case, and normally much smaller. Thus, since the rate of chemical reactions $(dC/dt) \sim A\exp(-E/RT)$, the solution of kinetic equations of a thermal reaction of the type Eq. (4.13) and allowing for the initial conditions ($[C_A] = [C_A^{(0)}]$ for $t = 0$) under known isothermal conditions, has the following form:

$$([C_A]/[C_A^{(0)}]) = \exp[-\mathcal{M}(L^2/y^2)\varphi(y)] \tag{4.14}$$

$$([C_A]/[C_A^{(0)}]) = \frac{1}{1+[C_A]\mathcal{M}(L^2/y^2)\varphi(y)} \tag{4.15}$$

when $T \sim t^{1/2}$ (see Eq. (4.8)), and

$$([C_A]/[C_A^{(0)}]) = \exp[-\mathcal{M}M\psi(z)] \tag{4.16}$$

$$([C_A]/[C_A^{(0)}]) = \frac{1}{1+[C_A^{(0)}]\mathcal{M}M\psi(z)}, \tag{4.17}$$

when $\tau \sim t$ (see Eq. (4.9)). Functions $\phi(y)$ and $\psi(z)$ in Eqs. (4.14--4.17) are

$$\varphi(y) = \varphi_1(y) + \varphi_2(y) = e^{-y}(1-y) - y^2\,\mathrm{Ei}(-y) \tag{4.18}$$

$$\psi(z) = \psi_1(z) + \psi_2(z) = (1/z)e^{-z} + \mathrm{Ei}(-z), \tag{4.19}$$

where $y = Lt^{1/2}$; $z = Mt^{-1}$; $L = (E/R)[\varkappa/2(1-r)](1/I)\sqrt{\pi/a}$, $([L] \sim \sec^{-1})$; $M = (E/R)[\varkappa/2(1-r)](1/I)(1/ak)$ $([M] \sim \sec)$; E is the activation energy of the corresponding type Eq. (4.13) reaction; R is the universal gas constant; A is a factor of the reaction rate; and Ei(z) is an exponential integral function. In the case of known solutions for Eqs. (4.11) and (4.14--4.17), Eq. (4.12) has the following form:

$$(\sigma_n J^n / \mathcal{A}) > \varphi(y),\ (\sigma_n J^n / \mathcal{A}) > z\psi(z) \tag{4.20}$$

for reactions of the first order, and

$$(\sigma_n I^n / [C_A^{(0)}]\mathcal{A}) > \varphi(y),\ (\sigma_n I^n / [C_A^{(0)}]\mathcal{A}) > z\psi(z) \tag{4.21}$$

for reactions of the second order.

Calculations show that the value of parameters $\alpha_1 = (\sigma_n J^n / A)$ and $\alpha_2 = (\sigma_n J^n / A[C_A^{(0)}])$ -- which determine, respectively, the value of τ_{cr} for reactions of the first and second order -- are always less than a unity. Actually, for condensed media, $A \simeq 3 \times 10^{10}$ $\sec^{-1}$ and $A[C_A^{(0)}] \simeq 10^{12}$ $\sec^{-1}$, correspondingly for mono- and bimolecular reactions. Since the absorption cross sections σ_n for single, 2- and 3-photon absorption are $\sigma_1 \simeq 10^{-(20--22)}\,\mathrm{cm}^2$, $\sigma_2 \simeq 10^{-50}\,\mathrm{cm}^4 \cdot \sec \cdot \mathrm{mole}^{-1} \cdot \mathrm{photon}^{-1}$ and $\sigma_3 \simeq 10^{-(85--90)}\,\mathrm{cm}^6 \cdot \sec^2 \cdot \mathrm{mole}^{-1} \cdot \mathrm{photon}^{-2}$, clearly, for optical densities $J < 10^{30}$ $\mathrm{photon} \cdot \mathrm{cm}^{-2} \cdot \sec^{-1}$, condition $\alpha_1 \ll 1$ is always fulfilled for reactions of the first order, and $\alpha_2 \ll 1$ for reactions of the second order. However, if the optical density is exceedingly high ($J \geq 10^{30}\,\mathrm{photon} \cdot \mathrm{cm}^{-2} \cdot \sec^{-1}$), $\alpha_1 \leq 1$ and $\alpha_2 \leq 1$.

The analysis of functions $\phi(y)$ and $\psi(z)$ -- which are terms in the original inequalities (4.20) and (4.21) -- shows that in the case when $\alpha_1 \ll 1$ and $\alpha_2 \ll 1$, y and z which determine the value of τ_{cr}, should be much greater than 1. In such a case, the asymptotic

solution of inequalities (4.20) and (4.21) leads to the following values of τ_{cr} for the first (i = 1) and the second (i = 2) orders of reaction:

$$\frac{L^2}{[\log(2/\alpha_i)]^2} > \tau_{cr}, \quad i = 1,2 \tag{4.22}$$

for the case when a surface absorption of the entire pulse energy is assumed, and

$$M/[\log(1/\alpha)] > \tau_{cr}, \quad i = 1,2 \tag{4.23}$$

for the case of bulk absorption of pulse energy ($\varphi(y) \simeq (2/e^y y)$ for $y >> 1$ and $\psi(z) \simeq (1/z^2 e^z)$ for $z >> 1$).

If $\alpha_i \leq 1$, the solution of inequalities (4.20) and (4.21) -- found from the asymptotic expression for functions $\varphi(y)$ and $\psi(z)$ in the region $y << 1$ and $z << 1$, has the following expression:

$$(4L^2/(1-\alpha_i)^2) > \tau_{cr}, \quad i = 1,2 \tag{4.24}$$

for reactions of the first (α_1) and (α_2) order in the case of surface emission of heat, and

$$[M(1-C)/(1-\alpha_i)] > \tau_{cr}, \quad i = 1,2 \tag{4.25}$$

for the case of bulk emission of the pulse energy.

In the case when values for α_1 and α_2 lie in the region $0.1 \leq \alpha_i \leq 0.9$, inequalities (4.20) and (4.21) must be solved by a method of successive approximations. However, approximate calculations of τ_{cr} can easily be obtained if one assumes that in this region, y and z vary within $0.1 \leq y(z) \leq 2.0$. Thus, in the case of surface emission of heat the following equation can be used for calculating τ_{cr}:

$$DL^2 > \tau_{cr} \tag{4.26}$$

where $0.25 \leq D \leq 100$, and for the bulk absorption correspondingly

$$D'M > \tau_{cr} \tag{4.27}$$

where $0.5 \leq D' \leq 10$.

The next important problem is to find the upper limit of values for the optical flux density for which reactions in a medium are always photochemical and, consequently, the concept τ_{cr} looses its sense. In other words, it becomes important to evaluate the critical value of the optical flux I_{cr} (or J_{cr}) for which a stationary thermal field is created in the specimen for which the rate of the photochemical reaction always exceeds the rate of the thermal reaction. The solution of the steady state problem shows that the temperature field has the form of $T(x) = [I(1-r)/\varkappa k_n]e^{-k_n x}$. If one assumes the near-surface temperature ($x \to 0$) and the fact that the rate of a photochemical reaction is considerably greater than that of a thermal reaction, the following expression is obtained:

$$\log (1/\alpha_i)T < (E/R), \quad i = 1,2 \tag{4.28}$$

where $T(x = 0) = I(1-r)/k_n/\varkappa$.

The upper (critical) value of the optical flux density may be found by solving a transcendental inequality

$$\log(1/\alpha_i)J < [E/R(1-r)]\varkappa k_n(1/\gamma) \tag{4.29}$$

where γ is a factor for converting I ($cal \cdot cm^{-2} \cdot sec^{-1}$) into J ($photon \cdot cm^{-2} \cdot sec^{-1}$). Therefore, it can be said that at densities $J < J_{cr}$, there exists in the medium a steady-state temperature field for which the primary role is played by photochemical reactions.

The foregoing analysis was made clearly under the assumptions that the rate of photochemical reaction is independent of the temperature and that the laser pulse duration τ considerably exceeds the characteristic relaxation time τ_{rel} of energy transfer from one set of degrees of freedom to others. The latter assumption imposes certain limitations on the applicability of obtained results;

without this assumption, however, in a case where $\tau < \tau_{rel}$, the problem under consideration would lose its sense. In other words, if $\tau_{cr} < \tau_{rel}$, the inapplicability of the proposed calculation system is evident and, further, the impossibility of a photochemical reaction is demonstrated within the conditions of the problem.

The model proposed by Barashev and Tal'roze was demonstrated on the example of a two-photon chemical reaction of decomposition of AgCl which was observed elsewhere.[#] Tal'roze's calculations based on the experimental parameters from this work showed $\tau < 6.8 \times 10^{-3}$ sec.

C. REACTION RATE CONTROL

The effect of radiation on a reacting mixture was considered, at one time, as a means of speeding up the chemical reaction in the mixture. We now know that exothermic reactions are capable of producing population inversion of the energy levels. The radiation which acts on a system of inverted energy levels tends to equalize their population by way of stimulated transitions. In the course of this, a portion of energy liberated in the reaction may be extracted from the system by way of amplification of radiation which acts on the reacting mixture. This means that the effect of radiation may be such as to retard the development of a reaction. The reaction deceleration may be strictly thermal in nature and it may also occur as a result of changes in the kinetics of the excited and stable reaction products.

1. Effect of Radiation on the Explosion Limits

In a paper submitted approximately 2 1/2 years ago, but published only recently, this question is discussed by Orayevskiy and demonstrated further on the example of a $H + Cl_2$ mixture [40]. The effect of radiation on the thermal explosion limits is considered.

[#] Rousseau, D. L., G. E. Leroi and G. L. Link, J. Chem. Phys., 42, 4048, 1965.

Orayevskiy assumes that in the process of an elementary act which yields energy, a portion of energy is distributed over the rotational and translational components, causing a rapid increase in the temperature of the reacting mixture. Another portion of the energy is distributed over the vibrational levels, the distribution being inversely proportional to certain pairs of v-r transitions. The equation for the thermal explosion limit is written in the following form:

$$w(T)Q[1 - \eta(\sigma I/(1 + \sigma I))] + \varkappa I = \lambda(T-T_0) \tag{4.30}$$

where $w(T)$ is the reaction rate, λ is a coefficient proportional to thermal conductivity, Q is the energy released in the reaction, I is the intensity of incident radiation, σ is the coefficient which depends on the cross section of stimulated emission and the relaxation of inverted v-r energy levels, η is that portion of the vibrational energy which can be released from the mixture in the form of radiation under an infinitely strong optical flux, and $\varkappa$ is the coefficient of absorption of the incident radiation. Equation (4.30) can be rewritten in the following form:

$$q - [(\alpha/(1 + n)) - \beta]n = 0 \tag{4.31}$$

where $q = w(T)Q - \lambda(T - T_0)$ is the excess coefficient of the explosion limit in the absence of radiation, $\alpha = \eta Q w(T)$, $\beta = \varkappa/\sigma$, and $n = \sigma I$. If n is bounded by roots n_{max} and n_{min} of Eq. (4.31)

$$n_{min} < n < n_{max} \tag{4.32}$$

then

$$q - [(\alpha/(1 + n)) - \beta]n < 0 \tag{4.33}$$

i.e., an explosive reaction does not occur even if in the absence of radiation the condition for explosion is satisfied ($q > 0$). In such a case, radiation quenches the reaction. However, the reaction

termination is possible only in the case if

$$\begin{matrix} \alpha < \beta \\ q < \alpha + \beta - 2[\alpha\beta]^{1/2} \end{matrix} \tag{4.34}$$

The existence of the lower level of optical intensity, which is capable to suppress the development of a reaction is explained by the fact that as the energy is extracted from the reacting system by way of stimulated transitions, a competing process of relaxation occurs which tends to thermalize this energy. Since the stimulated transition cross section is small at such small incident radiation intensities, practically all of the energy released in the reaction is used to heat the system.

At light intensities greater than the upper limit n_{max}, energy removal by the stimulated emission cannot compensate the heating of reagents due to light absorption. The condition $\alpha < \beta$ defines an obvious requirement that the energy due to the stimulated emission should exceed the absorbed energy for small light intensities. The second portion of Eq. (4.34) becomes more graphic if $\beta = 0$. It then becomes

$$q < \alpha \tag{4.35}$$

If $q > \alpha$, then the amount of heat released in the system is so great that an explosion occurs even when the maximum possible energy $\eta w(T)Q$ is removed from the system via the stimulated emission. Absorption reduces this critical value of q, so that the latter becomes equal to $\alpha + \beta - 2[\alpha\beta]^{1/2}$.

Orayevskiy applies the above analysis to a real case of an exothermic (ΔE = 45 kcal/mole) reaction of $H + Cl_2 \rightarrow HCl^* + Cl$. His calculations show that the effect of radiation on the reacting system may, in principle, decrease the effective heat of reaction by almost 10 kcal/mole.

Considering the fact that energy released in the chemical reaction is distributed among the various degrees of freedom, the rate of the explosion reaction depends on whether the energy given

off to the r-t transitions of the reaction products is sufficient for a thermal explosion to develop. The translational energy is rapidly distributed over the system increasing its temperature, whereas the vibrational energy relaxation is a process which takes more time. Therefore, if

$$w(T)Q(1 - \eta_0) > \lambda(T - T_0) \tag{4.36}$$

(where $1 - \eta_0$ is a portion of energy distributed over r-t degrees of freedom of the reaction products), a thermal explosion may occur much faster than it does in the vicinity of the limit which is determined by the following expression:

$$w(T)Q = \lambda(T - T_0) \tag{4.37}$$

The above occurs when the total rate of all the elementary acts which lead to the release of energy is greater than the rate of vibrational relaxation. Naturally, the rate at which the explosion develops, as it progresses from limit (4.37) to limit (4.36), increases continually and the introduction of "limit" (4.36) is strictly conventional.

Because a thermal explosion may occur without a loss of the vibrational energy beyond limit (4.36), the vibrational energy of the excited reaction products may be used for the production of stimulated emission at fast reaction rates.

2. Non-Equilibrium Dissociation

A number of chemical kinetics problems requires the attainment of rapid reaction rates under non-equilibrium conditions characterized by low gas temperatures and large vibrational energy content. For example, in high-power cw chemical lasers (e.g., $HF^* + CO_2$), one of the important problems is to produce comparatively large concentrations of free atoms or radicals at low gas temperatures. This is achievable provided the rate of molecular dissociation is sufficiently fast.

One way of attaining fast dissociation rates at low gas temperatures could be -- according to Gordeyets et al. [41] -- the use of polyatomic molecules in which the vibrational excitation is passed onto a mode whose dissociation limit energy D is greater than the minimum dissociation energy of molecule D_{min}. In such a case, a molecule may decompose by way of predissociation, i.e., by way of transition of a molecule into the continuous spectrum from a vibrational level with an energy greater than D_{min}. The rate of such a transition is normally high due to mode interactions in the upper levels. Thus, the rate of dissociation is determined by the probability of molecules populating the k + 1 level and the population of level k whose number is given by:

$$E_k = k[E_1-(k-1)\Delta E] \leq D_{min} \leq E_{k+1} = (k+1)[E_1-k\Delta E) \tag{4.38}$$

where E_1 and ΔE are, respectively, the energies of the lower level of an oscillator and its anharmonicity in °K. If k lies near level $n^*(i^*)^{\neq}$ or even $k < n^*(i^*)$, v-t processes or the radiative decay of this level exert little effect on its population. The latter can be considerably large for a sufficiently large vibrational energy content, and it can thus ensure a rapid dissociation rate. The non-equilibrium energy can be accumulated by a number of pumping methods: optical, thermal, chemical, electrical, or via vibrational transfer with another molecule with its own non-equilibrium energy. Assuming $k < n^*(i^*)$, the expression for the dissociation rate of a polyatomic molecule is

$$c = zN\frac{1}{\theta}N_1\beta Q_{10}^{10}(1+I_k')^{-1} \approx zN\frac{1}{\theta}(k+1)\beta Q_{10}^{10}\exp\left(-\frac{D_{min}}{T}\right)\times$$
$$\times\exp\left[kE_1\left(\frac{1}{T}-\frac{1}{T_1}-\frac{\gamma_0}{3D}\right)\right](1+I_k')^{-1}. \tag{4.39}$$

$^{\neq}$ $n^* = \frac{3}{8}\frac{\log(\beta A)}{\gamma_0}\frac{E_1}{\Delta E}$ $\qquad i^* = \log(\frac{z\beta Q_{10}^{01}}{A_{10}})(\frac{2}{3}\gamma_0 + \frac{E_1}{2T})^{-1}\frac{E_1}{2\Delta E}$

The above expression differs from a similar expression for diatomic molecules in two respects. First, for $T_1 > T$, the rate of non-equilibrium dissociation of a polyatomic molecule is much greater than that of diatomic molecules even at low (room) temperatures T. The recent Karlov experiments with BCl_3 dissociation by 10.6μ radiation [42] clearly demonstrate the applicability of the above formula. Second, the dependence of dissociation rate of a polyatomic molecule on a gas temperature is possibly anomalous. It can be seen from Eq. (4.39) that for a constant vibrational energy content (or T_1 = const), v does not increase with T for $T < T_1$, as one would expect, instead it falls off.≠ This is demonstrated in Fig. 56 for the case of $BCl_3(\nu_3)$ molecule at T_1 = const.

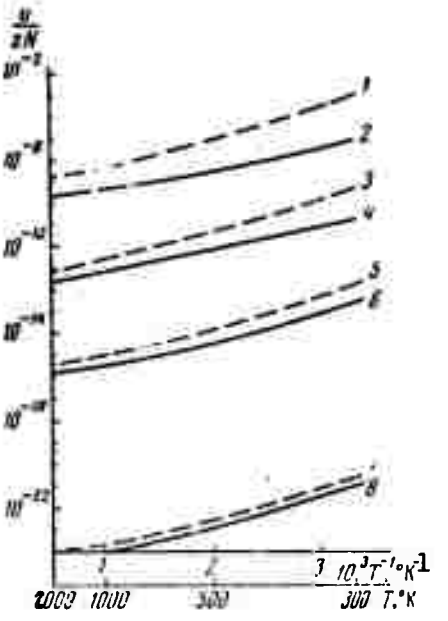

Fig. 56

Dependence of gas temperature T on probability of dissociation v/zN for $BCl_3(\nu_3)$; BCl_3 - BCl_3 collisions. Curves 1 and 2 -- T_1 = 3000°K, 3 and 4 -- 2000, 5 and 6 -- 1500, 7 and 8 -- 1000. Calculation made with (curves 2, 4, 6, 8) and without (1,3,5,7) assumption of dissociation effect on population of upper levels.

≠An increase in v with T for T_1 = const. may occur if either $k < n^*(i^*)$ fails to hold or if normal thermal dissociation takes over.

The foregoing indicates that the strong dependence of v on T_1 provides a means of control over the dissociation by way of manipulating the gas temperature and the vibrational energy content.

Thus, molecules with excess energy may act as active centers for the reaction. For example, under normal conditions, the vibrational energy of HCl^* molecules formed in the reaction $H + Cl_2 \rightarrow HCl^* + Cl$, is insufficient to produce branched chains. By increasing this energy -- say, by way of nonresonant vibrational energy transfer -- one may achieve the desired branching: $HCl^* + Cl_2 \rightarrow HCl + Cl + Cl$.

The kinetics of nonresonant transfer and some examples of its possible application in gas-dynamic and chemical lasers was treated theoretically by Gordeyets et al. [43]. The article -- which proceeds from the solution of rate equations for anharmonic oscillators and harmonic oscillators with dissimilar frequencies -- is an analysis of the vibrational energy distribution and the effect of two-photon transitions on the energy distributions. An earlier work by the same authors considered the kinetics of vibrational transfer in anharmonic oscillators with single-photon transitions [1]. However, the approach involving distributions with single-photon transitions tends to limit their area of applicability and fails to describe the many aspects of vibrational relaxation.

D. EFFECT OF ANHARMONICITY

A laser controlled initiation of a chemical reaction can be achieved by means of the resonance excitation of vibrational levels of a molecule. The calculation of the level population for a system of anharmonic molecules was made by Orayevskiy and Savva in [44]. This work deals with the excitation of the Morse oscillator, and HCl and HI molecules are cited as examples.

The dependence of vibrational energy $W/D = 1 - c(\Omega^2, P_o)$ on the square of the frequency is shown in Fig. 57a for different values of P_o, where $P_o = eE_o/\omega_{10}\sqrt{2mD}$), D is the dissociation energy, $\Omega = \omega/\omega_{10}$, e is the effective charge, and m is reduced mass. The study shows that the linear portion of the right hand side branches of the resonance curve can be well expressed by the expression:

$$W/D = 1 - \Omega_+^2 + 1.82P \tag{4.40}$$

When the laser frequency is

$$\Omega_p = [1 - 3(P_o/2)^{2/3}]^{1/2} \tag{4.41}$$

the maximum energy stored in a molecule is

$$W_{max}/D = 3(P_o/2)^{2/3} + 1.82P \tag{4.42}$$

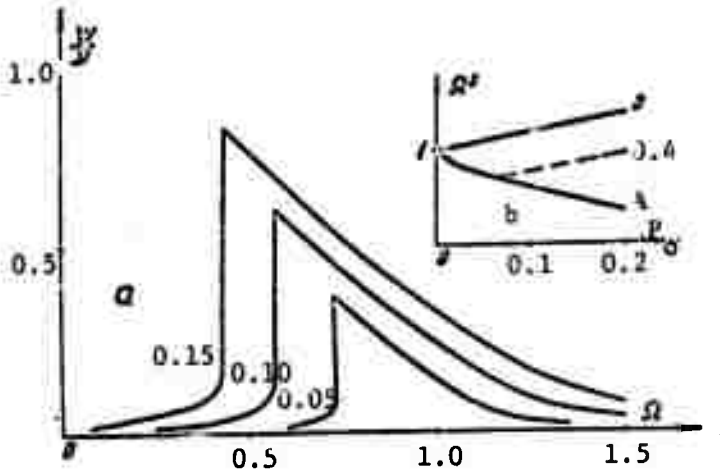

Fig. 57

The resonance regions

Eqs. (4.40--4.42) can be used to qualitatively evaluate the possibility of laser activation of molecules. A chemical reaction proceeds at a considerable rate if the molecule involved has an energy which exceeds the activation energy $W_a \leq D$.

In Fig. 57b, the region between the 0.4-line and curve A corresponds to the formation of active molecules for the reaction with $W_a/D = 0.4$.

The laser activation of molecules is selective whereas thermal activation is not. For example, the excited gas mixture of HCl and HI molecules may predominantly initiate reaction HCl + X or reaction HI + X. Figure 58 shows the resonance regions for these molecules for the condition where W_a = (D-2.5)ev for both molecules. The energy of the molecule inside the cone exceeds the activation energy, i.e., the reaction proceeds at a rapid rate.

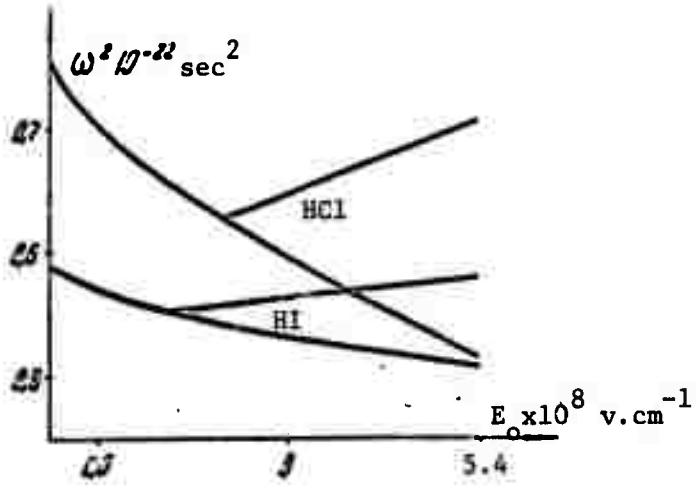

Fig. 58

Regions in which a chemical reaction takes place.

Figure 59a shows the population of the Morse oscillator with 22 levels in the case of radiation with frequencies ω_{10}, $\omega_{10}-3\Delta$, $\omega_{10}-6\Delta$ and for L = 1.2. Figure 59b shows the total population of 10 upper levels of the same oscillator as a function of laser frequency. Knowing the number of active molecules induced by the laser, the rate of the chemical reaction can be made quantitatively.

The power required to densely populate the levels near the dissociation limit is somewhat high. Moreover, for such intensities undesirable effects begin to appear. However, the required powers for populating several levels are fully tenable. The relaxation of a

vibrational subsystem occurs much faster than the v-t relaxation. This has led the authors to propose the following method of resonance pumping. A radiation with frequency $\omega \sim \omega_{10}$ effectively populates one or several lower vibrational levels while higher levels are populated by way of rapid v-v transfer. The population is preserved during a period which is small in comparison with v-t relaxation.

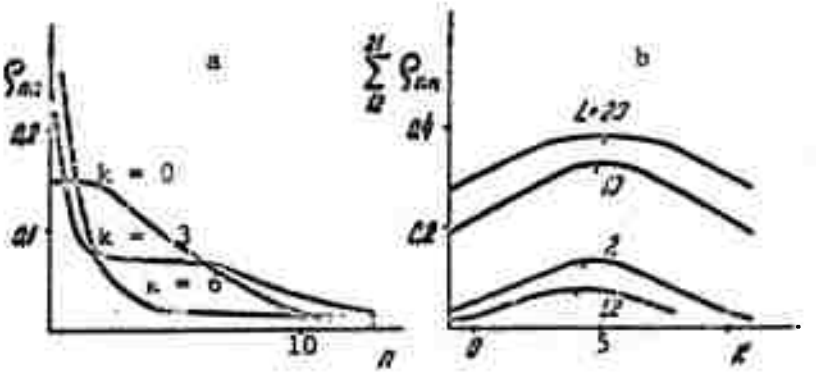

Fig. 59

Excitation of vibrational levels by radiation

E. SELECTIVE DISRUPTION OF CHEMICAL BONDS

A serious obstacle which prevents the solution of the problem of selective breaking of bonds by means of laser radiation is the molecular anharmonism. In the majority of molecules, the v-t relaxation processes occur on the lower levels and proceed much slower than processes involving one degree of freedom. As a result of anharmonism, v-t relaxation begins to take over on the high levels well below the dissociation limit. The dissociation of molecules is hardly probable until such time as the heating of the gas by radiation absorption gives rise to diffusive propagation of excitation among these levels. Karlov showed that in the case of polyatomic molecules -- such as BCl_3 -- vibrational predissociation is possible without the heating of the gas [42]. In the physical sense, this stands in contrast with the work of Orayevskiy [44] insofar as the process is determined by the selective interaction of radiation with one of the vibrational degrees of freedom and the v-v relaxation of excitation. In such a case, the vibrational temperature may considerably

exceed the translational temperature of the medium, a fact which was pointed out earlier by Artamonova et al. [1].

A somewhat different approach was taken by Afanas'yev et al. who looked at a non-steady-state self-consistent problem for the case of molecular-gas dissociation under resonant laser radiation, under the conditions where the laser pulse duration is limited by v-t relaxation (t_m) only [45]. A derivation was made of the analytical expressions for the vibrational temperature θ and the dissociation constant $\gamma = k/t_c$, where t_c is the v-v relaxation.

$$\gamma = \frac{1}{2t_c}\alpha\left(\frac{h\omega}{\mathcal{E}^*}\right)^2 \frac{(\mathcal{E}^*/\theta)^2}{1+\alpha\mathcal{E}^*/\theta}, \tag{4.43}$$

$$\exp\left(-\frac{\mathcal{E}^*}{\theta}\right) = \frac{\alpha}{2}\left(\frac{h\omega}{\mathcal{E}^*}\right)^2 \frac{\mathcal{E}^*/\theta}{1+\alpha\mathcal{E}^*/\theta}, \alpha = \frac{I\sigma t_c}{\mathcal{E}^*}. \tag{4.44}$$

where $\mathcal{E}^*$ is the threshold energy (close to the activation energy) above which molecules are populated by way of resonance collisions only.

The above equations suggest that for small fields ($\alpha \to 0$), the dissociation constant is actually proportional to laser flux density. On the other hand, in the case of large fields ($\alpha \to \infty$), the vibrational temperature and the dissociation constant tend to a finite limit which corresponds to the bleaching of the system associated with the saturation effect. Using Karlov's [42] and Artamonova's [1] experimental data ($t_c = 10^{-6}$sec, $t_m = 10^{-3}$sec, $h\omega \approx 0.1$ ev, $\mathcal{E}^* \approx 2$ ev, $\sigma = 10^{-17}$cm^2 (pressure ~ 100 torr), $I \approx 10^2$w$\cdot$cm^{-2}), Afanas'yev showed that $\theta \approx 0.2$ ev and $\gamma \approx 10^3$sec^{-1}. This indicates that under the above conditions, $\gamma t_m \sim 1$ and a considerable portion of molecules is dissociated prior to v-t relaxation.

Afanas'yev claims that his results can be directly applied to the case of decomposition of a vibrationally excited molecule due to chemical reaction.

F. TWO-STEP PHOTOEXCITATION

The selective disruption of certain bonds can be accomplished by a two-step photoexcitation. Proposed recently by Karlov et al., this method postulates that a molecule can be excited by two lasers: via the resonant absorption of ir radiation and irradiation by an optical or near-uv radiation.[≠] The wavelengths of the latter must be such so as to ensure photodissociation from those ground energy levels which are populated by way of absorption of ir laser radiation and by collisions, but whose vibrational relaxation nas not yet substantially been affected by anharmonicity.

The parameters of a laser required for this task were derived from the following equations:

$$\frac{dx}{d\tau} = -x + \frac{w_1}{(1+x)^2} - w_2 \frac{m-x}{1+x}\left(\frac{x}{1+x}\right)^m$$

$$\frac{dc}{d\tau} = -w_2\left(\frac{x}{1+x}\right)^m \frac{c}{1+x} \qquad (4.45)$$

where $c = \sum_n f_n$ and $x = \frac{1}{c}\sum_n n f_n$, where f_n is the normalized probability of level populations so that $c + f_g = 1$ and f_g is the dissociation cross section of a molecule; $\tau = t/t_v$, where t_v is the v-t relaxation and $w_{1,2} = \frac{\sigma_{1,2} J_{1,2}}{h\nu_{1,2}} t_k$, σ_1 is the resonant in absorption cross section; σ_2 is the photodissociation cross section, $h\nu_{1,2}$ and $J_{1,2}$ is, respectively, photon energy and flux density of ir and optical radiation. It was assumed that photodissociation occurs during the transfer from the m-th vibrational level to the repulsion term or the unstable portion of the excited term.

Equations (4.45) were derived from a system of equations for the population of a harmonic oscillator, and their solution, although simple, is difficult to visualize. Assuming that m = 10, and if $w_2 x^m (1+x)^{-(m+1)} > 1$, a substantial portion of molecules becomes

---

[≠] Recently, two-step photodissociation of HCl by the fundamental and the second harmonic of a pulsed Nd-glass laser was reported by Ambartsumyan and Letokhov at the CLEA 71 meeting in Washington, D.C.

dissociated well before a noticeable vibrational relaxation. If $w_1 = 50$, $x = 3$ and the bulk of molecules decays in $\tau = 70/w_2$. The numerical example shows that at pressure $p = 10$ torr, t_v for many molecules is $\sim 10^{-3}$ sec and $\sigma_1 = 10^{-16}$--10^{-17} cm^2, both decreasing $\sim 1/p$. For $h\nu_1 = 2 \times 10^{-13}$ erg, $w_1 \approx 1$ if $J_1 \approx 0.2$--2 $w \cdot cm^{-2}$. If $\sigma_2 = 10^{-19}$ cm^2 and $h\nu_2 = 4 \times 10^{-12}$ erg, $w_2 \approx 1$ for $J_2 = 4 \times 10^3$ $w \cdot cm^{-2}$. Clearly, two-step dissociation at presently achievable densities can occur more rapidly than the vibrational relaxation.

Although he has yet to perform the experiment, Karlov thinks that CF_3I molecules are well suited for two-step dissociation. The resonant excitation of CF_3I by 10.6μ CO_2 laser could produce about 10 vibrational levels which would be sufficient for the dissociation of these molecules by the second harmonic of an Nd-glass laser.

An interesting conclusion which can be drawn from these experiments is that dissociation of molecules by broadband optical sources may be considerably speeded up under the resonant pumping which vastly increases the number of photodissociation channels in a molecule.

G. DIRECTIONAL REACTIONS INITIATED BY 10.6μ RADIATION

1. Karlov's Experiments

About a year ago, Karlov showed that gaseous BCl_3 will dissociate rapidly under the effect of 10.6μ CO_2 laser radiation [42]. Under the experimental conditions, the laser frequency and the vibrational frequency of the BCl_3 molecule ν_3 were resonant and the dissociation occurred as a result of cascade population of higher vibrational levels. At that time, Karlov stated that the production of atomic chlorine by way of dissociation should lead to the formation of chemically active centers. For this reason, irradiation of stable gas mixtures involving BCl_3 could initiate a controllable chemical reaction.

In a very recent work, Karlov et al. report on having accomplished this goal through the initiation of a chain reaction by means of CO_2 laser radiation, which was accompanied by a detonation wave [47]. The authors found that when mutually inert gases H_2 and BCl_3 were irradiated by 10.6μ CO_2 laser radiation, a rapid chemical reaction

occurred whose front propagated in the form of a cylindrical detonation wave.

The experiment was carried out for a mixture of H_2:BCl_3 = 20:1, at the total pressure of 1 atm. The pulsed CO_2 laser radiation consisted of nearly-rectangular 600 w pulses with the duration of 30 μsec and pulse rise of ~0.5 μsec. The laser radiation was focused by a system of salt optics into a nearly parallel beam with a 0.3 cm diameter which was directed along the axis of the cell containing the experimental mixture. The cell consisted of a thick-walled brass cylinder 10 cm long and 4 cm bore. The input window was hermetically sealed by a crystalline ZnSe plate and the output and side windows were covered with salt flats. The cell was equipped in fast piezoelectric transducers located at the lateral walls. The optical fluorescence and ir absorption spectra of the gas mixture were observed, the former through a side window by means of FEU-62 photomultiplier and through the end window by means of high-speed movie camera SKS-1M.

When the laser radiation was coupled to the H_2 + BCl_3 mixture, an explosion reaction occurred which was accompanied by intensive optical fluorescence and a sharp jump in the pressure. The fluorescence occurred with a certain delay, the duration of which depended on the partial pressure of BCl_3, the intensity of laser radiation, and also on the purity of the original reagents. The luminous region propagated from the axis to the cell periphery in the form of a cylindrical shell. While expanding, this region narrowed and became brighter. The fluorescence was at its maximum when the luminous region reached the cell walls. At the same time, the pressure attained its maximum of 40--50 atm. The time of propagation of the fluorescence wave was 0.5 μsec. During that time, the gas in the laser beam region continued to luminesce, and when the luminescent layer reached the cell walls, fluorescence was quenched. In the meantime, at the cell center, secondary fluorescence occurred in a region with a diameter greater than the laser beam diameter and continued for several milliseconds.

The spectroscopic study of the line intensity of vibrational absorption ν_3 of the BCl_3 molecule at the time of the explosion confirms an irreversible disappearance of this gas during the expansion of the detonation wave.

Figure 60 shows the shape of the pumping pulse (a) and the temporal dependence of the optical fluorescence intensity (b), and gas pressure (c).

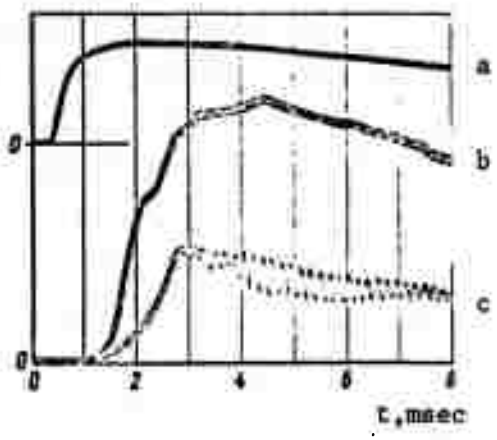

Fig. 60

Shape of 10.6μ pumping pulse (a) and the temporal dependence of optical fluorescence intensity (b) and gas pressure (c).

The dynamics of laser-induced reaction appears to be similar to the processes of propagation of combustion waves in laminar flows in closed vessels.[≠] In Karlov's case, chain reactions occur at the detonation wavefront, in which higher boranes are formed and decomposed and the chlorination of hydrogen occurs as a result of the production of atomic chlorine and active radicals BCl and BCl_2 in the laser beam region.

The flame velocity in the primary wave reaction was calculated to be from 0.5 to 2 m/sec. Karlov also suggested that the secondary fluorescence gives rise to reaction waves with high combustion rates at the cell walls. This leads to the occurrence of pressure waves which are well delineated in Fig. 60c.

[≠] A figure showing a film of the propagation of the reaction wave is included in the same paper. The quality of the photograph, however, renders it useless for reproduction in this report.

2. Basov's Experiments

In recently published articles [48,49], Basov et al. studied experimentally the effect of 10.6μ radiation on a number of the following gaseous systems:

N_2F_4 - NO	N_2F_4 - NO - Xe	SiH_4
N_2F_4 - NO - N_2	N_2F_4 - N_2O	SiH_4 - BCl_3
N_2F_4 - NO - NF_3	N_2F_4 - H_2	SiH_4 - SF_6
N_2F_4 - NO - CF_4	N_2F_4 - CH_4	SF_6 - NO
	N_2F_4 - BCl_3	

The light absorbing substances were N_4F_4, SF_6, BCl_3 and SiH_4. The laser intensity was from 20 to 70 w in a ~2--9 mm diameter beam. The exposure time was generally < 0.5 sec and the gas mixtures were kept in cylindrical cells 100 mm long and 20 mm bore terminated with AgCl windows.

The experimental results are shown in Table 8 and Fig. 61.

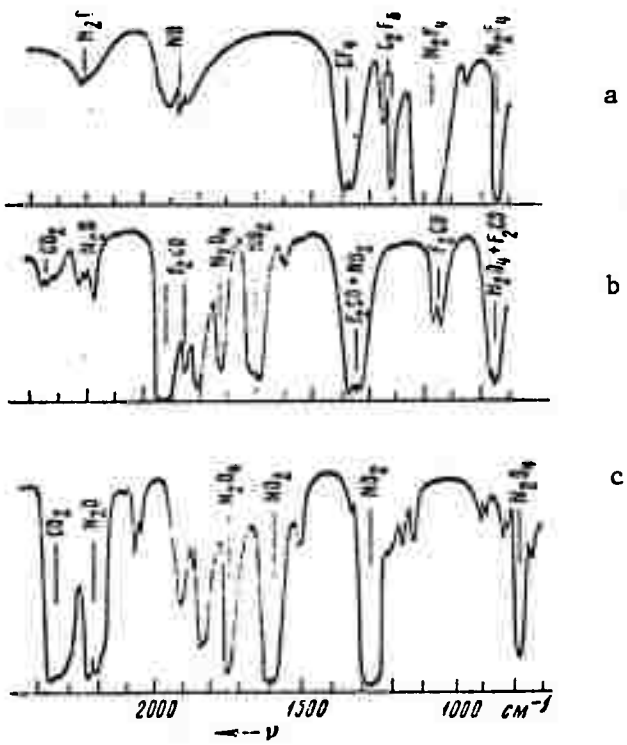

Fig. 61

IR absorption spectra a -- original mixture N_2F_4 (100 torr), NO (200 torr), CF_4, C_2F_6; b -- Mixture after irradiation experiment #5, NO_2, F_2CO; c -- Mixture after irradiation experiment #6, NO_2, CO_2, N_2O.

Table 8

Basov's Experiments with Laser Induced Reactions

Exp. no.	Reagents and partial pressures, torr		Laser intensity, w, times irradiated, n, exposure time	Reaction products and final pressure P_f, torr
			A. Beam d ≈ 8 mm [48]	
1	N_2F_4	60	20 w	no reaction
	NO	150	1 min	
	CF_4, C_2F_6	~5		
2	N_2F_4	100	~20 w	N_2F_4, NO, FNO,
	NO	200	~5 min	CF_4, C_2F_6, N_2
	N_2	460		
	CF_4, C_2F_6	~10		
3	N_2F_4	100	~20 w	N_2F_4, NO, FNO,
	NO	200	beam focused on	CF_4, C_2F_6, N_2,
	N_2	460	AgCl window for	some NF_3
	CF_4, C_2F_6	10	2--3 min	
4	N_2F_4	60	30 w	NO_2, CO_2, N_2
	NO	150	3×10^{-2} sec	
	CF_4, C_2F_6	6		
5	N_2F_4	100	50 w	NO_2, F_2CO, N_2
	NO	200	< 0.1 sec	194 torr
	CF_4, C_2F_6	10		
6	N_2F_4	100	70 w	NO_2, CO_2, N_2O,
	NO	200	< 0.1 sec	N_2
	N_2	460		
	CF_4, C_2F_6	10		
7	N_2F_4	100	50 w	no reaction
	CF_4, C_2F_6	10	< 1 sec	
	N_2	650		
8	SF_6	100	50 w	SF_6, F_2SO, NO,
	NO	200	< 0.1 sec	traces CO_2, N_2O
				unknown substances
9	SF_6	300	50 w	SF_6, F_2SO, NO
	NO	200	< 0.1 sec	traces CO_2, N_2O
				470 torr
10	SF_6	100	50 w	no reaction
			~10 sec	
			B. Beam d ~ 2 mm [48]	
11	N_2F_4	100	30 w	NF_3, FNO, FNO_2,
	NO	200	3×10^{-2} sec	CO_2, F_2CO, N_2,
	CF_4, C_2F_6	10		traces CF_4, C_2F_6,
				N_2O, 236 torr
12	N_2F_4	100	30 w	NF_3, NO_2, CO_2 (20%),
	NO	100	< 1 sec	NO, N_2O, N_2, CF_4
	CF_4	200		

Table 8 (cont.)

Reagents and partial pressures, torr		Laser intensity, w, times irradiated, n, exposure time	Reaction products and final pressure P_f, torr
		C. Beam d = 9 mm [49]	
N_2F_4 NO	100 100	40 w	FNO, N_2, F_2, 262 torr, fluorescence
N_2F_4 NO N_2	100 200 460	70 w	NO_2, N_2O, N_2 fluorescence
N_2F_4 NO CF_4	100 100 200	30 w	NF_3, NO, CO_2 (10%), CF_4, N_2
N_2F_4 N_2O_4	300 150	40 w n = 3	NO_2 (49%), NF_3 (38%), N_2O (5%), FNO_3, N_2, 512 torr, weak fluorescence
N_2F_4 H_2	50 100	50 w	N_2, HF, $N_2F_4 + 2H_2 = 4HF + N_2$, fluorescence
N_2F_4 CH_4	228 114	50 w	CF_4 (22%), HF, N_2, $N_2F_4+CH_4=CF_4 + 4HF+N_2$, 534 torr
N_2F_4 BCl_3	114 114	50 w n = 3	BF_3, fluorides, N_2, fluorescence when n = 1 289 torr
SiH_4	228	50 w n = 3	Si, H_2 (34%), $SiH_4 \equiv Si + 2H_2$, 22% conversion, fluorescence for n = 1,2, 284 torr
SiH_4 BCl_3	112 112	40 w n = 3	BCl_2H, SiH_3Cl, $SiH_4+BCl_3=BCl_2H+SiH_3Cl$, B_2H_6, fluorescence for n = 1--3, 234 torr
SiH_4 SF_6	300 100	40 w	SiF_4, H_2, S, $SiH_4+2/3SF_6=SiF_4+2H_2+2/3S$, fluorescence, 698 torr

The reactions are, above all, dependent on light intensity which when below ~40 w and pressures <200 torr, failed to induce a noticeable reaction for short exposure times. At longer exposure times, reactions occurred as thermal processes (experiments 1 and 2). At intensities of 30 watts and up, a bright green-yellow flare was observed which occurred immediately after the diaphragm was opened (experiments 4--6). As a result of the reaction, NO_2, CO_2 (or F_2CO) were formed, and were fully reacting with N_2F_4, CF_4 and C_2F_6. The mass spectroscopic analysis showed the presence of nitrogen. The pressure after the reaction decreased (in experiment 5, the mixture pressure went down from 300 to 194 torr). The dilution of the reacting mixture by nitrogen caused additional formation of nitrogen oxide. In experiments 2--7, the absence of NF_3 is conspicuous. The irradiation of a single N_2F_4 molecule did not produce an optical flare. Only a small decrease in pressure was observed.

Processes occurring in systems N_2F_4 - NO - $CF_4(C_2F_6)$ - N_2 in which NO_2, CO_2, CF_2O, and N_2O were formed in the absence of NF_3, CF_4 and C_2F_6 in the reaction products, were only possible either when the system was heated to temperatures in excess of 1500°K, or with the participation of vibrationally excited molecules.

The conditions of irradiation in experiments 2 and 3 favor the thermal reaction. In experiment 3, the cell had a low transmission window on which the laser radiation was focused. The window was heated in the laser beam, a fact which was evidenced by the slow fluorescence of the window material. In experiment 2, the cell was irradiated by a 20 watt beam for approximately 5 minutes. The reaction occurred without a flare.

Different reaction products were observed in experiments with 2-mm beam, the basic product being NF_3 and the principal remaining products being FNO, CF_4, and C_2F_6 (experiments 11 and 12). In these experiments, only the axial portion of the gas volume was irradiated. The presence of F_2CO and CO_2 indicate that CF_4 undergoes transformation. Highly indicative of this is experiment 12 in which the initial mixture contained 50% CF_4 and ~20% CO_2 was obtained after the reaction. In addition to this, the presence of NF_3 and FNO indicate that the reaction is thermal.

On the other hand, irradiation of the SF_6 and NO mixture has led to an immediate reaction accompanied by a flare. The reaction product contained F_2SO. The conversion of SF_6 and NO occurred only partially. The mass-spectrometric analysis showed an absence of nitrogen. The reaction changed little when the SF_6:NO ratio changed (experiments 8 and 9). The irradiation of a single molecule of SF_6 did not produce the reaction (experiment 10).

The Basov experiments suggest that all of the above reactions (with the exception of those involving Si) begin exothermally rather than as a dissociation of vibrationally excited molecules, with chemical properties other than those inherent to ground-state molecules.

The Basov experiments also provide a means for evaluating the upper temperature level for the heating of a mixture as a result of the absorption of laser radiation. In the case of laser-induced reaction between SF_6 and NO, the threshold was ~50 watt, and the exposure time was not greater than 0.1 sec. The energy absorbed in this period was ~5j. The energy was absorbed in the volume $V = \frac{\pi}{4} \times \frac{1}{k}$ cm^3, where k is the coefficient of absorption of SF_6 at 10.6μ. At a pressure of 300 torr, k was $\leq$ 0.3--0.5 cm^{-1} and V ≈ 2--3 cm^3, and this enables one to evaluate the temperature of the heated mixture ΔT which, in this case, was $E/(c_V V) < 700°$.

Calculations for the N_2F_4 + NO mixture are of the same order (experiment 4), where the exposure time prior to the reaction did not exceed 3×10^{-2} sec. In this case, $\Delta T \simeq 200°$. Calculations showed that the most probable explanation for the obtained results can be found if one assumes that the chemical reaction in these mixtures is initiated by the vibrationally excited molecules. The population of high vibrational levels may occur by way of cascade transitions from lower vibrational levels onto higher levels either through molecular collisions or through photoexcitation. The latter possibility should not be discarded *a priori* since at high pressures, the widths of the absorption resonances may exceed the energy defect due to anharmonicity.

The important question to be answered is how many photons are required to activate a molecule in order to carry out a certain reaction? The chemical reaction itself can act as a source of photons, and if the photon emission compensates or exceeds the losses due to initiation, the entire process may be branched- or chain-branched.

V. BEAM PUMPED LASERS

Electron beam pumping of molecular mixtures is a recent major advance in chemical laser excitation. This technique provides more uniform volumetric initiation of gases than, say, optical flash photolysis. For example, Gregg of LRL had used 1.2-Mev electrons to excite H_2 + N_2F_4, NF_3, BF_3, and SF_6 mixtures and produced 10--100mj 50--1000nsec laser pulses. The importance of Gregg's work has been recognized particularly at the Lebedev Institute and at the Institute of Nuclear Physics of the Siberian Branch of the Academy of Sciences: two leading centers with on-going chemical laser research and a ready access to particle accelerators.

Five different Soviet groups are working independently on increasing the gain of gas lasers by way of exciting the laser gas-discharge region with a charged particle beam. The first group, headed by Lebedev's Prokhorov, observed a considerable increase in the output power of a CO_2 laser due to pumping by 2.8-Mev protons [50]. Also at the Lebedev Institute, Afanas'yev has experimented with gaseous xenon, neon, air and nitrogen pumped by 0.5-Mev electrons [51]. The third group under Faynberg at the Physico-Technical Institute of Low Temperatures of the Academy of Sciences UkrSSR, had used a pulsed low-energy electron beam to pump an argon-ion laser discharge [52]. Dolgov-Savel'yev at the Institute of Nuclear Physics experimented with 0.5-Mev electrons applied across the discharge of a CO_2 laser [53]. The most recent effort in this field is due to Basov et al. at the Lebedev Institute [54,55]. Unlike all the others, whose experiments were carried out at atmospheric or sub-atmospheric gas pressures, Basov kept his working gas (CO_2) at a pressure of ~16--20 atm.

All five agree that the interaction of a particle beam with the gas discharge tends to noticeably increase the laser output power by virtue of the uniform excitation at high pressures. The role of the electron beam is to provide conditions suitable for a streamerless development of discharge. The actual excitation energy is basically provided by the external field.

A. LOW PRESSURE MIXTURES

In the Dolgov-Savel'yev experiment [53], the laser consisted of a glass tube 50 cm long and 2 cm bore filled with pure and Ar- or Xe-doped CO_2 at pressures ranging from 1 to 30 torr. The optical cavity was made up of two 2-m curvature mirrors with Al coatings. The discharge electrodes were inside the glass tube. The laser beam was extracted through an NaCl aperture in one of the mirrors. The electron beam was coupled to the tube through 1.5-cm dia. 50-μ thick beryllium-foil "window" in the middle portion of the tube. The laser was capable of a steady state output at CO_2 pressures below 30 torr. At higher pressures, laser action was quenched. The power lost by the electron beam in passing through a 3-cm path in a gas was ~100--200 w.

The experimental results are shown in Figs. 62 and 63.

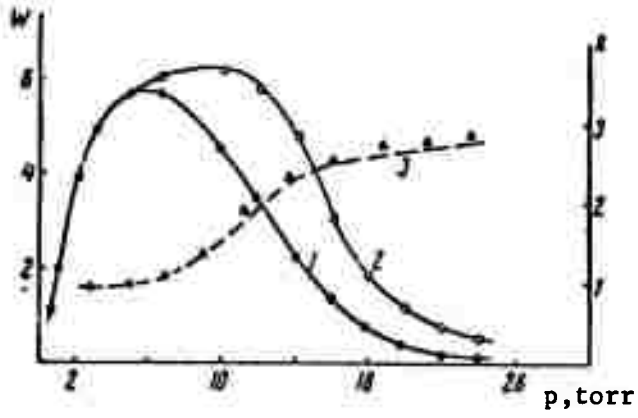

Fig. 62

Laser output power W for different pressures in pure CO_2 when pumped by pulsed discharge (1) and by pulsed discharge and particle beam (2); K is the ratio of (2) to (1) and is shown as curve (3).

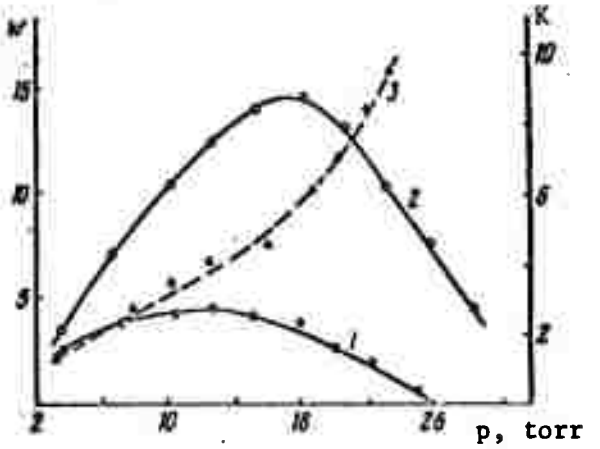

Fig. 63

Laser output power W in a CO_2 + Xe mixture (CO_2 pressure 3 torr, Xe pressure varied from 0 to 20 torr). Curves (1) -- (3), as in Fig. 61.

In Fig. 62, the effect of beam pumping (curve 2) is at first negligible at small pressures; as the CO_2 concentration increases, so does the beam effect, in spite of the fact that the discharge input power considerably exceeds the power imparted by the beam. Curve 3 is the power ratio for the beam-assisted and discharge-only curves, and it smoothly increases from 1 to 2.5--3.

In an Xe- or Ar-doped CO_2, the output power considerably increases with an increase in the total pressure (Fig. 63). Power measurements carried out at near-threshold conditions and CO_2 pressures of 10 torr produced the following results:

	pump power	laser output power
beam-assisted	9 kw	2.5 w
without beam	7.8 kw	1 w

An investigation of the effect of the e-beam on discharge parameters failed to detect noticeable changes in the discharge current and voltage in the tube. This has led the authors to conclude that an electron beam must not be considered as merely a source which provides additional ionization. In this connection, they feel

that perhaps the most probable mechanism explaining the gain enhancement by means of an e-beam is the change in the electron energy distribution function, particularly noticeable in CO_2 mixtures with argon or xenon.

Energetic beams are strongly scattered by gases and in the case of the above experiments, a 1 koe coaxial magnetic field was required to maintain the e-beam over the entire beam-gas interaction length (50 cm).

B. HIGH-PRESSURE MIXTURES

In the Basov experiments [54,55], a $CO_2 + N_2 + H_2O$ + He mixture was electrically discharged between two plane parallel titanium foil electrodes. The electron beam was pulsed into the discharge cell through an aperture in one of the electrodes, its energy being ~1.2 Mev, duration 20 nanosec, and current density 50 amp/cm^2.

The active laser region was 0.4 x 1 x 4 cm, and the output energy was extracted through a semi-transparent Ge-substrate silver mirror (10% transmission at $\lambda \simeq 2\mu$). The laser threshold voltage for a $CO_2 + N_2 + H_2O$ mixture (partial pressures 3.5 atm:11.5 atm:15 torr) was 19 kv and the electrical gas breakdown in the absence of an electron beam occurred at 32 kv (electrode gap 0.4 cm, active region 4 cm). The electron beam energy amounted to 1% of the energy stored in a $10^{-2}\mu$f condenser.

Figure 64 shows the dependence of the threshold electric field on the gas pressure. A decrease in the laser threshold at high pressures indicates a comparatively weak effect of quenching collisions on the population inversion of CO_2 molecules. An increase in the working mixture pressure causes an increase in the discharge breakdown voltage. This, in turn, calls for a greater energy per cm^3 of gas. The duration of the laser pulse and its delay with respect to ionization pulse are reduced as a result of an increasing frequency of collisions between N_2 and CO_2 molecules (see Fig. 65).

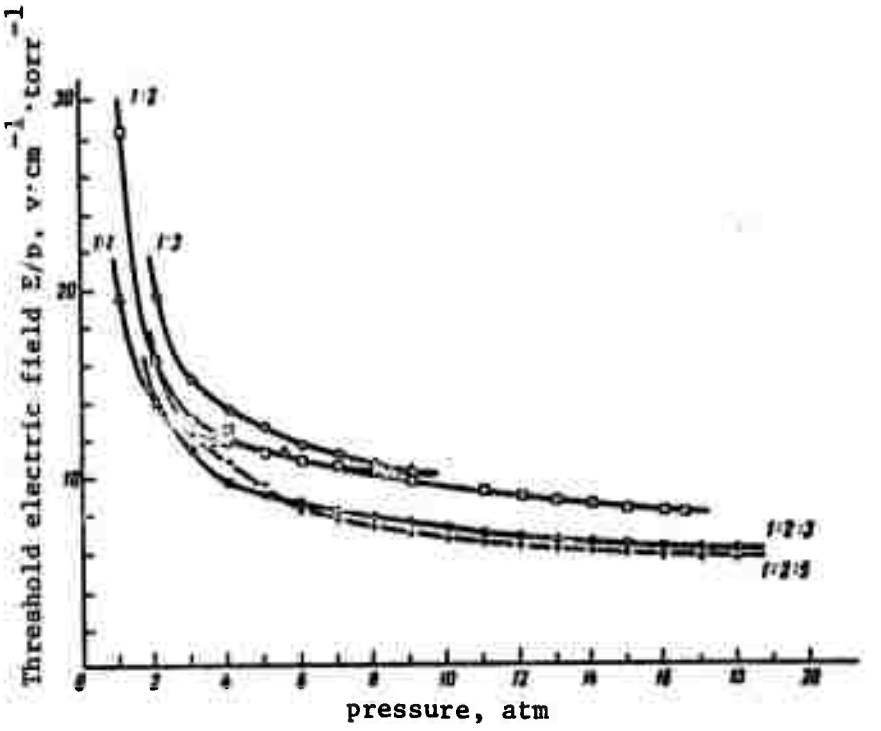

Fig. 64

Dependence of $(E/p)_{thresh}$ on mixture pressure. Numbers near curves show CO_2:N_2 and CO_2:N_2:He mixture composition. Water vapor was present in all mixtures at ~10 torr pressure.

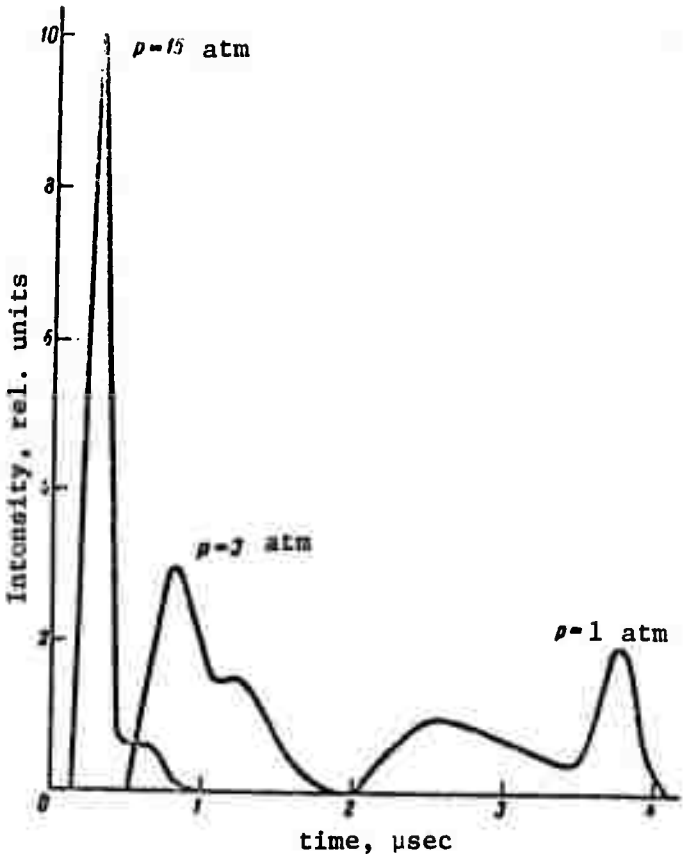

Fig. 65

Shape of laser pulse at different pressures. Discharge to threshold energy ratios at different pressures are: 1 atm -- ~1.5; 3 atm -- ~1.1; 15 atm -- ~1.02. CO_2:N_2 = 1:2.

Laser action was also observed for other mixture compositions, particularly in the absence of water vapor but with He added; it was quenched, however, when the pressure was reduced to 2 atm. The limiting pressure of the cell was ~25 atm.

The experiments produced laser pulse widths of ~200 nanosec. The coefficient of energy transfer from excited N_2 to CO_2 was ~30% which suggests that the Basov system behaves very much like the existing $N_2^* \rightarrow CO_2$ resonant transfer lasers in which the limiting efficiency is ~40%. Where it differs is in the possibility to produce ultrashort pulses -- and thus higher energies -- by manipulating

the CO_2 pressure. The spacing between the rotational components of a CO_2 line is ~5 x 10^{10}Hz; when the line is shock broadened, these components are apart by ~2 x 10^7 Hz/torr. The rotational lines will overlap at a pressure of ~2 x 10^3 torr, the linewidth of the laser transition being on the order of 5 x 10^{11} Hz. This would seem to indicate that at fairly high pressures, the self-mode locking will produce pulses with the duration of ~10 picosec.

Although he was unable to measure the overall efficiency of the system because of catastrophic problems at the output mirror, Basov estimates this to be in the region of 20--30% for CO_2. The estimated energy density of the device is ~200j/liter at 10.6μ. Virtually nothing is known about the beam quality of this laser. However, its suitability for heating of dense plasmas to Kev temperatures and for CTR was underscored by Basov at the recent laser-plasma interaction meeting in Hull, England [56].≠

During the past year, Basov used highly energetic electron beams (of the order of 1 Mev) to produce both superradiance [57] and stimulated emission [58] in a liquid xenon at $\lambda \approx 1760$Å. The power output of the vacuum uv Xe laser was of the order of several kw multimode and the beam divergence was a disappointing 7°. Nevertheless, this laser is tunable over ~100Å around 1760Å. In this respect, it appears to hold a considerable advantage over the gaseous hydrogen line lasers currently under development at IBM and NRL. Despite pessimism which generally beclouds the development of short-wavelength lasers, the Soviets are giving a serious consideration to beam-pumped liquid He and Ne as vacuum uv laser candidates at wavelengths down to 600Å [59].

≠High-pressure (~20 atm) beam-pumped gaseous xenon was reported at the same meeting to lase at 1672Å with a 50% conversion efficiency.

LIST OF PUBLICATIONS AND ABBREVIATIONS

Soviet publications scanned for this report have been abbreviated in order to save time and space. A list of these abbreviations and their expanded forms follows:

DAN SSSR	Akademiya Nauk SSSR. Doklady
FAiO	Fizika atmosfery i okeana
FiKhOM	Fizika i khimiya obrabotki materialov
FMiM	Fizika metallov i metallovedeniye
FiTP	Fizika i tekhnika poluprovodnikov
FTT	Fizika tverdogo tela
IFZh	Inzhenerno-fizicheskiy zhurnal
IVUZ. F	Izvestiya vysshikh uchebnykh zavedeniy. Fizika
IVUZ. R	Izvestiya vysshikh uchebnykh zavedeniy. Radiofizika
IzvAN SSSR. MZhiG	Akademiya Nauk SSSR. Izvestiya. Mekhanika zhidkosti i gaza
IzvAN SSSR. NM	Akademiya Nauk SSSR. Izvestiya. Neorganicheskiye materialy
IzvAN SSSR. Ser. khim.	Akademiya Nauk SSSR. Izvestiya. Seriya khimicheskaya
KhVE	Khimiya vysokikh energiy
KiK	Kinetika i kataliz
KE	Kvantovaya elektronika
KSpF	Kratkiye soobshcheniya po fizike
MiTOM	Metallovedeniye i termicheskaya obrabotka metallov
OiS	Optika i spektroskopiya
OMP	Optiko-mekhanicheskaya promyshlennost'

PiTE	Pribory i tekhnika eksperimenta
RiE	Radiotekhnika i elektronika
RZhF	Referativnyy zhurnal. Fizika
SiK	Steklo i keramika
TVT	Teplofizika vysokikh temperatur
UFN	Uspekhi fizicheskikh nauk
UFZh	Ukrainskiy fizicheskiy zhurnal
VAN SSSR	Akademiya Nauk SSSR. Vestnik
VLU	Leningradskiy gosudarstvennyy universitet. Vestnik
ZhETF	Zhurnal eksperimental'noy i teoreticheskoy fiziki
ZhETF P	Zhurnal eksperimental'noy i teoreticheskoy fiziki. Pis'ma v
ZhFKh	Zhurnal fizicheskoy khimii
ZhPKh	Zhurnal prikladnoy khimii
ZhPMTF	Zhurnal prikladnoy mekhaniki i tekhnicheskoy fiziki
ZhPS	Zhurnal prikladnoy spektroskopii
ZhTF	Zhurnal tekhnicheskoy fiziki

REFERENCES

1. Ksander, Y., Soviet Chemical Laser Research: Pulsed Lasers, The Rand Corporation, R-921-ARPA, November 1971.
2. Basov, N. G., V. I. Igoshin, Ye. P. Markin, and A. N. Orayevskiy, "Dynamics of Chemical Lasers," KE, No. 2, 1971, pp. 3-24. An edited translation of this article was published by The Rand Corporation, WN-7519-ARPA, August 1971.
3. Basov, N. G., V. T. Galochkin, V. I. Igoshin, L. V. Kulakov, Ye. P. Markin, A. I. Nikitin, and A. N. Orayevskiy, "Spectra of Stimulated Emission in the Hydrogen-Fluorine Reaction Process and Energy Transfer from DF to CO_2," unpublished report.
4. Dolgov-Savel'yev, G. G., V. F. Zharov, Yu. S. Neganov, and G. M. Chumak, "Vibrational-Rotational Transitions in a Chemical Laser Based on $H_2 + F_2$ Mixture," ZhETF, Vol. 61, No. 1, 1971, pp. 64-71.
5. Igoshin, V. I. and A. N. Orayevskiy, "Kinetics of an HCl Chemical Laser," KhVE, Vol. 5, No. 5, 1971, pp. 397-403.
6. Balakhnin, V. P., V. I. Yegorov, and Ye. I. Intezarova, "ESR Study of the Kinetics of Elementary Reactions of Atomic Oxygen," 2. "The Reaction O + HCl = OH + Cl," KiK, Vol. 12, No. 2, 1971, pp. 299-303.
7. Orayevskiy, A. N. and V. A. Shcheglov, "Analysis of Propagation of Photodissociation Waves in Gases with Allowance for Chemical Reactions," ZhETF, Vol. 59, No. 3, 1970, pp. 845-856.
8. Orayevskiy, A. N. and V. A. Shcheglov, "Analysis of the Propagation of Photodissociation Waves in Gases Allowing for Chemical Reactions," KSpF, No. 5, 1970, pp. 3-7.
9. Basov, N. G., V. T. Galochkin, L. V. Kulakov, Ye. P. Markin, A. I. Nikitin, and A. N. Orayevskiy, "Chemical Laser Based on a $D_2 + F_2 + CO_2$ Mixture," KSpF, No. 8, 1970, pp. 10-14.
10. Basov, N. G., V. V. Gromov, Ye. L. Koshelev, Ye. P. Markin, A. N. Orayevskiy, D. S. Shapovalov, and V. A. Shcheglov, "A CW DF-CO_2 Chemical Laser," ZhETF P, Vol. 13, 1971, pp. 496-498.
11. Vasil'yev, G. K., Ye. F. Makarov, V. G. Papin, and V. L. Tal'roze, "A Study of Vibrational Energy Transfer from HF and DF Molecules to CO_2 Molecules," ZhETF, Vol. 61, No. 1, 1971, pp. 97-100.
12. Leypunskiy, I. O., I. I. Morozov, and V. L. Tal'roze, "Mass-Spectroscopic Measurement of Rates in Reactions of Atomic Hydrogen and Fluorine with CH_3I and CF_3I," DAN SSSR, Vol. 198, No. 6, 1971, pp. 1367-1370.
13. Dodonov, A. F., G. K. Lavrovskaya, I. I. Morozov, and V. L. Tal'roze, "Mass-Spectroscopic Measurement of the Rate Constant of an Elementary Fluorine-Hydrogen Reaction," DAN SSSR, Vol. 198, No. 3, 1971, pp. 622-624.

14. Kapralova, G. A., Ye. M. Margolina, and A. M. Chaykin, "Rate Constants of Certain Reactions of the Vibrationally Excited Hydrogen Molecules Reacting with Fluorine," DAN SSSR, Vol. 197, No. 3, 1971, pp. 624-626.

15. Kapralova, G. A., Ye. M. Margolina, and A. M. Chaykin, "Mechanism of the Fluorine-Hydrogen Reaction," DAN SSSR, Vol. 198, No. 3, 1971, pp. 634-637.

16. Shutov, G. M. and Ye. Yu. Orlova, "The Methodology for the Kinetic Studies of Reactions with Complex Stoichiometry," ZhFKh, Vol. 45, No. 4, 1971, pp. 832-833.

17. Azatyan, V. V. and L. B. Romanovich, "The Use of the Explosion Limit Method in the Study of Reactions of Oxygen Atoms and Hydroxyl Radicals with an Inhibitor," AN SSSR. Izv. Seriya Khim., No. 5, 1971, pp. 941-946.

18. Safaryan, M. N. and Ye. V. Stupochenko, "The Kinetics of Thermal Decay of Diatomic Molecules in an Inert Gas at High Temperatures," KhVE, Vol. 5, No. 3, 1971, pp. 195-201.

19. Adkhamov, A. A. and M. Nasriddinov, "The Kinetic Theory of Relaxation Processes in Polyatomic Gases," In: Sb. "Teplofiz. svoystva gazov." M., "Nauka" [Sbornik on "Thermophys. Properties of Gases," Moscow,"Nauka"], 1970, pp. 185-187.

20. Losev, S. A., O. P. Shatalov, and M. S. Yalovik, "The Anharmonicity Effect on Relaxation Times in Adiabatic Excitation and Vibrational Deactivation of Molecules," DAN SSSR, Vol. 195, No. 3, 1970, pp. 585-588.

21. Medvedev, B. A., M. A. Teytel'boym, and A. Ye. Shilov, "The Chemical Activation of the $CHFCl_2$ Molecule in the Reaction $\cdot CHCl_2 + F_2 \rightarrow CHFCl_2 + F$," KiK, Vol. 12, No. 2, 1971, pp. 269-275.

22. Medvedev, B. A., M. A. Teytel'boym, and A. Ye. Shilov, "The Mechanism of the Gas Phase Reaction of Chlorofluoromethane with Molecular Fluorine," KiK, Vol. 12, No. 3, 1971, pp. 749-751.

23. Pariyskaya, A. V. and V. I. Vedeneyev, "The Fluorination Mechanism of Methane and Its Fluorine Derivatives," 2. "Difluoromethane," KiK, Vol. 12, No. 2, 1971, pp. 293-298.

24. Vedeneyev, V. I. and A. V. Pariyskaya, "The Mechanism of Fluorination of Methane and Its Fluorine Derivatives," 1. "A Comparison of Fluorination Rates of CH_4, CH_3F, CH_2F_2, CHF_3," KiK, Vol. 12, No. 1, 1971, pp. 21-26.

25. Pariyskaya, A. V. and V. I. Vedeneyev, "The Mechanism of Fluorination of Methane and Its Fluorine Derivatives," 3. "Methyl Fluoride," KiK, Vol. 12, No. 3, 1971, pp. 543-548.

26. Skorobogatov, G. A., "Formal Kinetics of Reactions in Photodissociation Gas Lasers," VLU, No. 4. Fizika i khimiya, No. 1, 1970, pp. 144-157.

27. Skorobogatov, G. A. and V. Ye. Khomenko, "The Role of Chain Reactions in the Kasper-Pimentel Perfluoroalkyliodide Lasers," VLU, No. 10. Fizika i khimiya, No. 2, 1970, pp. 170-174.

28. Belousova, I. M., O. B. Danilov, N. S. Kladovikova, and I. L. Yachnev, "Quenching of Excited Atoms in a Photodissociation Laser," ZhTF, Vol. 40, No. 7, 1970, pp. 1562-1564.

29. Andreyeva, T. L., S. V. Kuznetsova, A. I. Maslov, I. I. Sobel'man, and V. N. Sorokin, "Study of Excited Iodine Reactions by Means of a Photodissociation Laser," ZhETF P, Vol. 13, 1971, pp. 631-635.

30. Andreyeva, T. L., V. I. Malyshev, A. I. Maslov, G. Ya. Solov'yev, and V. N. Sorokin, "Study of a Q-Switched Iodine Laser," KSpF, No. 10, 1970, pp. 71-77.

31. Dudkin, V. A., I. N. Knyazev, and V. I. Malyshev, "IBr Recombination Photodissociation Laser in a Periodically Pulsed Mode," KSpF, No. 5, 1970, pp. 32-37.

32. Volkov, V. N. and I. G. Zubarev, "Study of Spectral Composition and Linewidth of Emission from a C_3F_7I Photodissociation Laser," KSpF, No. 1970, pp. 10-16.

33. Velikanov, S. D., S. B. Kormer, V. D. Nikolayev, M. V. Sinitsyn, Yu. A. Solov'yev, and V. D. Urlin, "Determination of the Lower Limit of the Fluorescence Linewidth of the $5^2P_{1/2}$-$5^2P_{3/2}$ Transition of Atomic Iodine in a Photodissociation Laser," DAN SSSR, Vol. 192, No. 3, 1970, pp. 528-530.

34. Beterov, I. M., Ye. A. Matyugin, and V. P. Chebotayev, "Measurement of Relaxation Constants by the Three-Level Laser Spectroscopy," ZhETF P, Vol. 12, No. 4, 1970, pp. 174-177.

35. Kochelap, V. A. and S. I. Pekar, "Kinetics of Lasers Based on Light Induced Chemical Reaction in a Steady-State Regime," UFZh, Vol. 15, No. 7, 1970, pp. 1057-1067.

36. Kochelap, V. A., "Thermally Pumped Photostimulated Chemical Reactions," UFZh, Vol. 15, No. 6, 1970, pp. 1213-1216.

37. Kochelap, V. A. and S. I. Pekar, "Theory of Stimulated Radiative Chemical Reaction in Gases and Its Application in Lasers," ZhETF, Vol. 58, No. 3, 1970, pp. 854-864.

38. Pekar, S. I. and V. A. Kochelap, "Einstein Relationships for the Stimulated Chemiluminescence and Their Applicability to High-Pressure Chemical Lasers," DAN SSSR, Vol. 196, No. 4, 1971, pp. 808-811.

39. Barashev, P. P. and V. L. Tal'roze, "The Competition Between Thermal and Photochemical Mechanisms of Substance Transformation in the Field of a Pulsed Laser," KhVE, Vol. 5, No. 1, 1971, pp. 30-36.

40. Orayevskiy, A. N., "The Explosion Limits in the Radiation Field," KhVE, Vol. 5, No. 2, 1971, pp. 118-120.

41. Gordiyets, B. F., A. I. Osipov, and L. A. Shelepin, "Non-equilibrium Dissociation Processes and Molecular Lasers," ZhETF, Vol. 61, No. 2, 1971, pp. 562-574.

42. Karlov, N. V., Yu. N. Petrov, A. M. Prokhorov, and O. M. Stel'makh, "Dissociation of BCl_3 by CO_2 Laser Radiation," ZhETF P, Vol. 11, No. 4, 1970, pp. 220-222.

43. Gordiyets, B. F., A. I. Osipov, and L. A. Shelepin, "Kinetics of Nonresonant Vibrational Exchange and the Molecular Lasers," ZhETF, Vol. 60, No. 1, 1971, pp. 102-113.

44. Orayevskiy, A. N. and V. A. Savva, "Laser Induced Molecular Vibrations and the Chemical Reactions," KSpF, No. 7, 1970, pp. 50-55.

45. Afanas'yev, Yu. V., E. M. Belenov, Ye. P. Markin, and I. A. Poluektov, "Nonequilibrium Dissociation of a Molecular Gas by Resonant Laser Radiation with an Allowance for V-V Collisions," ZhETF P, Vol. 13, 1971, pp. 462-464.

46. Karlov, N. V., Yu. B. Konev, and A. M. Prokhorov, "The Use of Lasers for the Selective Breaking of Chemical Bonds," ZhETF P, Vol. 14, 1971, pp. 178-181.

47. Karlov, N. V., N. A. Karpov, Yu. N. Petrov, A. M. Prokhorov, and O. M. Stel'makh, "Excitation of a Detonation Wave During the Initiation of Chain Reactions in Gas Mixtures by CO_2 Laser Radiation," ZhETF P, Vol. 14, 1971, pp. 214-217.

48. Basov, N. G., Ye. P. Markin, A. N. Orayevskiy, and A. V. Pankratov, "Photochemical Effects of Infrared Radiation," DAN SSSR, Vol. 198, No. 5, 1971, pp. 1043-1045.

49. Basov, N. G., Ye. P. Markin, A. N. Orayevskiy, A. V. Pankratov, and A. N. Skachkov, "Stimulation of Chemical Processes by Infrared Laser Radiation," ZhETF P, Vol. 14, 1971, pp. 251-253.

50. Andriakhin, V. M., Ye. P. Velikhov, S. A. Golubev, S. S. Krasil'nikov, A. M. Prokhorov, V. D. Pis'mennyy, and A. G. Rakhimov, ZhETF P, Vol. 8, 1968, pp. 346-349.

51. Afanas'yev, Yu. V., E. M. Belenov, O. V. Bogdankevich, V. A. Danilychev, S. G. Darznik, and A. F. Suchkov, "The Possibility of Building Pulsed Gas Lasers with Electron Beam Pumping in the Electrical Field," KSpF, No. 11, 1970, pp. 23-27.

52. Tkach, Yu. V., Ya. G. Faynberg, L. I. Bolotin, Ya. Ya. Bessarab, N. P. Gadetskiy, Yu. N. Chernen'kiy, and A. B. Berezin, ZhETF P, Vol. 6, 1967, pp. 956-958.

53. Dolgov-Savel'yev, G. G., V. V. Kuznetsov, Yu. L. Kos'minykh, and A. M. Orishich, "A Possibility of Designing a CO_2 Laser with Electron Beam Pumping," ZhPS, Vol. 12, No. 4, 1970, pp. 737-739.

54. Basov, N. G., E. M. Belenov, V. A. Danilychev, and A. F. Suchkov, "High-Pressure Pulsed CO_2 Laser," KE, No. 3, 1971, pp. 121-122.

55. Basov, N. G., E. M. Belenov, V. A. Danilychev, O. M. Kerimov, I. B. Kovsh, and A. F. Suchkov, "High-Pressure Gas Lasers," ZhETF P, Vol. 14, No. 7, 1971, pp. 421-426.

56. Meeting on Laser-Plasma Interaction, Hull, England, September 1971.

57. Basov, N. G., O. V. Bogdankevich, V. A. Danilychev, G. N. Kashnikov, O. M. Kerimov, and N. P. Lantsov, "Superradiance of Condensed Xenon Excited by Fast Electrons," KSpF, No. 7, 1970, pp. 68-74.

58. Ksander, Y., A Soviet Vacuum UV Laser, The Rand Corporation, WN-7504-ARPA, July 1971.

59. Private communication from A. N. Orayevskiy (Lebedev Institute).

AUTHOR INDEX